Development of Field-deployable Nucleic Acid Testing Platforms

By:

Tianyu Dong

A Thesis Submitted to the Department of Chemistry

In Partial Fulfillment of the Requirements for the

Degree of Master of Science

Faculty of Mathematics & Science, Brock University

St. Catharines, Ontario

Abstract

This thesis is focused on the development of field-deployable nucleic acid testing platforms to allowed rapid detection and quantification of nucleic acids. Two distinct platforms suitable for nucleic acid testing in resource-limited settings were developed. First, a paper-based diagnostic device was developed. The principle of this paper-based device was based on the unique interfacial interaction of DNA and the DNA intercalating dye with cellulose on chromatographic paper. Second, a colorimetric reader was developed. The principle of the reader was based on measuring the absorbance change of a chromogenic substrate which is triggered by DNA and DNA intercalating dyes under light illumination. The performance of both devices was tested using synthetic DNA, nucleic acid amplicons, and actual parasites nucleic acid samples collected from school-age children in rural areas of Honduras.

Acknowledgements

I would like thank my supervisory Dr. Feng Li for giving me the opportunity to pursue graduate studies at Brock University and provide me support throughout my thesis project. I would also like to thank my committee members Professor Art Van der Est, Professor Theocharis Stamatatos, and Professor Tomáš Hudlický for providing me with suggestions and advice for my thesis project. I would like to acknowledge all of the members of Dr. Li's group who have support me throughout my thesis project. I would thank to Guan Wang and Hayam Monsour for aiding me in fabricate devices and collaborating on several experiments in my projects. I would like to recognize Professor Ana L. Sanchez and her group in Honduras, without their hard-working team our group would never have had clinical samples to test. I would like to thank Jesse Vanloon in Dr. Yan's group for proof-reading my dissertation. I would especially like to thank my parents for the continuous support and strength that they gave me in order to study in foreign country. I hope have made you proud.

Table of Contents

Abstract I

Acknowledgements II

List of Figures VI

List of Tables VIII

List of Schemes IX

List of equation X

List of Abbreviations XI

Chapter 1 Introduction and Literature Review 1

Contribution Statement 1

1.1 Introduction 1

1.2 Historical 2

1.2.1 Paper as a Detection Platform for NAT 2

1.2.2 Manipulating Nucleic Acid Samples Using μPAD. 4

Sample preparation using μPAD. 5

In-device nucleic acid amplification. 7

NAT using highly integrated sample-in-answer-out μPADs. 9

1.2.3 Signal Transduction Strategies for Nucleic Acids Detection in μPAD. 13

Lateral flow assays. 13

Intercalating dyes. 17

Hybridization probes. 17

Synthetic biology approaches. 21

Chapter 2 Development of Quantitative Paper-Based DNA Reader (qPDR) for Distance-Based Quantification of Nucleic Acids 24

Contribution statement 24

2.1 Introduction 24

2.2 Result and Discussion. 25

2.2.1 Device Fabrication and Assay Principle. 25

2.2.2 Chromatography Behavior of Nucleic Acid and SG on qPDR. 29

2.2.3 Effects of SG and Other Auxiliary Reagents on DNA Quantification Using qPDR. 31
Effects of SG Concentration on DNA Quantification. 31
Effects of Ionic Strength on DNA Quantification. 32
Effects of Urea on DNA Quantification. 33
Effects of Polyethylene Glycol Concentration on DNA Quantification. 34
Effects of Surfactants on DNA Quantification. 35
2.2.4 Deploying qPDR for NAT. 37
Assay Validation Using Synthetic DNA. 39
2.2.5 Sequence-Specific Nucleic Acid Quantification by Integrating qPDR with PCR. 42
2.2.6 Quantification of Soil-transmitted helminth (STH) Infections Using qPDR with PCR. 44
2.2.7 Distance-based Quantification of Mercury ion (Hg^{2+}) using qPDR. 47
2.3 Conclusion 50
Chapter 3 Fast Light-Activated Substrate cHromogenic (FLASH) Platform for Nucleic Acid Quantification. 51
3.1 Introduction. 51
3.2 Result and Discussion. 52
3.2.1 Principle of FLASH Assay. 52
3.2.2 FLASH Reader Fabrication and Performance Test. 53
FLASH Reader Fabrication and Working Principle. 53
Validation of FLASH Reader for NAT. 54
3.2.3 Integration of FLASH Reader with PCR. 56
3.2.4 Integration of FLASH Reader with LAMP. 59
3.2.5 FLASH strip. 60
3.3 Conclusion. 64
Chapter 4 Conclusion and Future Work. 65
Chapter 5 Experimental Section 67
5.1. Experimental Section for Chapter 2. 67
5.1.1 Materials and Reagents. 67
5.1.2 qPDR Fabrication. 68

5.1.3 Nucleic Acid Quantification Using qPDR. 69
5.1.4 Effects of SG and Other Auxiliary Reagents on Distance-based DNA Quantification Using qPDR. 72
Effects of Ionic Strength on DNA Quantification. 73
Effects of Urea on DNA Quantification. 73
Effects of Polyethylene Glycol Concentration on DNA Quantification. 73
Effects of Surfactants on DNA Quantification. 73
5.1.5 Quantification of PCR Amplicons Using qPDR. 74
5.1.6 Clinical STH Samples. 74
5.1.7 Quantification of STH Samples Using qPDR. 75
5.1.8 Quantification of Mercury ion (Hg^{2+}) using qPDR. 76
5.2 Experimental Section for Chapter 3. 76
5.2.1 Materials and Reagents. 76
5.2.2 Fabrication of FLASH Reader. 79
5.2.3 NAT using the FLASH Reader. 82
5.2.4 Validation of the FLASH reader Performance. 82
5.2.5 Preparation of HBV Containing Human Serum Samples and DNA Isolation. 83
5.2.6 Clinical STH Samples. 83
5.2.7 Deploying FLASH PCR for STH Infections. 83
5.2.8 Direct PCR. 84
5.2.9 LAMP. 85
5.2.10 Gel Electrophoresis. 85
5.2.10 Distance-based NAT Using FLASH Strip. 86
References 87

List of Figures

Figure 1.1 Manipulating nucleic acid samples using μPAD.

Figure 1.2 Nucleic acid detection by lateral flow strip.

Figure 1.3 Different nucleic acid signal readout strategies on paper-based devices.

Figure 1.4 Synthetic biology approaches on paper-based devices.

Figure 2.1 Retention distances of 3 dsDNA samples (S1-3) and 3 ssDNA samples (B1-3) on qPDR.

Figure 2.2 Chromatography behaviors of SG on qPDR.

Figure 2.3 Effect of SG concentrations on the quantification of dsDNA and the background (ssDNA).

Figure 2.4 Effects of ionic strength on the performance of distance-based quantification of DNA using qPDR.

Figure 2.5 Effects of urea on the performance of distance-based quantification of DNA using qPDR.

Figure 2.6 Effect of PEG 100,000 on the migration distances of SG I in the presence of 500 nM dsDNA and 500 nM ssDNA.

Figure 2.7 Effects of surfactant on the performance of distance-based quantification of DNA using qPDR.

Figure 2.8 Typical distance-based nucleic acid testing using qPDR.

Figure 2.9 Concentration dependency of the retention distance d_R on the concentration of dsDNA.

Figure 2.10 Quantification of PCR amplicons on qPDR.

Figure 2.11 Quantification of genomic DNA by using PCR and qPDR.

Figure 2.12 qPDR and gel electrophoresis picture of worm samples after PCR amplification.

Figure 2.13 Distance-based quantification of Hg^{2+} using T-rich ssDNA probe.

Figure 2.14 Distance-based quantification of Hg^{2+} using different T-rich ssDNA probes

Figure 3.1 The Jablonski diagram shows a plausible mechanism for the FLASH reaction.

Figure 3.2 Design and operation of FLASH reader.

Figure 3.3 FLASH reader performance tests.

Figure 3.4 Quantification of STH infections by using FLASH PCR.

Figure 3.5 Analyzing clinical parasitic worm samples using PAGE gel.

Figure 3.6 Quantification of LAMP amplicons by FLASH reader.

Figure 3.7 Colorimetric detection on qPDR by pre-deposited TMB.

Figure 5.1 Procedures of converting an image of DNA quantification on qPDR into a chromatogram.

Figure 5.2 Schematic illustration of the housing (**a**) and electrical (**b**) designs of the FLASH reader.

List of Tables

Table 5.1 Synthetic DNA sequences.

Table 5.2 Retention distance measured by 59 people.

Table 5.3 PCR templates and primers.

Table 5.4 LAMP templates and primers.

List of Schemes

Scheme 2.1 Schematic Illustration of the Fabrication Process **(A)** and the Assay Principle **(B)** of qPDR.

Scheme 3.1 Workflow for visual, colorimetric detection and/or quantification of genetic biomarkers in diverse biological and clinical samples using the FLASH system.

List of equation

Equation 1: % greyscale intensity = (X-Min)/(255-Min) * 100%

List of Abbreviations

µPAD	paper-based analytical device
1D	one-dimensional
3D	three-dimensional
AgNPs	silver nanoparticles
AL	Ascaris lumbricoides
APS	ammonium persulfate
ASV	anodic stripping voltammetry
CTAB	Cetrimonium bromide
CV	crystal violet
DENV	dengue virus
d_R	retention distance
dsDNA	double-stranded DNA
FLASH	Fast Light-Activated Substrate cHromogenic
FRET	fluorescence resonance energy transfer
HBV	hepatitis B virus
hCG	human chorionic gonadotropin
HDA	helicase dependent amplification
HIV	human immunodeficiency viruse
ICP	ion concentration polarization
ITP	isotachophoresis
LAMP	loop-mediated isothermal amplification
LE	leading electrolyte
LFA	lateral flow assay
LRET	luminescence resonance energy transfer
MµBs	magnetic microparticles
NAT	Nucleic acid testing
PAGE	polyacrylamide gel electrophoresis
PCR	polymerase chain reaction
PEG	polyethylene glycol
POCT	point-of-care testing
QDs	quantum dots
qPDR	quantitative paper-based DNA reader
RBS	ribosome binding site
RCA	rolling circle amplification
RNA	Ribonucleic acid
RPA	recombinase polymerase amplification
SDA	strand displacement amplification
SDS	sodium dodecyl sulfate
SG	SYBR Green I

SHERLOCK	specific high-sensitivity enzymatic reporter unlocking
ssDNA	single-stranded DNA
STH	Soil-transmitted helminth
TE	trailing electrolyte
TEMED	N,N,N′,N′-tetramethylethylenediamine
TMB	3,3’,5,5’-tetramethylbenzidine
TT	Trichuris trichiura
UCNPs	upconversion nanoparticles
WHO	world health organization
ZIKV	Zika virus

Chapter 1
Introduction and Literature Review

Contribution Statement

The contents of Chapter 1 section 1.1, and 1.2 were modified from a recent review titled "Shaping up field-deployable nucleic acid testing using microfluidic paper-based analytical devices".[1] Reprint with permission from Dong, T.; Wang, G. A.; Li, F. Shaping up field-deployable nucleic acid testing using microfluidic paper-based analytical devices. *Anal. Bioanal. Chem.* **2019**, 411, 4401-4414. Copyright 2019 Springer Nature.

I am the lead author of this paper and contributed to 100% of the writing with revision from other authors.

1.1 Introduction.

Nucleic acid testing (NAT) is a technique that detects genetic markers from clinical or biological samples and has been shown to have an indispensable role in disease diagnosis and monitoring. Standard NATs often require a wet lab environment and may lead to extensive sample manipulation and expensive instrumentation; thus, NATs are predominately performed at centralized clinical laboratories. Miniaturization of standard NATs into a simple portable point-of-care testing (POCT) platforms may aid in the rapid diagnosis at the patient bedsides or the doctor's office.[2] Deploying simple NATs for field-based diagnosis is also critical for monitoring and managing viral, bacterial, and parasitic infections in low-middle income countries that lack industrialization, where widespread infections can cause serious morbidity and death.[3-5] Despite recent efforts in integrating standard NATs with advanced approaches in microfluidics,[6-7] nanotechnology,[8-10] and

synthetic biology,[11-16] rapid and broad adoption of these technological innovations remains challenging. The qualitative and insensitive nature of many detection platforms, such as lateral flow devices, may limit the use of NATs to be used for accurate and quantitative analyses.[15-16] To be used as a POCT in resource-limited settings, an ideal NAT shall meet the "ASSURED" criteria developed by world health organization (WHO), which include affordable, sensitive, specific, user-friendly, rapid & robust, equipment-free, and delivered to end users.[17]

The overall project referred to here is to develop field-deployable platforms that are capable of nucleic acid quantification with high fidelity in a resource-limited setting that meets the requirements outlined by the WHO. Paper-based devices were selected as a topic of interest because NATs are portable and do not require an experienced individual with an academic background to deploy an NAT. Additionally the success of pregnancy test strip has motivated us to use cellulose paper as a test platform. Beside the paper-based devices, portable electronic POCTs devices have been extensively used because of their low-cost to manufacture *via* microfabrication technologies and capability of measuring various parameters depending on the complexity of the system.[18] The electronic POCTs devices outlined here is a colorimetric reader designed to perform a colorimetric analysis via a photooxidation reaction with chromogenic material.

1.2 Historical.rr

1.2.1 Paper as a Detection Platform for NAT.

Paper with low-cost and unique capillary action behaviour has naturally been recognized as one of the best engineering materials for realizing field-deployable NAT.[19-

[21] Typically, paper-based devices compose of a polymer of β-linked D-glucose or more commonly known as cellulose.[22] The intermolecular and intramolecular hydrogen bonding are the forces that holds cellulose chains together to compose cellulose fibers. Cellulose is insoluble in weak acid, base, and common organic solvents. Strong acids cause the acid-catalyzed hydrolysis of cellulose chains and result in the chemical degradation of cellulose chains.[23] Diverse analytical and microfluidic devices made partially or entirely out of paper, generally known as microfluidic paper-based analytical devices (μPAD), have been created and used as a test platform for NAT in recent years.

The idea of μPAD was first introduced by Martinez[24] in 2007, opening the possibility of creating sophisticated microfluidic systems by simply patterning diverse designs on papers. They examined the use of patterned/partitioned hydrophilic chromatography paper for the purpose of bioassays comprising of hydrophilic polymeric cellulose separated by hydrophobic lines of SU-8 photoresist, a patented epoxy-based polymer that was etched onto the paper using photolithography. The partitioning of the paper allowed for the manipulation of biological fluids allowing multiple diagnostic assays to take place on a single strip of paper.

Comparing to other analytical devices, μPAD offers several unique advantages towards field-based applications. Paper is a widely available and low-cost material that can be readily manufactured, modified, and patterned. Papers of varying sizes, thicknesses, pore sizes, and chemical modifications are widely available and well-defined channels can be easily created through a range of printing and patterning techniques, such as wax-printing, ink-jet printing, screen-printing, photolithography, laser direct-writing, or even hand-writing.[19] Paper can also be physically modified by cutting to form designed shapes.

More complicated multi-dimensional paper circuits can also be achieved by simply folding and unfolding the paper with designed channel. Because of the hydrophilicity and porosity, μPADs can generate and control liquid flows via capillary action without the need for external pumps. Paper possesses a high surface area to volume ratio; this suggests that paper can absorb higher amount of fluids than other microfluidic platforms. External power supplies, such as electricity, can also be used for the manipulation (e.g., electrophoresis) or detection (e.g., electrochemical detection) of nucleic acids in μPAD. Also, due to the high surface area to volume ratio, paper can store higher amount of fluids than other microfluidic platforms. Paper is also an environmentally friendly material that can be easily disposed of and degraded. When handling samples containing infectious pathogens or biohazards, it is also possible to minimize the risks of users and potential contamination by simply burning devices. These advantages have driven the development of diverse μPADs for clinical diagnosis, environmental monitoring, and food safety surveillance.

1.2.2 Manipulating Nucleic Acid Samples Using μPAD.

A NAT involves three steps: nucleic acid sample preparation (isolation and purification), amplification, and detection. For field-based applications the overall goal is to miniaturize each step and eventually integrate all steps into a single portable device. As an example, μPADs offer a simple and inexpensive solution for NAT miniaturization with the addition of multi-dimensional analysis through folding/partitioning. The tunability of paper devices allows for sophisticated sample processing and the ability for highly integrated sample-in-answer-out μPADs which streamlines the steps for deploying an NAT.

Sample preparation using µPAD. Sample preparation is a step in NAT that is designed to extract and purify nucleic acids from complicated sample matrices to remove inhibitors for subsequent nucleic acid amplification. As an example, Whatman Flinders Technology Associates (FTA) cards are a commercially available paper-based device that allows for the preservation, extraction, purification, and allowed transportation of nucleic acids. To further enhance the in-device nucleic acid extraction, purification and liquid transportation, a variety of µPADs have recently been developed. In a study conducted by Fronczek.[25], they developed a one-dimensional (1D) paper device capable of extracting nucleic acids of *Salmonella Typhimurium* from field and clinical samples through filtering and chromatographic interactions between cellulose (or nitrocellulose) with varying components in the sample. determined that proteins, lipids, and other cell lysates were retained close to the inlet of the device while nucleic acids migrated further in the paper channel, thus separating the sample mixture. Using this simple µPAD, the nucleic acid extraction can be accomplished within 5 minutes. Despite the rapid partitioning of nucleic acids and proteins, the device created by Fronczek. possesses a minor caveat, being that the device requires the sample to be lysed and then dilution prior to loading. An ideal µPAD should allow direct raw sample preparation without the need for prior treatments. To achieve this goal, Govindarajan[26] introduced a three-dimensional (3D) paper origami device that integrates the lysis of the *E. coli* bacterial cells and nucleic acids extraction into a single device without using external equipment or treatment (Figure 1.1 A). This device was fabricated by stacking layers of Mylar sheets using repositionable adhesive and cellulose paper. All reagents including the lysis buffer, extraction buffer, and washing buffers were preloaded and dried on the different layers of the device to achieve the field-

ready sample preparation. Upon introducing the raw sample into the central inlet, a series of lysis, washing, and extraction steps could be activated by simply folding the designated layers of the paper origami. The overall extraction process starting from the raw sample can be completed within 1.5 hr without the use of external power or within 1 hr using a heater block with an extraction limit as low as 33 CFU/ml.

For samples containing only trace amount of nucleic acids, it is ideal to concentrate nucleic acids during the extraction step. One viable strategy is to integrate μPAD with electrokinetic extraction techniques, such as isotachophoresis (ITP) and ion concentration polarization (ICP). [27-29] ITP is an technique that is derived from electrophoresis. Unlike electrophoresis which separates charged molecules such as deoxy ribonucleic acid (DNA) according to size, ITP is used to selectively partition and concentrate ionic analytes such as nucleic acids from a complex mixture based on ionic mobility using an electric field and a discontinuous buffer system composing of a leading electrolyte (LE) and a trailing electrolyte (TE). In 2015, Li[27] reported a 3D multi-layered paper-based ITP device capable of concentrating DNA samples. As shown in Figure 1.1 B, the device consists of a series of wax-patterned filter paper that are folded on-top of one another in an accordion-like way. Each section of filter paper possesses a 2 mm diameter paper well and thee total thickness of folded paper device was 2 mm. The buffer system for the device is portioned between two reservoirs containing the LE and TE buffers, respectively, and is separated by a slip layer. Due to the short channel length, a high electric field of ~16 KV/m can be generated for ITP using two 9 V batteries. Using this device, over 100-fold enrichment was achieved for DNA having lengths of up to 1,517 bps within 10 min.

When integrating with ICP, μPAD can not only concentrate DNA but also separate DNA based on their sizes or separate double-stranded DNA (dsDNA) from single-stranded DNA (ssDNA). Recently, Gong[28] developed such an ICP-μPAD capable of simultaneously preconcentrating, separating, and detecting DNA fragments in clinical samples. The device was fabricated by patterning wax barriers on nitrocellulose paper, which defines two reservoirs connected by a sample channel (Figure 1.1 C). To enable ICP, one of the reservoirs is partially coated with a cation-selective nanoporous Nafion membrane while the other reservoir is devoid. After loading the reservoir with deionized water and loading the sample in the sample channel an electrical field was applied. This resulted in the partitioning and accumulation of anionic charged species such as DNA across the channel and close to the cathode end of the apparatus. Gong determined that the device was capable of separating, preconcentrating, and detecting 150 copies/mL of hepatitis B virus (HBV) DNA fragments in human serum samples within 10 min, allowing for early diagnosis of hepatitis B without the need for nucleic acid amplification.

In-device nucleic acid amplification. To enable the sensitive and specific detection of specific DNA or Ribonucleic acid (RNA) sequences, nucleic acid amplification is commonly required. An optimal μPAD for field-applicable NAT should provide an in-device nucleic acid amplification step. Nucleic acid amplification is most commonly carried out by polymerase chain reaction (PCR). As standard PCR requires a thermal cycling step. Thermo cycling is a procedure that involves repetitive heating and cooling cycles in order to denature, anneal, and extend target nucleic acid sequence. In-device PCR was found to be a challenge for in-field NAT. On the other hand, significant progress has been made to integrate μPAD with isothermal nucleic acid amplification techniques. The

in-device amplification was first reported by Rohrman[30] in 2012, where human immunodeficiency virus (HIV) DNA was amplified using isothermal amplification technique recombinase polymerase amplification (RPA) in a paper-tape hybrid origami device (Figure 1.1 D). Similar to the 3D paper-origami for sample preparation, the in-device RPA was also achieved by storing key assay reagents (master mix and magnesium acetate) into different layers and then activating the reaction by simply folding the device. A long sample wick strip with a wax-patterned hydrophobic arm was also created to facilitate direct sample introduction from the microcentrifuge tube and thus eliminated the need for pipetting. Here the use of an LFA as a readout, Rohrman was able to detect as low as 10 copies of HIV DNA. Similarly, in a study conducted by Liu[31] reported a paper-based device capable of carrying out target-induced rolling circle amplification (RCA) to produce massive quantities of DNA amplicons for the subsequent detection. ROC is an isothermal technique that is used to amplify circular molecules of nucleic acids such as plasmids. The paper device that was fabricated by Liu was designed by patterning a 96-microzone on a nitrocellulose paper with each test zone of being 4 mm in diameter. RCA reagents was printed onto the paper device within a pullulan sugar film, allowing the maintenance of more than 90% activity at 4℃ after 15 days. Liu determined that RCA was more proficient on paper than in solution, likely in-part to the higher local concentration of immobilized DNA, thus allowing for the detection limit of single digit picomolar level. In addition to RPA and RCA, other isothermal amplification techniques such as loop-mediated isothermal amplification (LAMP), strand displacement amplification (SDA), and helicase dependent amplification (HDA) have also been integrated into μPAD to achieve the in-device amplification of the target nucleic acids.[32-37]

NAT using highly integrated sample-in-answer-out μPADs. Fully integrated μPADs that streamline the sample preparation, nucleic acid amplification and detection are highly desirable to fulfill the final goal of field-deployable NAT at low-resource environment.[38] One of the first fully integrated μPADs was introduced by Connelly[39] in 2015, where they developed a 3D "paper machine" that fully integrated sample preparation, LAMP, and detection in a low-cost, single-use format. As shown in Figure 1.1 E, the device was designed to be a closed system that contains three layers of magnetic sliding strips that could be slid to control the serial introduction of a sample, wash buffer, amplification reagents, and detection reagents. The middle layer of the device contains a reaction disc fabricated using Whatman FTA paper. The operation of the device requires the sequential sliding of the middle layer through each port on the top and bottom layers followed by adding sample, washing buffer, LAMP Master Mix and incubation in 65℃ for 1 hr. Using this paper device, Connelly was able to detect as low as 1 copy of the synthetic dsDNA representing the *malB* gene fragment of *E. coli* and consistently detect 5 *E. coli* cells in human plasma.

To further push the development of μPAD for direct NAT in human blood sample, Xu[40] introduced a 3D origami paper device capable of whole blood nucleic acid extraction, separation, LAMP and multiplexed nucleic acid analyses in a single device (Figure 1.1 F). The device was fabricated by patterning wax onto multiple foldable layers of filter paper. A glass fiber disk was also inserted into the middle layer for nucleic acid extraction. The NAT was initiated by loading the human blood sample onto the glass fiber disk followed by folding the device to enable cell lysis and DNA extraction on the glass-fiber paper. The purified DNA was then transferred to the amplification panel by another folding step and

split to four independent paper wells where species-specific LAMP reagents were deposited; the system was sealed using an acetate film to prevent evaporation. Amplification was carried out at 63 °C for ~45 min and was examined under naked-eye detection with a handheld UV lamp. Xu concluded that the device that was fabricated was capable of simultaneous detection of multiple pathogens including *P. falciparum* (98%), *P. malariae* (96%), *P. vivax* (98%) from either finger-prick fresh blood sample or frozen blood were achieved within a single paper device. The NAT in whole blood sample can also be achieved using electrokinetic paper-based devices that enable nucleic acid separation and preconcentraion in a single step. In a study conducted by Bender[41] described an electrokinetic paper-based device that integrated ITP with RPA. This ce consisted of a glass fiber strip that connected with two electrolyte reservoirs. A plasma separation membrane was placed on the top of the strip in order to allow for the partitioning of plasma, coagulation factors (solid particles) where the plasma was allowed to wick onto the glass fiber strip. The operation of the device fabricated by Bender utilized TE buffer and LE buffer with RPA reagent into two reservoirs and the application of an applied electric field. The device was found to allow for the extraction of as DNA that was as low as 10^4 copies/ml, and simultaneously allowed for the concentration and amplification of the targeted DNA in a single step.

As nucleic acid amplification requires incubation at elevated temperatures, most abovementioned devices still require external reusable equipment such as incubator, water bath and heater, which not only adds the cost and complexity of the NAT, but also increases the risk of cross-contamination. To address this challenge, Tang[42] recently developed a fully disposable and integrated μPAD for nucleic acid extraction, amplification (HDA),

and detection using LFA for complex mechanical mixture (wastewater, milk, juice, and egg). Tang was able to detect *Salmonella typhimurium* using an apparatus that consisted of a sponge-based reservoir for extraction, an integrated battery, a positive temperature coefficient ultrathin heater, temperature control switch, and on-device dried reagents for HDA.

Despite the unique ability for liquid handling and sample processing using multi-dimensional paper devices, the detection of target nucleic acids or amplicons remains an analytical challenge. In comparison to standard solution-based assays, nucleic acid detection using μPADs is of lower sensitivity because of the variable paper composition and potential sample losses during the liquid transportation. As a result, the development for novel signal transduction strategies that are not only sensitive and specific to target nucleic acids in μPAD but are also simple, inexpensive and compatible with field conditions is required.

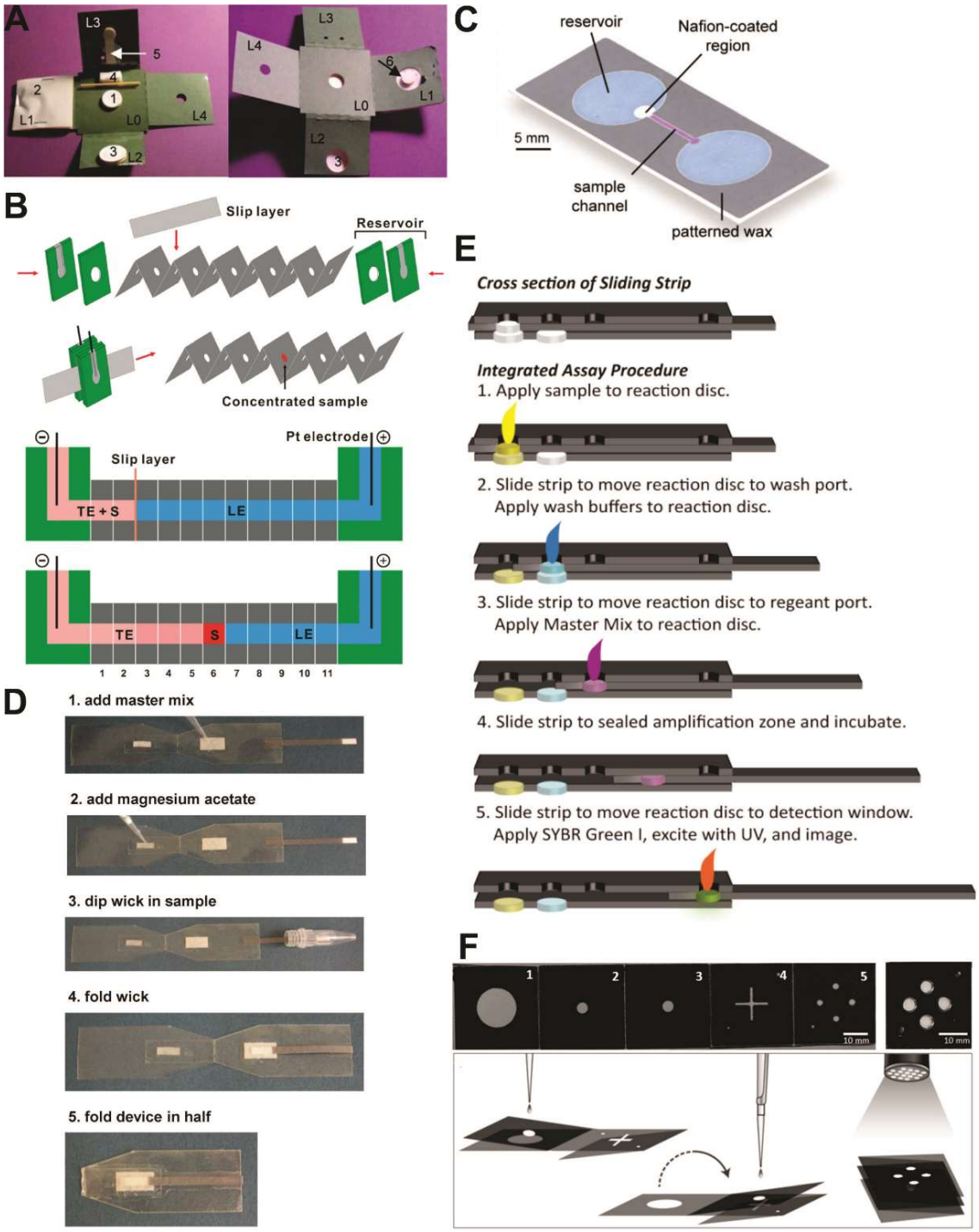

Figure 1.1 Manipulating nucleic acid samples using µPAD. **(A)** Front (left) and back (right) side view of the 3D µPAD (Reprinted with permission from ref [26], Copyright 2012, The Royal Society of Chemistry. **(B)** Multi-layer paper-based ITP platform for nucleic acid concentration (Reprinted with permission from ref [27], Copyright 2015, The Royal Society of Chemistry). **(C)** ICP-µPAD device for DNA preconcentration, separation and detection (Reprinted with permission from ref [28], Copyright 2015, American Chemical Society). **(D)** Schematic illustration of nucleic acid amplification by RPA on paper and plastic device

(Reprinted with permission from ref [30], Copyright 2012, The Royal Society of Chemistry). **(E)** 3D "paper-machine" that integrates DNA extraction, amplification and detection (Reprinted with permission from ref [39], Copyright 2015, American Chemical Society). **(F)** 3D μPAD for detecting nucleic acids from whole blood samples (Reprinted with permission from ref [40], Copyright 2016, Wiley).

1.2.3 Signal Transduction Strategies for Nucleic Acids Detection in μPAD.

Translation of nucleic acids or amplicons into detectable signals in paper-based devices is an important step to ensure sensitive and specificity of a designated NAT. The detection of specific nucleic acid sequences can be achieved by either direct capture through DNA hybridization or through amplification by using sequence specific primers. Colorimetric readout using lateral flow assays and fluorescent readout using DNA intercalating dyes are the two most commonly used signal transduction approaches in μPAD.[43-49] Advanced nucleic acid sensing strategies making use of CRISPR/Cas system[11,16,50], DNA hybridization probes[51-62], DNA nanotechnology[63-66], and synthetic biological approaches[67-68] have also been introduced to μPAD, representing a new trend for designing better paper-based NAT for field applications.

Lateral flow assays. LFAs, such as pregnancy tests, are one of the earliest paper-based immunoassays for POC diagnosis. LFAs can be readily used for NAT by labeling the target nucleic acids with affinity ligands or antigens such as biotin and digoxigenin.[43] The labeling can be achieved through PCR or isothermal amplification, where a set of two primers are labeled with two distinct ligands. In the presence of the target DNA or RNA, the double-stranded amplicon bearing both ligands can be captured at the testing line of LFA the use of a signal reporter such as gold nanoparticle or fluorescent dye is commonly used for subsequent colorimetric or fluorescence readout.[43-45] One caveat of LFA assays is

the potential for a false positive caused by the nonspecific amplification and the dimerization of primers. To address this challenge, Phillips[43] recently introduced a tagged strand displacement probe to LAMP (Figure 1.2 A). This probe was designed to bind to the targeted loop region of the LAMP products by toehold-mediated strand exchange, a reaction that is highly sequence specific due to the thermodynamic penalties of the initiating branch migration. In comparison to a direct labeling of LAMP primers, this probe eliminated false positive test bands in LFA. Using this strategy, Phillips has detected as few as 3.5 *Vibrio cholera* and 2,750 *E. coli* bacteria without any specious correlations.

In addition to modifications of the probs used for nucleic acid detection, the modification of the lateral flow strip surface with complementary DNA probes capable of capturing single-stranded amplicons through DNA hybridization is possible (Figure 1.2 B).[46] As lateral flow strip offers sufficient spatial resolution to position multiple DNA probes, multiplex nucleic acid detection can be achieved on a single LFA device. In addition to serving as a stand along paper-based device for NAT, LFAs have also been adapted to other μPADs to create fully integrated sample-to-answer devices.[38,42] Because of the simplicity, LFA is also an attractive low-cost engineering platform that translates emerging ultrasensitive and specific NAT into field-deployable diagnostic assays. One exciting example is the paper-based SHERLOCK (specific high-sensitivity enzymatic reporter unlocking) assay for the detection of Zika and Dengue viruses and gene mutations in clinical samples.[11,16,50] SHERLOCK is a novel nucleic acid detection platform which combines isothermal preamplification with Cas13 to detect single molecules of RNA or DNA.[11] Gootenberg in addition to SHERLOCK has introduced the second generation of SHERLOCK (SHERLOCKv2), where multiplexed detection could be achieved by using

four orthogonal CRISPR enzymes (LwaCas13a, CcaCas13b, PsmCas13b, and Cas12a) that preferentially cleave certain dinucleotide combinations when CRISPER RNA binds to its target.[50] By further engineering the cleavage substrates, commercially available LFAs can be used as readout for the SHERLOCKv2 assay. As shown in Figure 1.2 C, virus RNAs were first extracted from the clinical sample and then pre-amplified using RPA to accumulate the targets that trigger the collateral activities of Cas proteins through the binding to the CRISPR RNA. The substrate was designed to contain biotin at one end and FAM at the other end. As the lateral flow strip contained a streptavidin-modified control line and a protein A modified test line, abundant reporters accumulated anti-FAM antibody-gold nanoparticle conjugates at the control line. In the presence of the target nucleic acids, the cleavage of the reporter using the CRISPR-Cas machine reduced accumulation at the control line and result in signal on the test line. The paper-based SHERLOCK assay allowed the instrument-free detection of Zika virus (ZIKV) or dengue virus (DENV) ssRNA at 2 aM detection limit within 90 min.[16] Moreover, this paper-based detection system is also sensitive to single nucleotide mutations, which has been demonstrated by the detection of mutations in liquid biopsies of non-small cell lung cancer patients.[50]

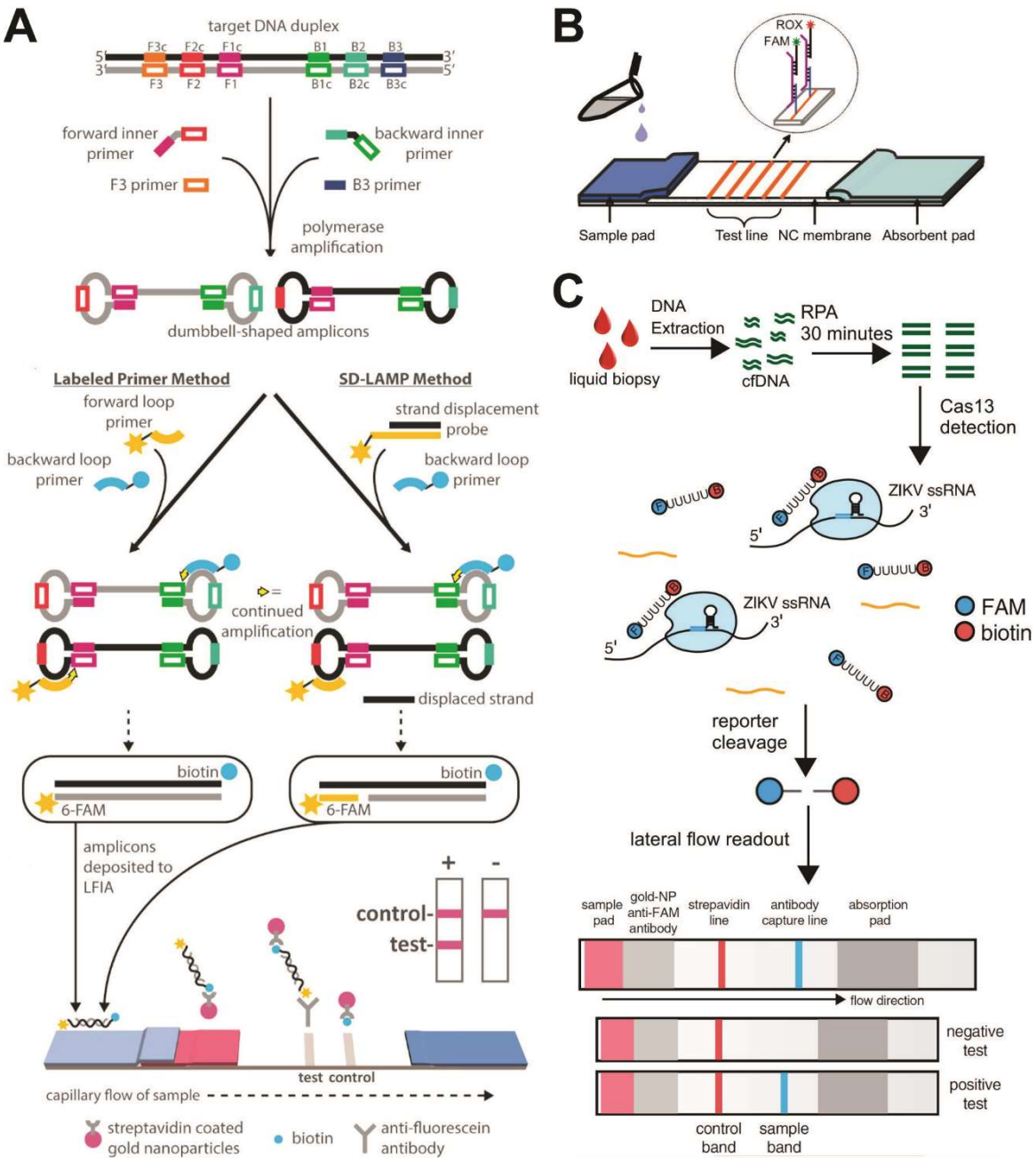

Figure 1.2 Nucleic acid detection by lateral flow strip. **(A)** Strategies for the detection of LAMP products using LFA (Reprinted with permission from ref [43], Copyright 2018, American Chemical Society). **(B)** Multiplexed detection of nucleic acids by capturing multiple DNA amplicons on a single lateral flow strip through hybridization (Reprinted with permission from ref [46], Copyright 2014, American Chemical Society). **(C)** Schematic illustration of a typical work flow of SHERLOCKv2 assay with LFA as a paper-based readout (Reprinted with permission from ref [50], Copyright 2018 American Association for the Advancement of Science).

Intercalating dyes. Despite the wide application to NAT, LFAs are generally qualitative and requiring additional modifications to the primers. To further push the quantification capacity and simplify the assay protocol, fluorogenic DNA intercalating dyes have been widely used in μPAD. Fluorogenic DNA intercalating dyes are the workhorses in biochemical laboratories for nucleic acid staining and quantification. Because of the strong intramolecular quenching, these dyes possess no or very low fluorescence in solution.[47-48] However, the binding of such dyes to nucleic acids or amplicons limits the self-quenching and thus turns on the fluorescence. As no labeling or washing steps are required, it is not surprising that intercalating dyes are one of the most widely used signal readout strategies in μPAD when nucleic acid amplification is involved. However, to facilitate the in-device visual detection of nucleic acids, an UV lamp or light box is required. To eliminate the need for external light sources, Roy[49] explored the visual, colorimetric detection of LAMP amplicons in μPAD using a chromogenic DNA intercalator, crystal violet (CV). CV is violet in color, however, can be converted into leuco crystal violet (LCV) in the presence of sodium sulfite. The binding of CV to dsDNA can effectively prevent this color transition and change the colorless LCV to the violet CV, allowing the colorimetric sensing of Sus scrofa (porcine) gene and Bacillus subtilis gene in paper. To fulfill the quantification capacity, tedious data extraction and analysis steps are required using imaging software (*e.g.,* ImageJ) after collecting the data using a digital camera.

Hybridization probes. Short synthetic DNA probes that are complementary to the target ssDNA or RNA are one of the most powerful approaches for the sequence-specific detection of nucleic acids. When combining with μPAD, a typical design involves the modification of the paper substrate with a capture DNA probe and the labeling of the target

with a detection DNA probe.[51-61] The sandwiched binding complex can then be detected through the detection DNA probe that is attached with an enzyme, a fluorescent dye, or a nanoparticle.[51-54] More advanced optical or electrochemical detection platforms have also been introduced to μPAD by further modifying the capture probes within the paper substrates with luminescent nanomaterials or microelectrodes or engineering the detection probes with advanced DNA nanotechnology approaches.[56-64] For example, Noor[55-56] has developed a series of paper-based solid-phase nucleic acid hybridization assays by chemically immobilizing quantum dots (QDs) as donors to enable fluorescence resonance energy transfer (FRET) assays (Figure 1.3 A). Comparing to conventional uses of QDs as passive fluorescent labels, the paper-based solid-phase FRET assays show several advantages, including the rapid hybridization kinetics (< 2 min), low detection limit (~ 300 fmol), and high multiplexity. The same group also explored the immobilization of upconverting nanoparticles (UCNPs) as energy donors that allowed the luminescence resonance energy transfer (LRET) on paper, where QDs could be used as sensitive fluorescence readout.[57-58] The paper-based FRET assay is also readily compatible with isothermal DNA amplification.[56] When integrating with HDA, Noor has detected as low as zeptomoles of target nucleic acids.

Electrochemical readout is also attractive for paper-based NAT, as microelectrodes can be easily printed on paper and the whole device can be miniaturized for field applications.[59-61] To achieve this goal, synthetic DNA probes modified with electrochemical labels have been used for the detection of specific sequences in μPADs. For example, Li[61] described a 3D paper-based electrochemical sensor called *o*slip-DNA (*o* stands for origami) for the detection of HBV. As shown in Figure 1.3 B, the device was

fabricated by first patterning channels using wax-printing on chromatographic paper and then removing the paper using razor blade to create hollow channels. The three electrodes were then added by stencil printing. To operate the *o*slip-DNA, one-step sample incubation was used to capture DNA-functionalized silver nanoparticles (AgNPs) onto DNA-functionalized magnetic microparticles (MμBs) through the target DNA. After washing the unbound AgNPs, the mixture was loaded to the inlet of the oslip-DNA and MμBs carrying AgNPs were captured directly at the working electrode by using a small rare-earth magnet. Once capturing the MμBs, the slip layer was pulled to a functional position, which resulted in the release of a strong oxidant ($KMnO_4$). $KMnO_4$ rapidly oxidized AgNPs and released large amounts of Ag^+ ions. The Ag^+ was then electrochemically deposited onto the working electrode and quantified using anodic stripping voltammetry (ASV). As the overall cost was estimated to be 0.36 USD and the detection of HBV-specific nucleic acids could be done within 5 min, this device holds good potential for field-based NAT, such as POC diagnosis. The detection limit of this device was 85 pM, suggesting a nucleic amplification step might be necessary to push the detection limit to the clinically relevant levels.

Beside designing and crafting new μPADs, it is also possible to engineer standard pregnancy test strips as readout for NAT using the concept and strategies in dynamic DNA nanotechnology. Du[15] introduced this idea, where human chorionic gonadotropin (hCG) was used as a label for DNA hybridization probes (Figure 1.3 C). The hCG-DNA probe was then designed to hybridize to LAMP products through a toehold-mediated strand displacement. When loaded onto the pregnancy test strip, the resulting hCG-LAMP complexes were too large to migrate and thus generated an "off" signal. An alternative "turn-on" assay was also designed, where hCG-DNA was released from a bulky three-way

junction reporter through a toehold-mediated strand displacement with the LAMP products. Using this assay, as few as 20 copies of Ebola virus templates could be detected in both human serum and saliva using a commercially available pregnancy test strip. Moreover, this assay could also be adapted to distinguish a common melanoma-associated SNP allele from the wild-type sequence. In addition to the toehold-mediated strand displacement reactions[15, 62], more advanced concept and strategies of the emerging DNA nanotechnology such as catalytic hairpin assemblies and hybridization chain reactions have also been integrated with μPADs as isothermal and enzyme-free signal amplifiers to enhance the analytical performance of paper-based NATs.[63-64]

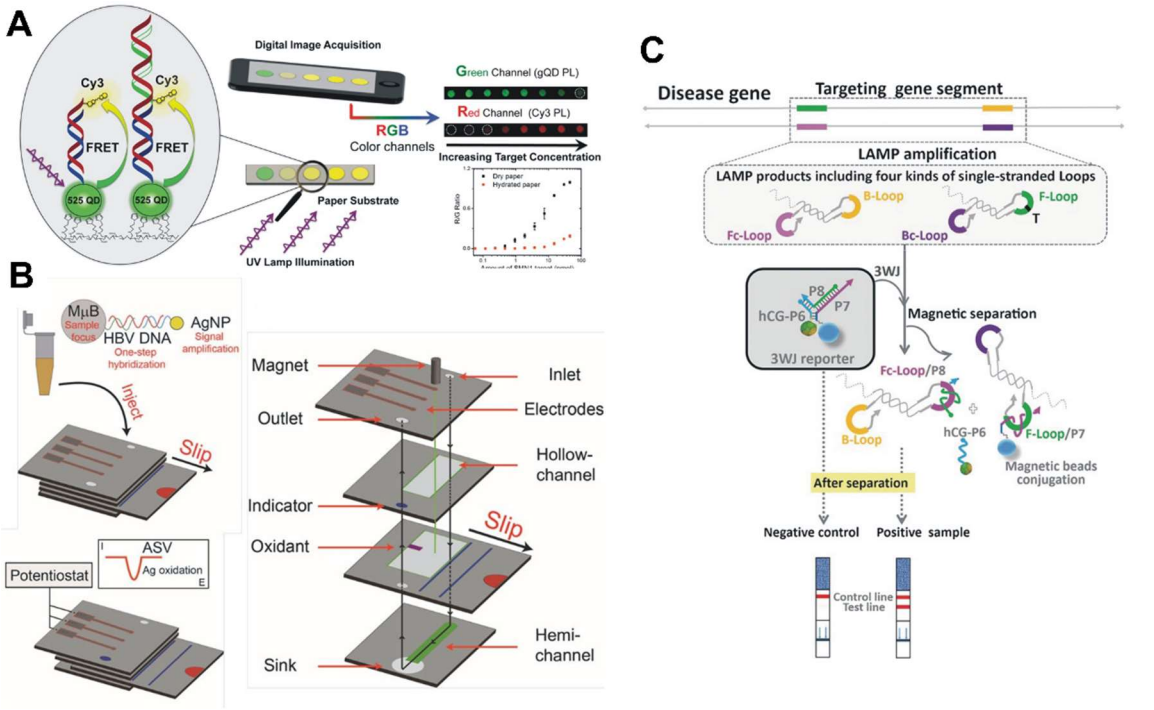

Figure 1.3 Different nucleic acid signal readout strategies on paper-based devices. **(A)** FRET-based DNA detection using quantum dot-modified paper device (Reprinted with permission from ref [56], Copyright 2014, American Chemical Society). **(B)** Electrochemical detection of HBV DNA using 3D *o*slip-DNA (Reprinted with permission from ref [61], Copyright 2015, American Chemical Society). **(C)** Method for the detection of LAMP product using a pregnancy test strip (Reprinted with permission from ref [15], Copyright 2017,

Wiley).

Synthetic biology approaches. Recent advances in the field of synthetic biology have yield several powerful synthetic gene networks capable of sensing the surrounding environment and generating a measurable output.[12, 65-66] One intriguing question is that can such powerful synthetic biological system be integrated into μPAD to create low-cost field-deployable NAT for diagnosis at resource-limited environments. To achieve this goal, two impactful synthetic biological approaches were developed by Green[65] and Pardee[66], including toehold switches and paper-based synthetic gene network. Toehold switches are a class of de-novo-designed prokaryotic riboregulators that activate gene expression in response to cognate RNAs with arbitrary sequences (Figure 1.4 A).[65] This system is composed of two RNA strands: the switch and the trigger. The switch RNA contains the coding sequence of the gene that is regulated by an upstream hairpin-based processing module containing both a strong ribosome binding site (RBS) and a start codon. The trigger RNA (the target) can hybridize to the hairpin through a toehold-mediated strand displacement reaction and expose the RBS and start codon, thereby initiating translation of the gene of interest. The system was designed such that the trigger RNA did not possess complementary bases to the RBS or the start codon and thus could be generalized as a sensor for any target nucleic acids. To further enable the use of toehold switches in μPAD. The same group also developed the paper-based synthetic gene network that was achieved by freeze drying cell-free biological components into paper to create materials with the fundamental transcription and translation properties of a cell (Figure 1.4 B).[66] These cell-like papers are stable at room temperature and can be activated by simply adding water. The on-paper colorimetric or fluorescent readout can be readily achieved by embedding

mRNAs for expression chromogenic enzymes such as LacZ or fluorescent proteins. By further integrating the paper-based protein expression system with mRNA sensors operated by toehold switches, the author has developed a panel of 24 sensors that could distinguish between the Sudan and Zaire strains of the Ebola virus (Figure 1.4 C). The same system has also been applied to the in-field diagnosis of ZIKV with clinically relevant sensitivity.[12] To do so, an isothermal RNA amplification technique known as NASBA (nucleic acid sequence-based amplification) was used to amplify and accumulate the trigger RNAs for the subsequent toehold switch reactions on paper (Figure 1.4 D). In a typical workflow, ZIKV RNAs were directly collected from serum or salvia samples and amplified using NASBA. The reaction mixture was then loaded onto the paper disk to rehydrate the reagents for the expression of the enzyme LacZ capable of converting the yellow chlorophenol red-b-D-galactopyranoside into the purple chlorophenol red on paper. The authors also combined NASBA with a CRISPR/Cas9 module that selectively cleaves the target DNA sequence possessing a PAM domain, which allowed the discrimination between American and African ZIKV.

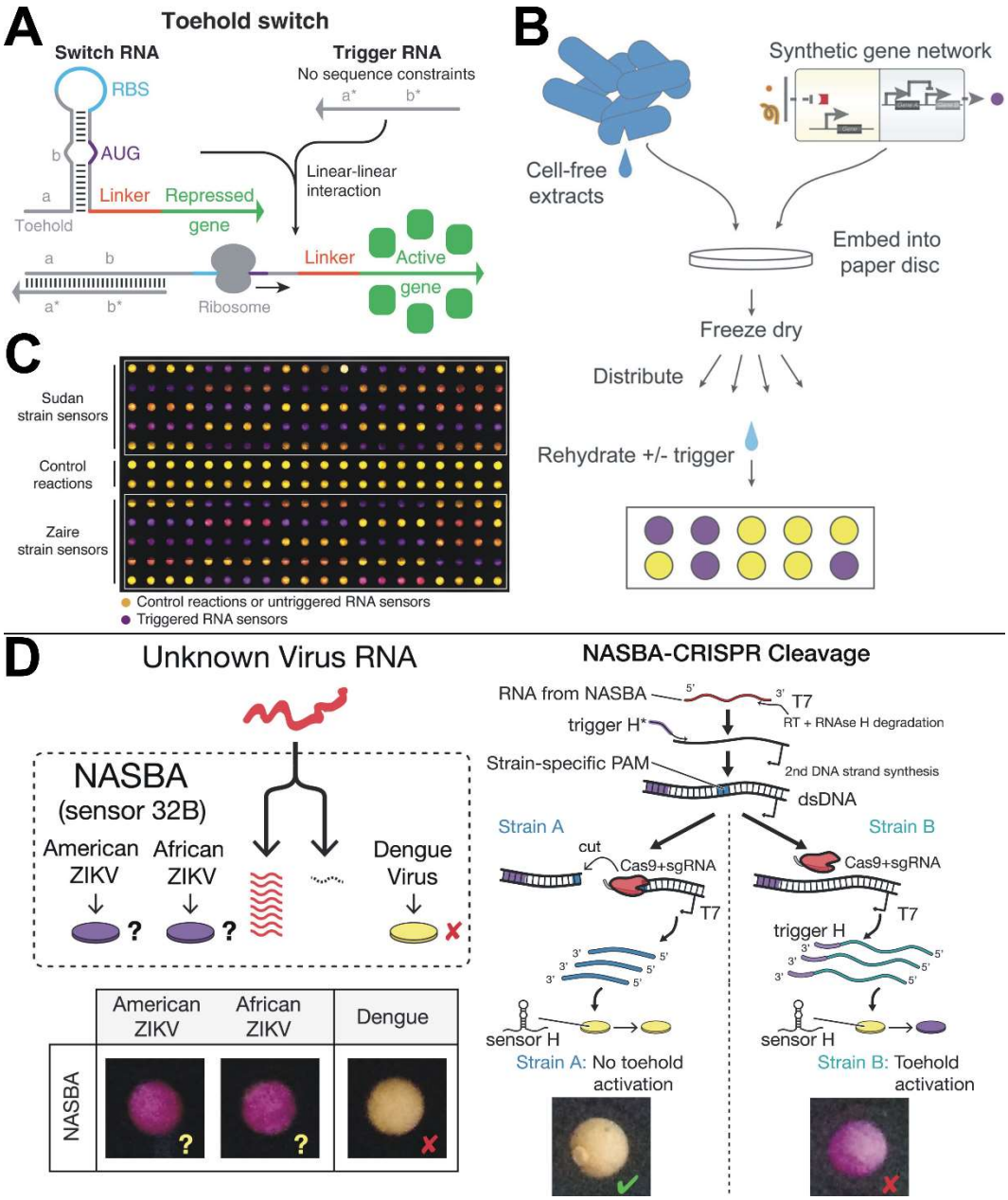

Figure 1.4 Synthetic biology approaches on paper-based devices. (**A)** Schematic illustration the concept of toehold switches (Reprinted with permission from ref [65], Copyright 2014 ELSEVIER). (**B)** Preparation and activation of paper-based synthetic gene network (Reprinted with permission from ref [66], Copyright 2014 ELSEVIER). (**C)** Diagnosis of Ebola viruses using a panel of paper-based synthetic biologic sensors (Reprinted with permission from ref [66], Copyright 2014 ELSEVIER). **(D)** In-field diagnosis of ZIKV and stain discrimination using NASBA and NASBA-CRISPER Cleavage assays (Reprinted with permission from ref [12], Copyright 2016 ELSEVIER）.

Chapter 2

Development of Quantitative Paper-Based DNA Reader (qPDR) for Distance-Based Quantification of Nucleic Acids

Contribution statement.

The contents of Chapter 2 section 2.1, 2.2.1 to 2.2.6, and 2.3 were modified from published paper "Paper-Based DNA Reader for Visualized Quantification of Soil-Transmitted Helminth Infections". [69] Reprinted with permission from Wang, A. G.; Dong, T.; Mansour, H.; Matamoros, G.; Sanchez, A. L.; Li, F., based DNA reader for visualized quantification of soil-transmitted helminth infections. *ACS Sens.* **2018**, 3, 205-210. Copyright 2018 American chemical Society.

Alex Guan Wang and I contributed equally on this paper. I have participated all experiments throughout the project, including device fabrication, experimental design, and data analyses.

2.1 Introduction.

Since first being introduced by Martinez in 2007, microfluidic paper-based analytical devices have found wide application in the detection of nucleic acids, proteins, small molecules, and metal ions in field-based settings. [21, 39, 70-71] While much attention has been focused on the design and fabrication of novel μPADs for flexible fluidic controls, it is also critical to develop signal readout strategies that are compatible with μPADs. [61, 72] As suggested by the World Health Organization, an ideal POC diagnostic tool for the

developing world should be “reader-free”, raising a key technical question on how to directly generate the digital readout without the need for electrical domains.[73] Recent efforts toward this challenge have revealed three types of physical readouts that are “digital” and thus are countable, including time[73-74], distance[75-76], and the number of colored segments.[77] This chapter is focused on the development of distance-based quantification method on μPAD.

During preliminary tests, the unique chromatographic behaviour of DNA and the fluorogenic DNA intercalation dye SYBR Green I (SG) on cellulose paper has been discovered by our group. This new-discovered chromatographic behaviour was incorporated into my paper-based device, termed quantitative paper-based DNA reader (qPDR). The qPDR translated the conventional fluorescence-based nucleic acid quantification into the measurement of distance as a readout. In this work, The chromatographic behavior of SG in qPDR was systematically studied with the aim to obtain the optimal experimental conditions for using qPDR. The practical applicability of qPDR to clinical samples was demonstrated by detecting nucleic acid samples of soil-transmitted helminth (STH) worms from Honduras. Beside the nucleic acid quantification, the ability of quantifying mercury ion (Hg^{2+}) on qPDR was demonstrated through the combination of functional nucleic acids and qPDR.

2.2 Result and Discussion.

2.2.1 Device Fabrication and Assay Principle.

As illustrated in Scheme 2.1 A and experimental section 5.1.2, qPDR containing a sample loading zone and a linear test zone was fabricated using a well-established wax

printing technique on cellulose paper. The thermometer shaped wax pattern consists of a round sample loading zone and a bar shape test zone with a distance mark (2mm spacing between each) and was printed onto a unmodified sheet of cellulose paper (Whatman No.1). The patterned paper was stacked onto a glass slide using paraffin wax to seal the bottom.

The mechanism of qPDR for nucleic acid analysis is on the basis of the unique interfacial interactions of SG with unmodified cellulose on the chromatographic paper. SG was found to be strongly retained by the cellulose matrix and was localized at the sample loading zone in the absence of DNA or in the presence of ssDNA (Scheme 2.1 B). SG can be effectively eluted into the testing zone by dsDNA because of the strong binding affinity between dsDNA and SG.

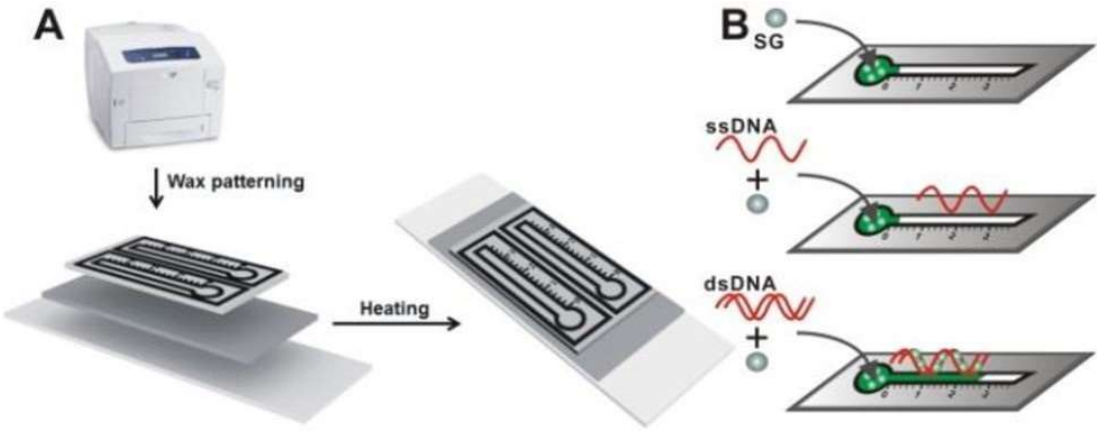

Scheme 2.1 Schematic Illustration of the Fabrication Process **(A)** and the Assay Principle **(B)** of qPDR. Reprinted with permission from Wang, A. G.; Dong, T.; Mansour, H.; Matamoros, G.; Sanchez, A. L.; Li, F., based DNA reader for visualized quantification of soil-transmitted helminth infections. ACS Sens. **2018**, 3, 205-210. Copyright 2018 American chemical Society.

To quantitatively study the distribution of SG throughout the qPDR device, it is also possible to convert the distribution of SG in the test zone into a chromatogram by taking digital photos (Figure 2.1). SG possesses green fluoresces and under goes

illumination by blue/UV light, next a picture of the qPDR device was taken and digitally enhanced where the green channel was separated out from original RGB picture to enhance the sensitivity (Figure 2.1 A and B). All pixels in green channel can be measured by greyscale which the value of each pixel only represents an amount of light. The 1.0mm* 30.0mm test zone of the green channel was chosen and digitalized into 20*600 pixels with a resolution of 50 μm per pixel by using free software ImageJ (Figure 2.1 C). The greyscale intensity was further processed by data normalization to reduce experimental error and improve data integrity. The equation used to convert greyscale intensity into % greyscale intensity is shown in equation 1.

$$\% \text{ greyscale intensity} = (X\text{-Min})/(255\text{-Min}) * 100\% \qquad \text{(equation. 1)}$$

X represents the value of average greyscale intensity of 20 pixels in each row of the selected test zone, Min represents the smallest average greyscale intensity from each row, and a value of 255 was used as the maximum value of the greyscale intensity.

The normalized greyscale intensity of pixels in each row of test channel versus the retention distance (d_R) was plotted into a chromatogram and a threshold of 15% was set for the measured retention distance (figure 2.1 D). A threshold of 15% was selected because the sensitivity matches that of the naked eye (details in Table 5.2 in experimental section).

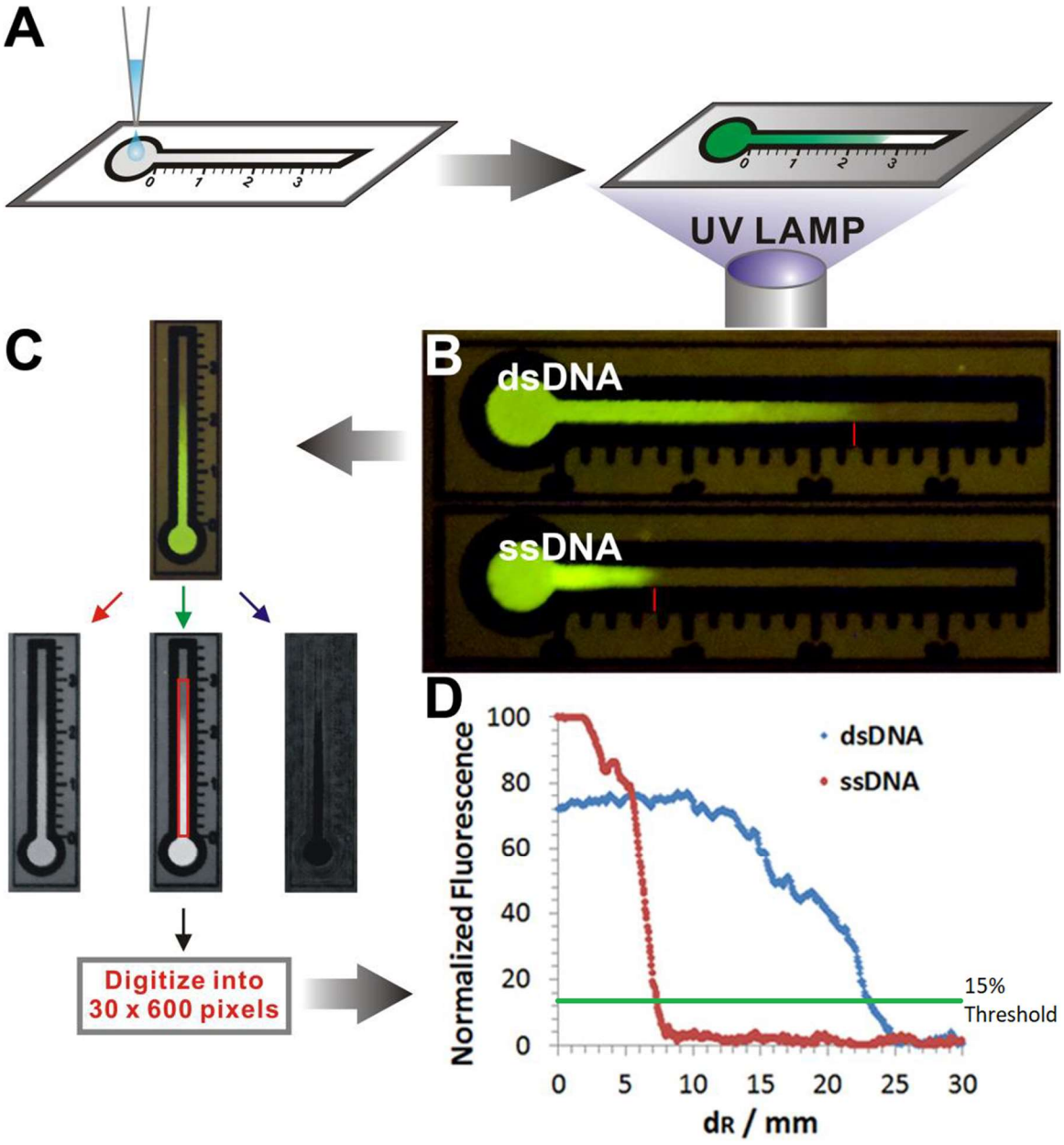

Figure 2.1 Procedures of converting an image of DNA quantification on qPDR into a chromatogram. **(A)** Schematic illustration of the procedure for sample loading and data collection using qPDR. **(B)** Typical fluorescent images of dsDNA/ssDNA-SG binding complexes captured using a smartphone camera. **(C)** Procedure for splitting color channels and digitizing the image using ImageJ. **(D)** Typical chromatograms of DNA-SG complexes extracted from the fluorescence images. The green line indicates the 15% threshold on the chromatogram. Reprinted with permission from Wang, A. G.; Dong, T.; Mansour, H.; Matamoros, G.; Sanchez, A. L.; Li, F., based DNA reader for visualized quantification of soil-transmitted helminth infections. ACS Sens. **2018,** 3, 205-210. Copyright 2018 American chemical Society.

2.2.2 Chromatography Behavior of Nucleic Acid and SG on qPDR.

qPDR operates in a similar manner compared to classic paper chromatography, in that classic paper chromatography is based on polarity and qPDR is based on the intramolecular interaction between the analyte (mobile phase) and the cellulose matrix (stationary phase). The eluting strength of a solvent is a measure of how long the solvent or reagent can elute the SG into the test channel on qPDR. The weak elution strength of aqueous solutions was examined by the strong retention of SG at the loading zone upon the addition of sample (Figure 2.2 A). In figure 2.2 A, the retention distance of SG remained less than 6 mm when the loading solution reached 28mm wicking distance. Use of an organic solvents such as DMSO was found to increase the elution strength (Figure 2.2 B, right). The low elution strength by aqueous solution and high elution strength by organic solvent confirmed the chromatographic nature of qPDR (Figure 2.2 C). The retention distance (d_R) was quantitatively determined by elution strengths which was adjusted by mixing aqueous and organic solvents in different ratios (Figure 2.2 D). The intercalation of SG and dsDNA offered an alternative way to adjust the elution strength of the mobile phase when using qPDR (Figure 2.2 E and F). The d_R was determined quantitatively by the concentration of dsDNA (Figure 2.2 G). The elution strength of high concentrations of ssDNA (500 nM) was found to be the same as the blank (Figure 2.2 F). When examining the fluorescence of SG- cellulose compared to SG in solution when plated on a glass slide (Figure 2.2 H). The magnitude of the fluorescence enhancement was found to be equivalent to that of the maximal concentrations of dsDNA (Figure 2.2 A and E).

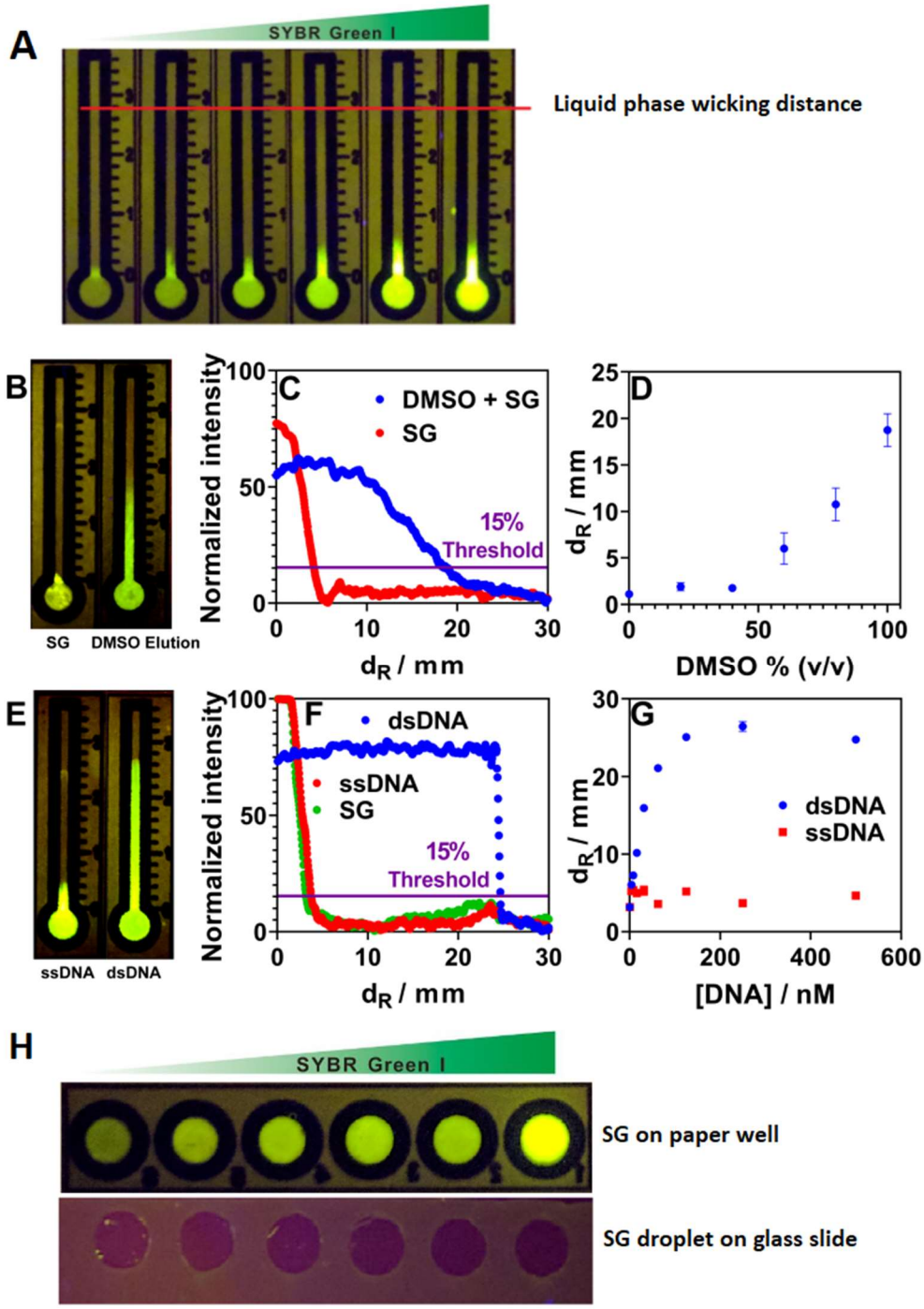

Figure 2.2 Chromatography behaviors of SG on qPDR. (**A**) Retention distances of varying concentrations of SG from 1.25 μM to 40.0 μM on qPDR. The red line indicated the solution wicking edge on qPDR. Reprinted with permission from Wang, A. G.; Dong, T.; Mansour, H.; Matamoros, G.; Sanchez, A. L.; Li, F., based DNA reader for visualized quantification of soil-transmitted helminth infections. ACS Sens. **2018,** 3, 205-210. Copyright 2018 American chemical Society. (**B**) A representative photo of 20 μM SG

eluted by water (left) and DMSO (right) in qPDR. (**C**) Chromatograms were constructed by extracting greyscale intensity of each pixel in the photo. dR was then determined by setting a threshold at 15% of the normalized intensity. (**D**) dR was plotted as a function of concentrations of DMSO. (**E**) A representative photo of 20 μM SG eluted by 500nM ssDNA (left) and 500nM dsDNA (right). (**F**) Chromatograms were constructed by extracting greyscale intensity of each pixel in the photo. dR was then determined by setting a threshold at 15% of the normalized intensity. (**G**) dR was plotted as a function dsDNA (or ssDNA) with concentrations ranging from 0 to 500nM. Each error bar represents one standard deviation from triplicate analyses. (**H**) Fluorescence of varying concentrations of SG from 0.625 μM to 20.0 μM on paper well and on glass slide.

2.2.3 Effects of SG and Other Auxiliary Reagents on DNA Quantification Using qPDR.

Effects of SG Concentration on DNA Quantification.

Since we are using the unique binding property of SG on cellulose paper as the key sensing mechanism, the concentration of SG was thought to play a critical role in maximizing the analytical performance of qPDR. First, the enhanced fluorescence of SG on cellulose depends on the concentration of SG. We found that as long as the SG concentration is higher than 10 μM, its distribution throughout qPDR can be clearly visualized upon blue light (490 nm) irradiation (Figure 2.3). Second, the migration distance of SG was also found to be affected by SG concentration. Increasing the SG concentration from 1.25 μM to 20 μM increases the dR of SG from 16.0 mm to 22.0 mm in the presence of 500 nM dsDNA (Figure 2.3). Further increasing SG concentration to 40 μM showed no significant change on retention distance of both dsDNA-SG and ssDNA-SG on qPDR. So the concentration of SG was set to 20 μM for the nucleic acid quantification assay on qPDR.

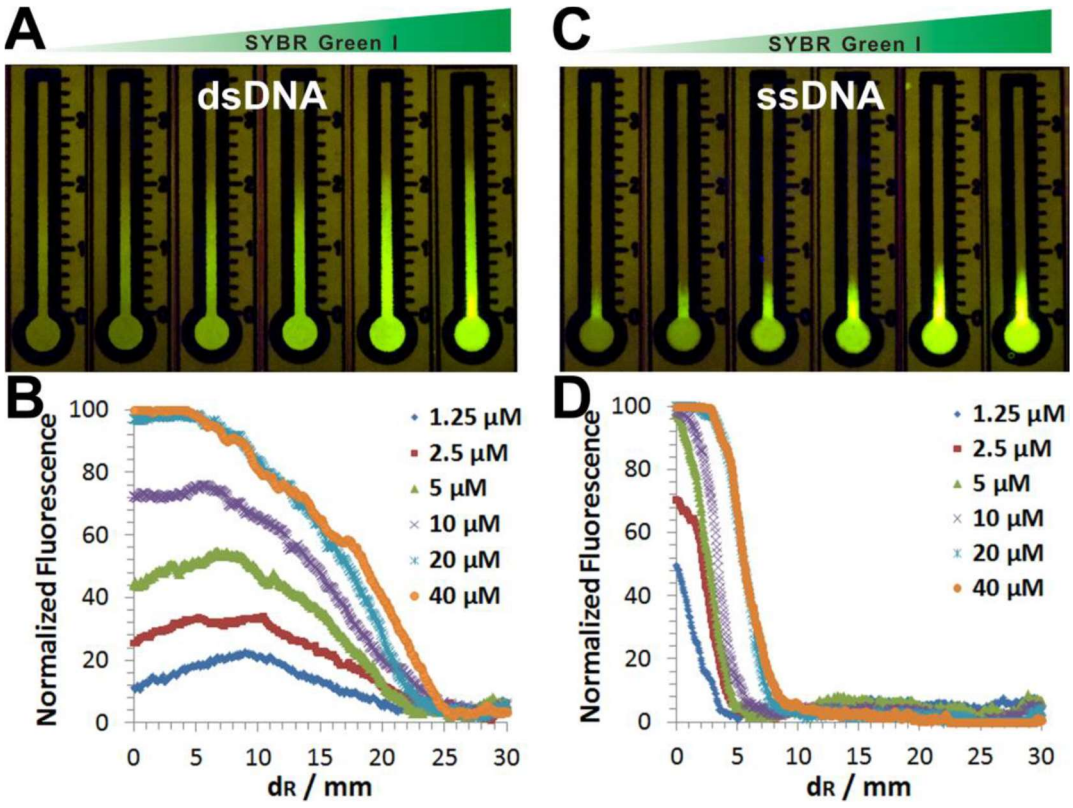

Figure 2.3 Effect of SG concentrations on the quantification of dsDNA and the background (ssDNA). Varying concentrations of SG from 1.25 µM to 40 µM were mixed with 500 nM dsDNA **(A, B)** or 500 nM ssDNA **(C, D)** and then loaded onto qPDR. Chromatograms (B, D) were extracted using ImageJ with the protocol outlined in Section 2.2.1. Reprinted with permission from Wang, A. G.; Dong, T.; Mansour, H.; Matamoros, G.; Sanchez, A. L.; Li, F., based DNA reader for visualized quantification of soil-transmitted helminth infections. ACS Sens. **2018,** 3, 205-210. Copyright 2018 American chemical Society.

Effects of Ionic Strength on DNA Quantification. The effect of ionic strength on the retention and DNA-mediated elution of SG were examined by altering the concentrations of Na^+ (Figure 2.4 A) or Mg^{2+} (Figure 2.4 B) ions. A 50-fold increase in ionic strength led to a two-fold increase in d_R for SG in the absence of DNA. The reduced retention of SG on cellulose suggests that electrostatic interactions play a significant role in retaining SG. DNA has a negatively charged phosphate-deoxyribose backbone that interacts strongly with ions[78]. The increase in ionic strength screens the negative charges of DNA and leads

to a reduction in d_R for dsDNA. This observation suggest that a low ionic strength needs to be maintained to achieve the optimal performance of distance-based DNA quantification using qPDR.

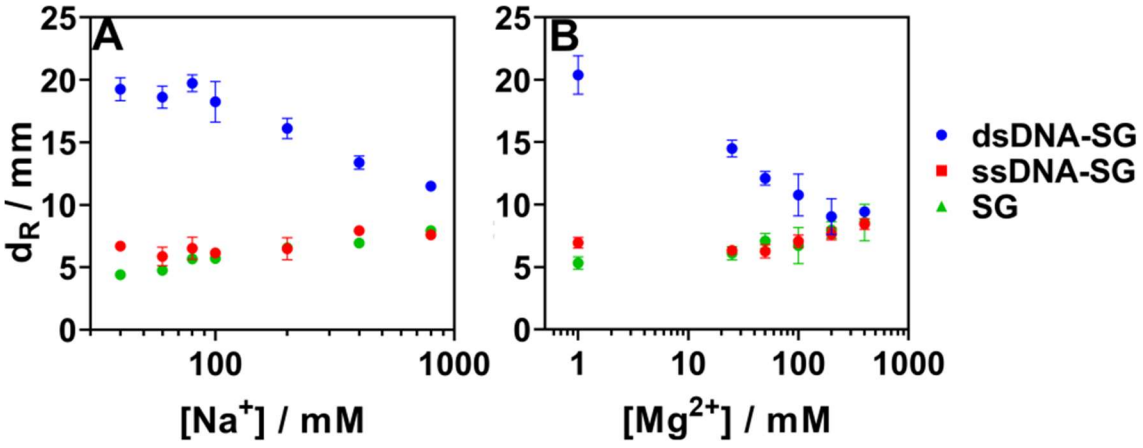

Figure 2.4 Effects of ionic strength on the performance of distance-based quantification of DNA using qPDR. The d_R of 20 μM SG in the presence or absence of 500 nM dsDNA or ssDNA was plotted against varying concentrations of **(A)** 0.1mM to 800mM Na^+, **(B)** 0mM to 400mM Mg^{2+}.

Effects of Urea on DNA Quantification. We next investigated the effect of urea on the analytical performance of qPDR under the assumption that urea may significantly disturb the hydrogen bonding between SG and cellulose. The d_R of SG was found to be doubled in the presence of 4 M urea, suggesting that hydrogen bonding was also involved for retaining SG on cellulose (Figure 2.5 A). The high concentration of urea also disturbs the double-helical structure of dsDNA and thus reduces the elution strength, evidenced by the reduction of d_R in the presence of urea (Figure 2.5B). d_R of SG was found to be doubled in the presence of 4 M urea, suggesting that hydrogen bonding was also involved for retaining SG on cellulose (Figure 2.5 A).

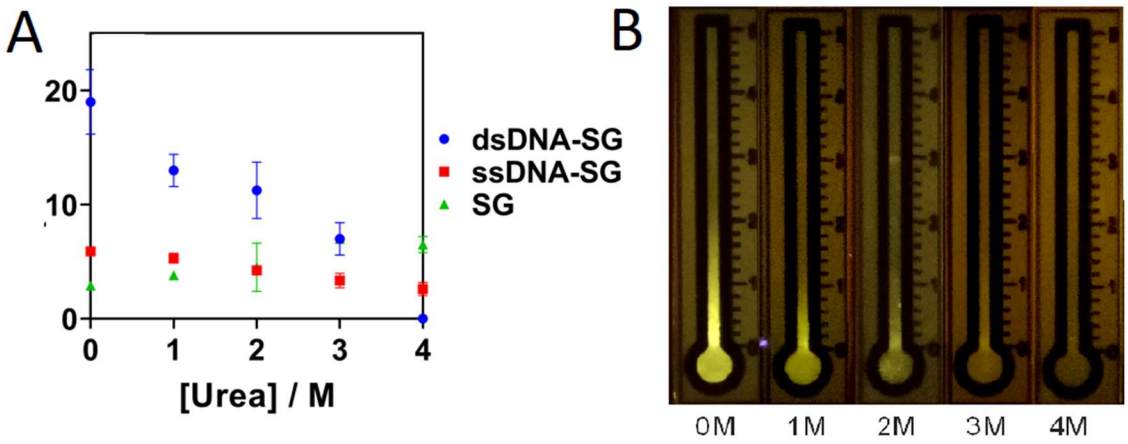

Figure 2.5 Effects of urea on the performance of distance-based quantification of DNA using qPDR. **(A)** The d_R of 20 µM SG in the presence or absence of 500 nM dsDNA or ssDNA was plotted against varying concentrations of urea from 0 to 4M. **(B)** Picture of 20µM SG-I with 500nM dsDNA in vary concentration of urea from 0M to 4M on qPDR.

Effects of Polyethylene Glycol Concentration on DNA Quantification. As dsDNA served as an eluting agent to release SG from the sample loading zone, the adsorption of dsDNA on cellulose would negatively impact the migration distance of dsDNA. The addition of high molecular weight polyethylene glycol (PEG, MW 100 kDa) was found to inhibited the adsorption of dsDNA on cellulose. As shown in Figure 2.7, increasing amount of PEG from 0 to 1 mg/mL effectively enhances d_R of SG in the presence of 500 nM dsDNA by 1.7-fold (Figures 2.6 A, B). The addition of PEG was also found to reduce the d_R of 500 nM ssDNA by a factor of 1.4 (Figure 2.6 C, D). The observed reduction of SG retention distance is likely a result of the increase in the viscosity of the sample solution, which reduced the flow rate and thus allowed the additional time for SG to be adsorbed by the cellulose in sample loading zone. The overall improvement of signal-to-background ratio was near 2.5 times at the optimal PEG concentration of 1 mg/mL. Further increasing

the amount of PEG to 10 mg/mL reduced the flow rate due to the increases in the viscosity and thus resulted in the reduction of d_R for dsDNA (Figure 2.6 A).

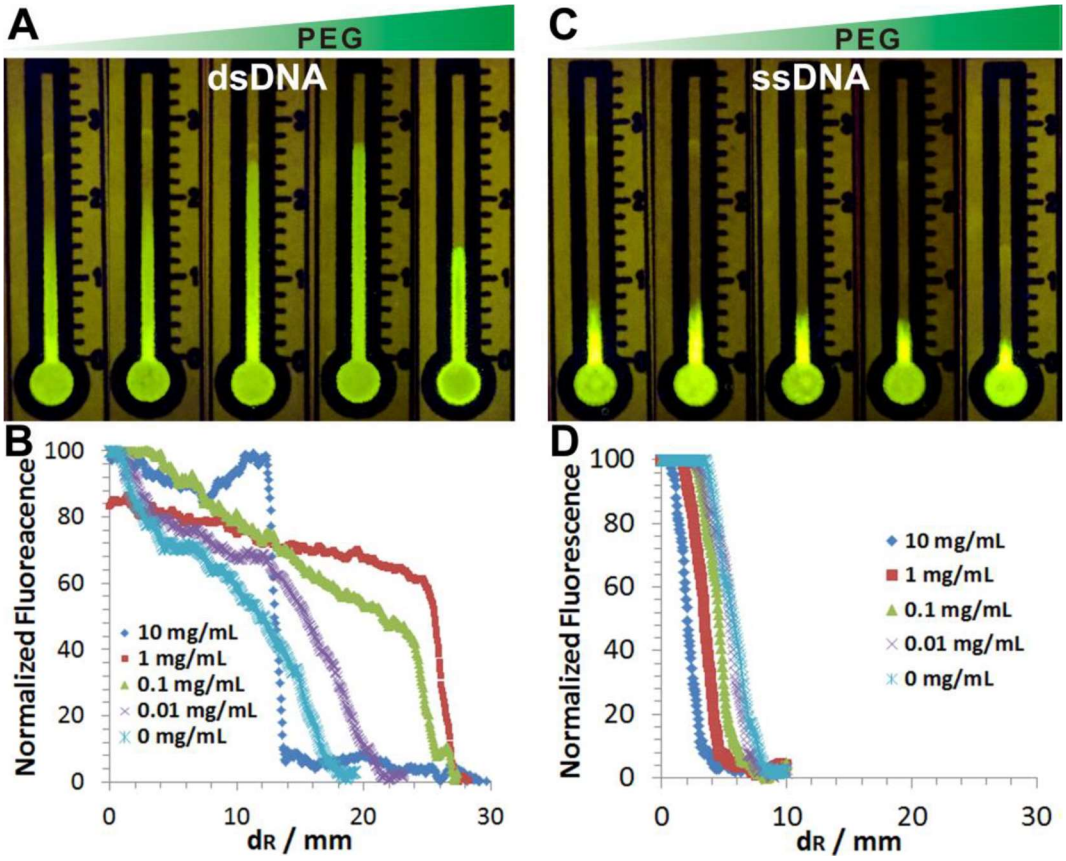

Figure 2.6 Effect of PEG 100,000 on the migration distances of SG I in the presence of 500 nM dsDNA and 500 nM ssDNA. Varying concentrations of PEG from 0 to 10 mg/mL were mixed with 20 μM SG I and 500 nM dsDNA **(A, B)** or 500 nM ssDNA **(C, D),** and then loaded into the paper device. Chromatograms (B, D) were extracted using ImageJ with the protocol outlined in previous Section 2.2.1. Reprinted with permission from Wang, A. G.; Dong, T.; Mansour, H.; Matamoros, G.; Sanchez, A. L.; Li, F., based DNA reader for visualized quantification of soil-transmitted helminth infections. ACS Sens. **2018,** 3, 205-210. Copyright 2018 American chemical Society.

Effects of Surfactants on DNA Quantification. As surfactant may help reduce the nonspecific adsorption of both SG and DNA on cellulose, the effects of three surfactants, TWEEN-20, CTAB, and SDS on the performance of qPDR was investigated. The addition of the non-ionic surfactant TWEEN-20 was found to reduced the retention of both SG and

SG-dsDNA complexes on qPDR (Figure 2.7 A). A maximal signal-to-background ratio was observed when fixing the amount of TWEEN-20 to be 0.1% (v/v). The slight decreases in d_R for SG-dsDNA complexes when kept increasing the concentration of TWEEN-20 was a result of increasing in the viscosity of the solution. Low concentrations (< 1 μM) of cationic surfactant CTAB was also found to increased the d_R of dsDNA-SG complex while the d_R of SG remains unchanged (Figure 2.7 B). However, high concentration (> 1 μM) of CTAB significantly reduced the electrostatic forces of dsDNA and led to a reduction of d_R for the SG-dsDNA complex (Figure 2.7 B). The anionic surfactant SDS was found to significantly reduced the elution strength of dsDNA, leading to a reduction of d_R (Figure 2.7 C). A sharp increase in d_R was found to all samples and controls when the concentration of SDS was greater than its critical micelle concentration (Figure 2.7 D), suggesting that the micelle could effectively encapsulate SG and prevent its retention to cellulose. The test of three surfactants suggested that low concentrations of surfactant may help improve analytical performance on qPDR. Non-ionic surfactant TWEEN-20 is the best choice because of its robustness across wide concentration ranges.

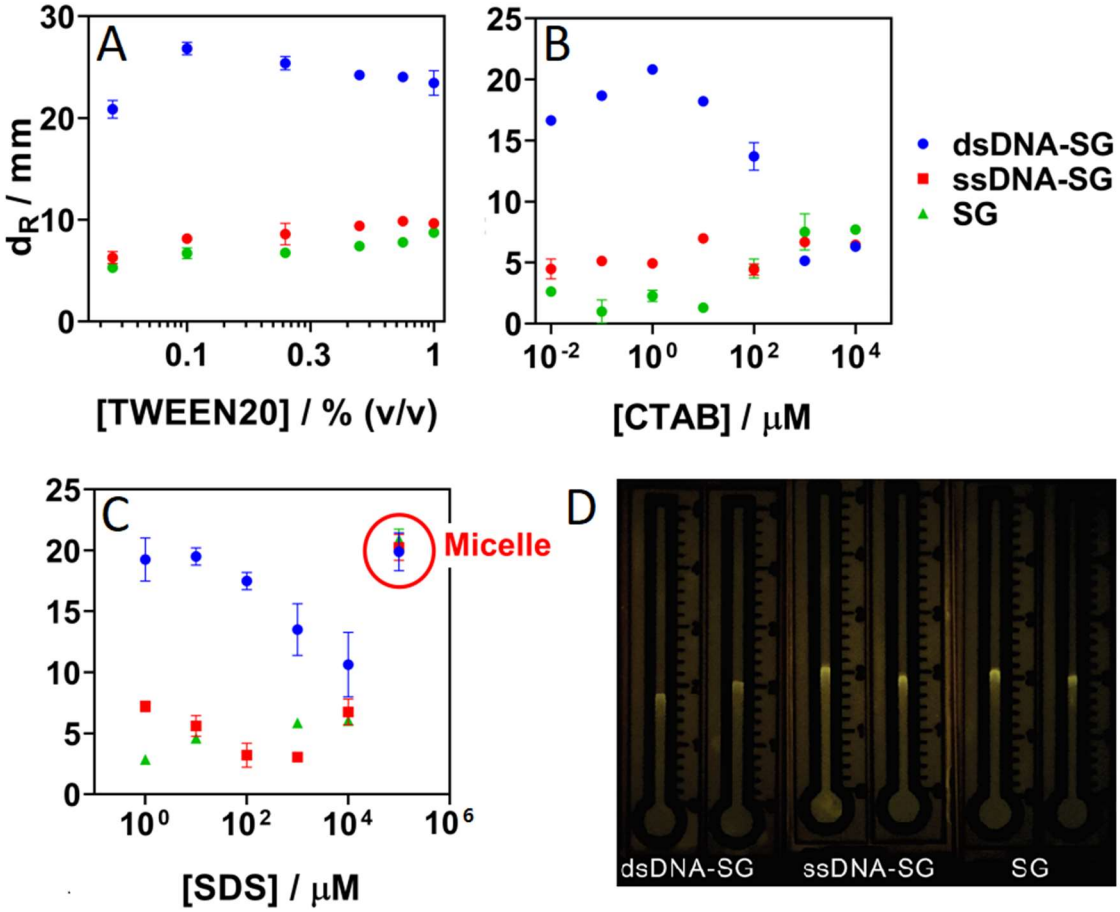

Figure 2.7 Effects of surfactant on the performance of distance-based quantification of DNA using qPDR. The d_R of 20 μM SG in the presence or absence of 500 nM dsDNA or ssDNA was plotted against varying concentrations of **(A)** TWEEN-20, **(B)** CTAB, and **(C)** SDS. **(D)** Picture of SDS micelle encapsulate SG on qPDR and prevent its retention to cellulose when SDS concentration at 10 mM.

2.2.4 Deploying qPDR for NAT.

Figure 2.8 shows a typical test of dsDNA and ssDNA using qPDR. The migration distances (d_R) of SG for dsDNA or ssDNA can be clearly visualized upon irradiating qPDR with a pocket-size blue-light box (Figure 2.8 A). A d_R of 22.0 mm was developed for 500 nM 44-bp dsDNA within 6 min, whereas the d_R for equal concentration of a 44-bp ssDNA was only 4.0 mm (Figure 2.8 B), suggesting that qPDR can effectively differentiate dsDNA over ssDNA. The binding affinity between SG and cellulose is stronger than that between

SG and ssDNA but much weaker than that between SG and dsDNA. Furthermore, the eluent strength of dsDNA is concentration dependent and thus the migration distance of SG in the test zone can be quantitatively determined by the concentrations of the dsDNA, making it possible to quantify dsDNA by simply reading the migration distance of SG in qPDR. This feature is highly useful for distance-based quantification of dsDNA, as the fluorescence intensity of SG is essentially independent of dsDNA. Therefore, it is possible to visualize the distribution of SG within qPDR in the presence of minute amount of dsDNA or in the absence of dsDNA.

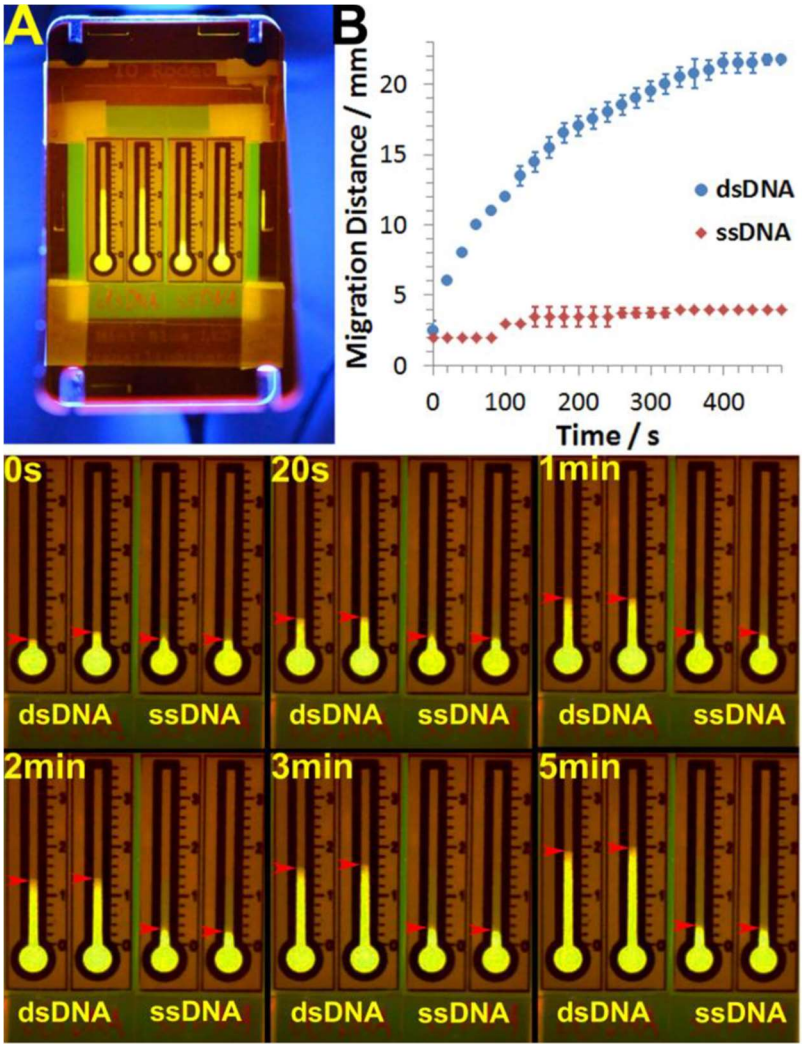

Figure 2.8 Typical distance-based nucleic acid testing using qPDR. **(A)** Typical setup of qPDR for visualized measurement of the migration distance of SG in the presence of 500 nM dsDNA and 500 nM ssDNA**. (B)** Kinetic measurements of SG migration in the test zone of qPDR in the presence of dsDNA and ssDNA. The migration distance for each data point was visually determined by the naked eye at a frequency of one snapshot per 20 s. The error bar represents one standard deviation from duplicated analyses. The bottom figure shows representative snapshots of qPDR in action at 0 s, 20 s, and 1, 2, 3, and 5 min. Reprinted with permission from Wang, A. G.; Dong, T.; Mansour, H.; Matamoros, G.; Sanchez, A. L.; Li, F., based DNA reader for visualized quantification of soil-transmitted helminth infections. ACS Sens. **2018,** 3, 205-210. Copyright 2018 American chemical Society.

Assay Validation Using Synthetic DNA. Having optimized the key assay parameters, we then challenged qPDR with varying concentrations of the 44-bp model DNA. Figure 2.9

shown a concentration dependency between the observed migration distance d_R and the concentration of dsDNA. In this proof-of-principle assay, the dynamic range of dsDNA was 17−63 nM dsDNA and the detection limit was 5 nM (Calculated from linear regression equation obtained from figure 2.9 D). The assay also revealed the high specificity to dsDNA over ssDNA, which was evidenced by the observation that d_R for 500 nM ssDNA was at the same level of a blank. Also, the d_R measured from digital picture (Figure 2.9 B) was identical as the measurement from the naked eye (Figure 2.9 C). This proved the possibility of nucleic acid quantification on qPDR by naked eye without the requirement of external measurement devices.

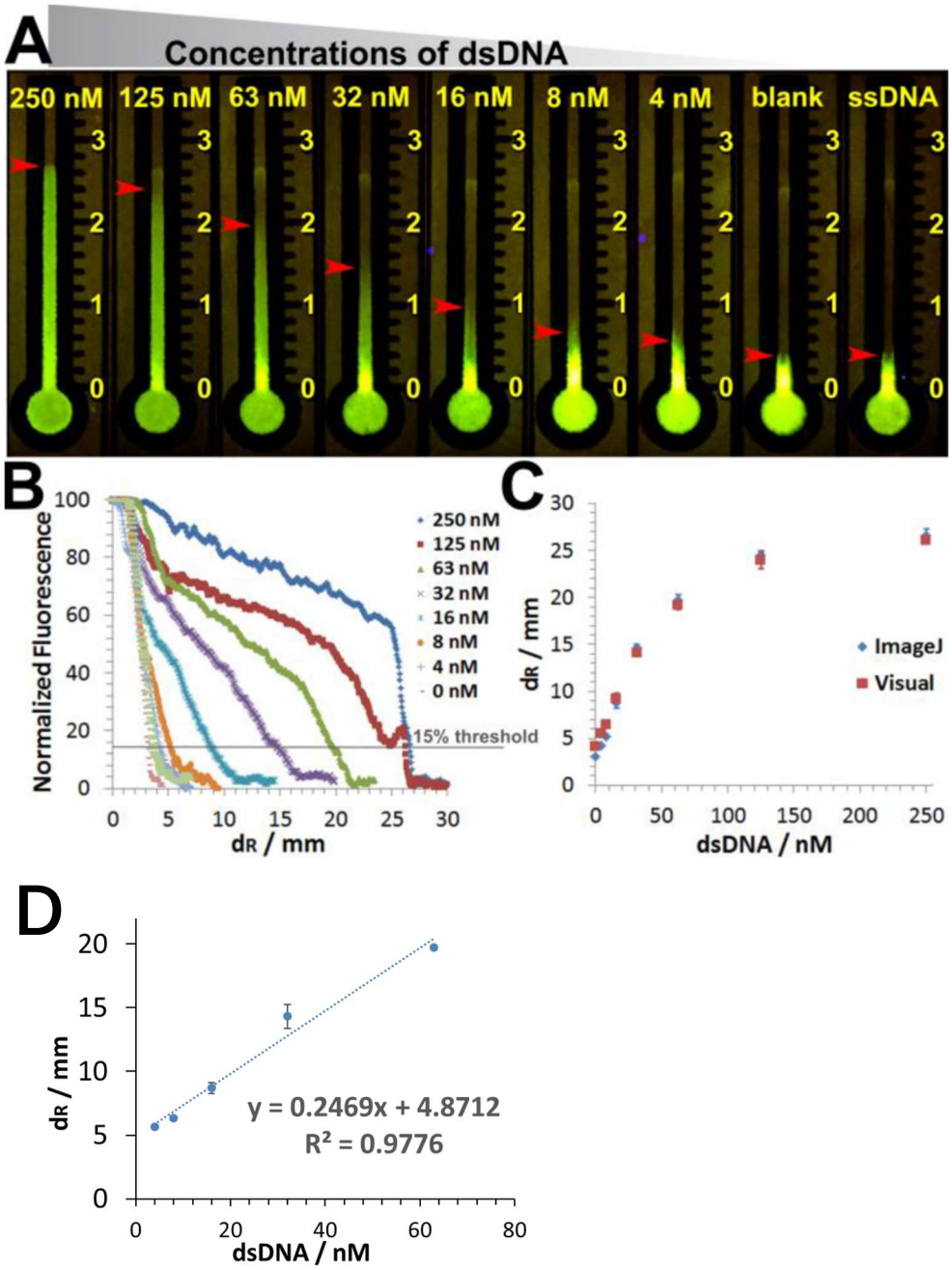

Figure 2.9 Concentration dependency of the retention distance d_R on the concentration of dsDNA. **(A)** Representative images of qPDR loaded with 20 μM SG, 1 mg/mL PEG, and varying concentrations of dsDNA from 4 nM to 250 nM or 500 nM ssDNA. Red bands indicate retention distances determined using visual examination. **(B)** Chromatograms of varying concentrations of dsDNA extracted using ImageJ. **(C)** Retention distance determined either from chromatograms extracted using ImageJ (blue) by direct reading using naked eyes (red) as a function of dsDNA concentrations. Each error bar represents one standard deviation from triplicate analyses. Reprinted with permission from Wang, A.

G.; Dong, T.; Mansour, H.; Matamoros, G.; Sanchez, A. L.; Li, F., based DNA reader for visualized quantification of soil-transmitted helminth infections. ACS Sens. **2018,** 3, 205-210. Copyright 2018 American chemical Society. **(D)** Dynamic range and linear regression of dsDNA on qPDR.

2.2.5 Sequence-Specific Nucleic Acid Quantification by Integrating qPDR with PCR.

Toward the disease diagnosis, the distance-based nucleic acid quantification using qPDR has to be sequence-specific. One viable solution is to selectively enrich the target nucleic acid with amplification strategies, such as PCR, LAMP, or RCA.[79] PCR was chosen because this technique has been widely accepted for disease diagnosis.[80] PCR amplicons that are typically much longer than the 44-bp model dsDNA was hypothesized to be favorable targets for qPDR, as longer dsDNA would provide more binding sites for SG. The compatibility of qPDR with PCR was characterized by using a 164-bp dsDNA standard. Figure 2.10 shows a typical test of the 164-bp DNA standard with concentrations varying from 1 aM to 1 pM using PCR amplification and then distance-based quantification using qPDR. The d_R difference between 1 aM and blank can be easily distinguished in figure 2.10 B. In contrast, a quantitative relationship was established when plotting d_R as a function of concentrations of DNA standard (Figure 2.10 D). The dynamic range was from 1 aM to 1 fM with a detection limit at 1 aM.

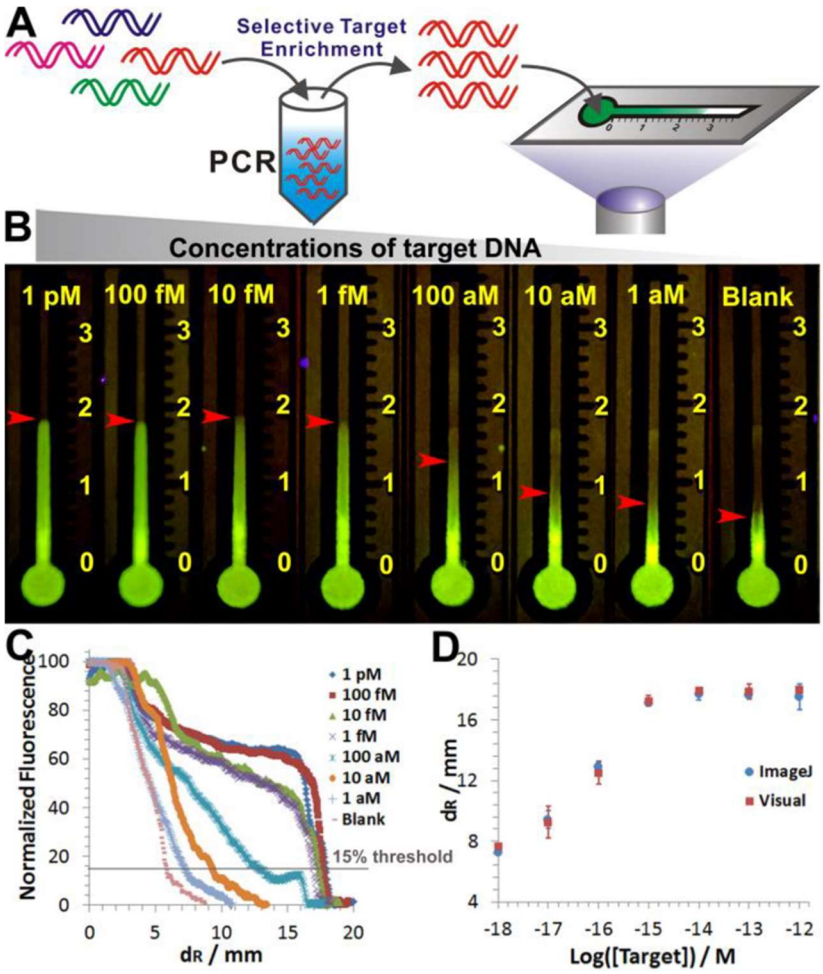

Figure 2.10 Quantification of PCR amplicons on qPDR. **(A)** Schematic illustrating the amplification of genetic DNA marker using PCR. DNA standards or genomic DNA samples were amplified using standard PCR protocol for 35 cycles and then mixed with 20 µM SG-I. The reaction mixture was then loaded onto the paper device for quantitative analyses. **(B)** Representative images of paper-based devices loaded with PCR amplicons of varying concentrations of DNA standards from 1 aM to 1 pM. **(C)** Chromatograms extracted using ImageJ for the quantitative analysis of PCR amplicons. **(D)** Migration distance determined either from chromatograms extracted using ImageJ (blue) or by direct reading using naked eyes (red) as a function of concentrations of DNA standards in 2 µL sample. Each error bar represents one standard deviation from triplicate analyses. Reprinted with permission from Wang, A. G.; Dong, T.; Mansour, H.; Matamoros, G.; Sanchez, A. L.; Li, F., based DNA reader for visualized quantification of soil-transmitted helminth infections. ACS Sens. **2018,** 3, 205-210. Copyright 2018 American chemical Society.

2.2.6 Quantification of Soil-transmitted helminth (STH) Infections Using qPDR with PCR.

Soil-transmitted helminth (STH) infections are a global health issue affecting nearly one-third of the world's population. Having confirmed that qPDR is fully compatible with PCR, we then challenged our device with clinical STH samples. All parasitic worm samples, including *Trichuris trichiura* (TT) and *Ascaris lumbricoides* (AL) were collected on-site at the rural areas of La Hicaca, Olanchito, Honduras, where STH prevalence in children is over 50% according to the estimation by the World Health Organization. Genome samples were then isolated from TT and AL worms that were expelled from school age children who had received chemotherapy (Figure 2.11 A). A pair of primers were designed to specifically amplify the 164-bp gene fragment on β-tubulin gene of TT. This gene fragment containing the codon 200 has been well validated for TT diagnosis and drug resistance tests. To be compatible with the need for on-site STH diagnosis, the genomic DNA samples were amplified using a low-cost smartphone controlled portable thermal cycler and qPDR devices post PCR analysis were read by the naked eye (Figure 2.11 B). Figure 2.11 B shows the relative migration distances ($\Delta d_R = d_R\text{sample} - d_R\text{blank}$) for 10 TT worm samples and 2 AL samples (original images in Figure 2.12 A). All 10 TT samples were found to be positive with varying levels of β-tubulin marker and the 2 AL samples were both negative. These results were further validated by performing a head-to-head comparison with PAGE results (Figure 2.12 B). As shown in Figure 2.11 C, results in both methods are very consistent, with 7 TT samples showing the same concentration levels and the other three samples showing minor inconsistencies. Unlike PAGE where limited quantitative information can be extracted from band

intensities (unless imaging software was applied), qPDR can generate digital readings (Δd_R) for all samples by visual examination.

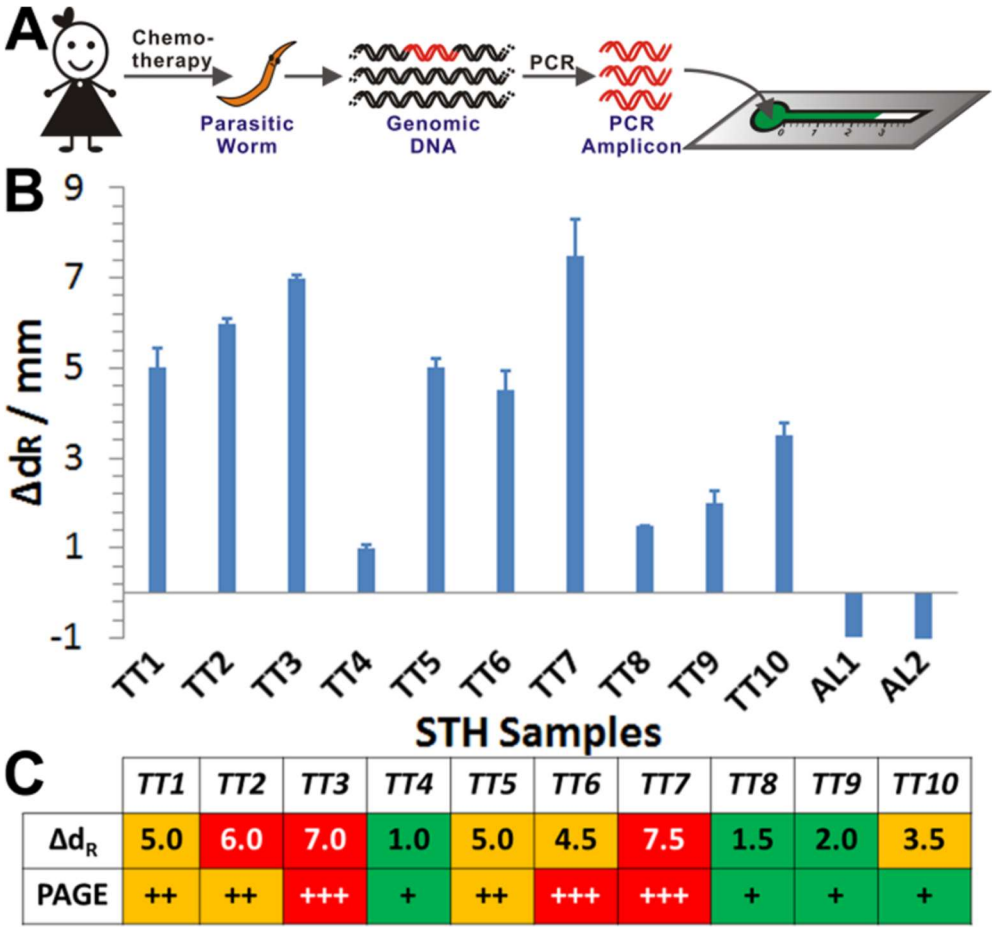

C

	TT1	TT2	TT3	TT4	TT5	TT6	TT7	TT8	TT9	TT10
Δd_R	5.0	6.0	7.0	1.0	5.0	4.5	7.5	1.5	2.0	3.5
PAGE	++	++	+++	+	++	+++	+++	+	+	+

Figure 2.11 Quantification of genomic DNA by using PCR and qPDR. **(A)** Schematic illustration of the procedure for the quantitative analysis of genomic DNA samples obtained from 10 *Trichuris trichiura* (TT) and 2 *Ascaris lumbricoides* (AL) worms that were collected from infected children in Honduras. **(B)** Relative migration distances (Δd_R) of genetic markers (β-tubulin gene) determined for each TT or AL sample. Each error bar represents one standard deviation from triplicate analyses. **(C)** Head-to-head comparison of Δd_R measured using qPDR with band intensities determined by PAGE (Figure 2-12 B) for each TT sample. To facilitate the quantitative comparison, levels of β-tubulin gene markers are arbitrarily classified into three groups with each assigned a distinct color (red for high level, orange for intermediate level, and green for low level). Results in qPDR are classified on the basis of Δd_R with $\Delta d_R > 5.0$ mm as "high" (red), 2.0 mm $< \Delta d_R \leq 5.0$ mm as "intermediate" (orange), and $\Delta d_R \leq 2.0$ mm as "low" (green). Results in PAGE were classified arbitrarily on the basis of the band intensity, with "+" standing for the lowest intensity and "+++" standing for the highest intensity. Reprinted with permission from Wang, A. G.; Dong, T.; Mansour, H.; Matamoros, G.; Sanchez, A. L.; Li, F., based DNA reader for visualized quantification of soil-transmitted helminth infections. ACS Sens. **2018,** 3, 205-210. Copyright 2018 American chemical Society.

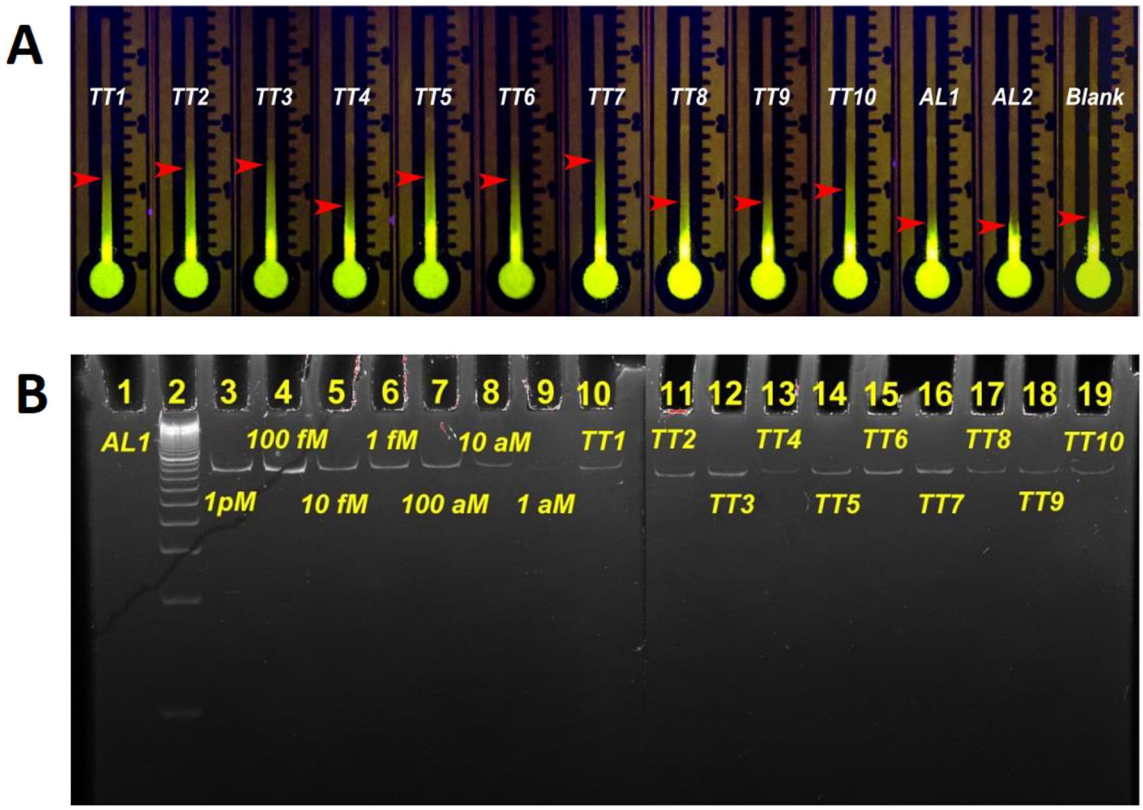

Figure 2.12 qPDR and gel electrophoresis picture of worm samples after PCR amplification. **(A)** Quantitative analysis of 12 genomic samples from STH worms, include 10 TT worms and 2 AL worms (negative controls), using qPDR. **(B)** Parallel analyses of PCR amplicons of DNA standards and STH worm samples using gel electrophoresis and qPDR. **Lane 1:** PCR amplicons from AL1; **Lane 2:** 20-bp DNA ladders; **Lane 3-10:** PCR amplicons from varying concentrations of DNA standards; **Lane 10-19:** PCR amplicons from 10 TT samples. Reprinted with permission from Wang, A. G.; Dong, T.; Mansour, H.; Matamoros, G.; Sanchez, A. L.; Li, F., based DNA reader for visualized quantification of soil-transmitted helminth infections. ACS Sens. **2018,** 3, 205-210. Copyright 2018 American chemical Society.

2.2.7 Distance-based Quantification of Mercury ion (Hg^{2+}) using qPDR.

Having demonstrated the uses of qPDR for measuring DNA at a point-of-care setting and the detection of STH infection using qPDR, we have also expanded the uses of qPDR for non-nucleic-acid targets such as Hg^{2+} ions. In Figure 2.13 A the recognition of Hg^{2+} was achieved using a variety of thymine (T)-rich ssDNA sequence probes ranging from a size of 22-bp (P1), 38-bp (P2) and 47-bp (P3) and was examined using varying

concentrations of Hg^{2+} (Figure 2.14 A, B, C). T-rich sequences bind strongly to Hg^{2+} through the formation of thermally stabilized thymine-Hg-thymine (T-Hg-T) bonds.[81] The formation of T-Hg-T bonds effectively converts an ssDNA into a dsDNA capable of eluting SG through intercalation. Thus, the distance-based quantification of Hg^{2+} can be achieved on qPDR.

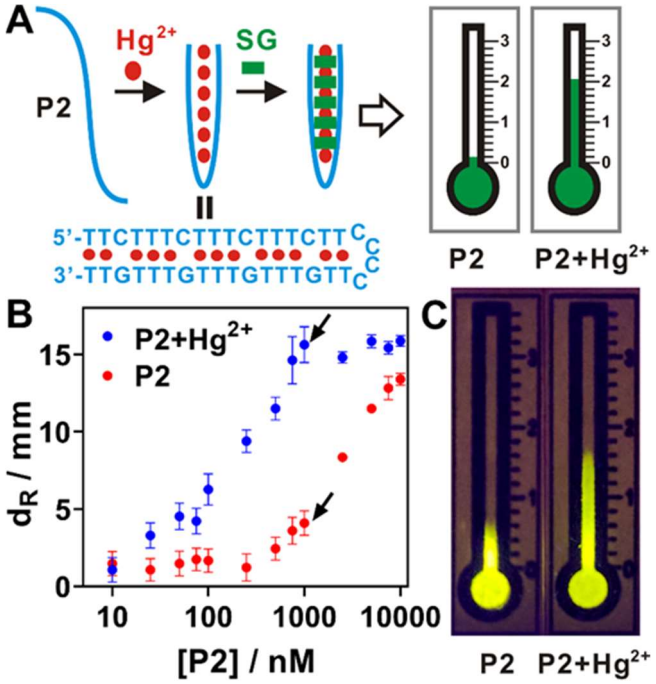

Figure 2.13 Distance-based quantification of Hg^{2+} using T-rich ssDNA probe. (**A**) Schematic illustration of the workflow for detecting Hg^{2+} using thymine-rich DNA probes (P2) and qPDR. (**B**) d_R was plotted as a function of P2 concentrations in the presence (blue dots) or absence (red dots) of 100 nM Hg^{2+}. (**C**) A representative image of qPDR for the distance-based detection of 100 nM Hg^{2+} using 1 μM of P2. Each error bar represents one standard deviation from triplicate analyses.

To maximize the analytical performance of qPDR for the detection of Hg^{2+} the concentration of the T-rich ssDNA probe (P2) was optimized for quantifying Hg^{2+}. In Figure 2.13 B the highest signal to background difference occurred at a concentration of 1

μM. The representative image of qPDR under this optimal condition is shown in Figure 2.13 C. P2 in comparison to P1 and P3 was found to be the optimal design as determined by the widest dynamic range and lowest LOD among the three designs (Figure 2.14 B). Under the optimal probe design (P2) and concentration (1μM), a detection limit of 10 nM Hg^{2+} was achieved (Figure 2.14 D). The superior analytical performance for quantifying Hg^{2+} confirms the possibility to expand qPDR for the detection of non-nucleic-acid analytes via the integration of synthetic nucleic acid probes.

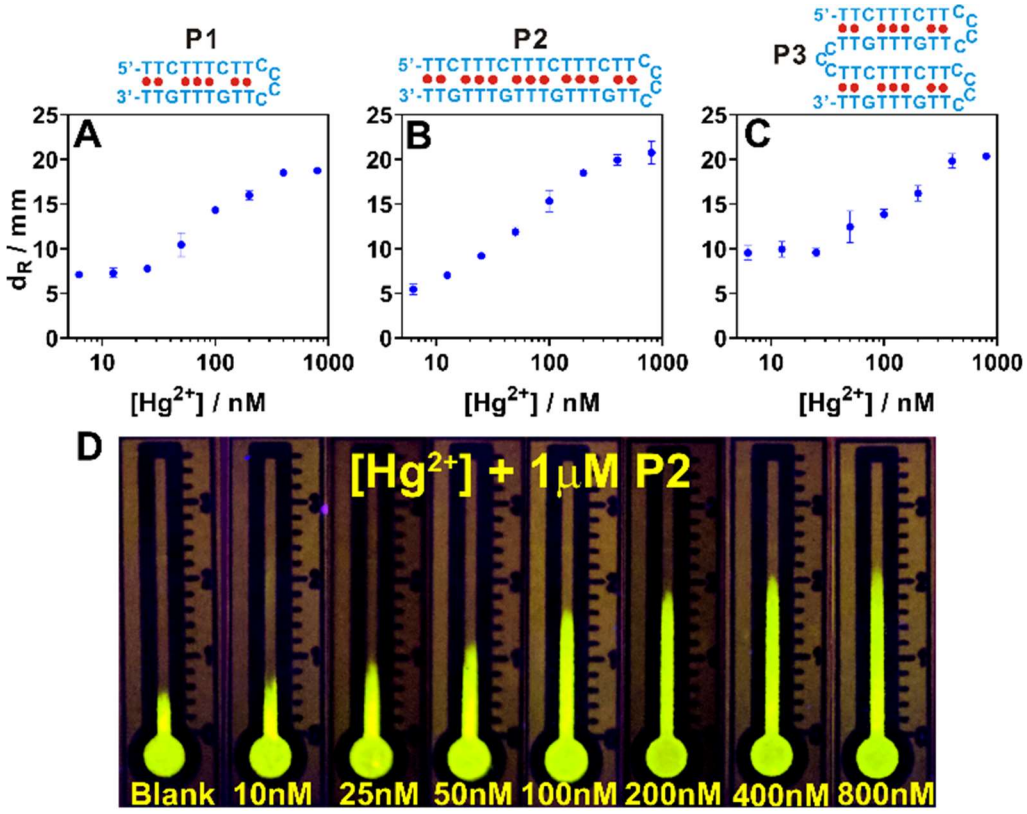

Figure 2.14 Distance-based quantification of Hg^{2+} using different T-rich ssDNA probes, including (**A**) a short T-rich probe (P1), (**B**) a long T-rich probe (P2), and (**C**) a tandem T-rich probe (P3). (**D**) A representative image of qPDR for the quantification of varying concentration of Hg^{2+} using 1 μM P2 as the detection probe. The concentration of all three probes were 1 μM.

2.3 Conclusion

In conclusion, we have developed a paper-based DNA quantification device that is geared towards on-site diagnosis. qPDR is fabricated using unmodified cellulose paper, is of low-cost, and can be mass produced using high throughput printers. qPDR harnesses the unique binding behaviors of SYBR Green I onto an unmodified cellulose paper holds great potential for the purpose of designing a novel sensing mechanism that utilizes DNA intercalating dyes and paper chromatography for nucleic acid quantifications. The use of migration distance over fluorescence intensity of SG for nucleic acid quantification eliminates the need for expensive fluorescence spectrophotometers. The chromatographic behavior of SG and nucleic acids on qPDR was systematically investigated as well as the effect of a series of auxiliary reagents with regards to the performance of qPDR. The results suggests that the retention of SG and DNA on cellulose is a combination of electrostatic forces, hydrogen bonding, and non-specific adsorption.

The qPDR is fully compatible with nucleic acid amplification methods such as PCR and can be readily integrated into disease diagnostic. The sequence-specific STH diagnosis from clinic samples was achieved by using qPDR and PCR amplification. As qPDR is PCR compatible, qPDR can be expanded from the application of STH diagnosis to other diseases by exchanging the PCR primers. Asides from nucleic acid quantification, we demonstrated the quantification of nanomolar Hg^{2+} using qPDR and T-rich DNA probes.

Chapter 3

Fast Light-Activated Substrate cHromogenic (FLASH) Platform for Nucleic Acid Quantification.

3.1 Introduction.

Standard NATs require extensive sample manipulation, expensive instrumentation, trained experts, and centralized clinical laboratories. NATs are rarely available to individuals in resource-limited areas because of the lack of access to well-developed diagnostic techniques. Miniaturization of equipment for standard NATs into simple POCT platform may aid in rapid diagnosis in resource-limited setting.

To overcome the current barriers on on-site NATs, we introduced fast light-activated substrate chromogenic (FLASH). FLASH is a universal colour generative technique that utilizes a series of redox reactions. Here a DNA intercalating dye is subjected to illumination and leads to the generation of active singlet oxygen ($^1O_2$) by energy transfer. Then an oxidize inactive chromogenic substrate is oxidized by singlet oxygen yielding the active chromogenic substrate and results in colour change. FLASH can be incorporated into a portable device that possesses a visual colorimetric readout that utilizes a beam of light (Scheme 3.1). Here two FLASH based platforms were engineered, the first platform consisted of a portable electronic FLASH reader and the second consisted of a a paper-based FLASH strip. The performances of FLASH on two platforms were tested by using synthetic DNA and clinical samples.

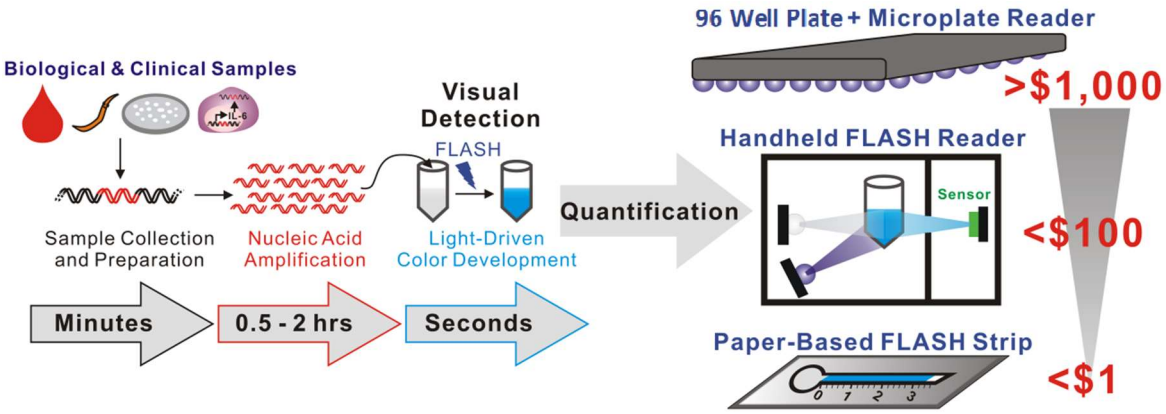

Scheme 3.1 Workflow for visual, colorimetric detection and/or quantification of genetic biomarkers in diverse biological and clinical samples using the FLASH system. For a diagnostic test, extracted DNA or RNA is first amplified via PCR or isothermal amplification and then detected using the FLASH assay. The detection of the appropriate target nucleic acid is indicated by a color change of the solution from colorless to blue. On-filed quantitative FLASH readout can be achieved using a handheld FLASH reader, or a paper-based FLASH strip.

3.2 Result and Discussion.

3.2.1 Principle of FLASH Assay.

DNA intercalating dye SG can be excited from its stable ground state to an excited singlet state upon irradiation using light. The relaxation process of an excited state SG results in emission of green fluorescence. In the presence of dsDNA the SG-dsDNA intercalation enhances the process of spin-forbidden intersystem crossing (ISC), an alternative relaxation pathway from the excited singlet state SG to the triplet state SG (Figure 3.1 left). In the presence of dissolved oxygen, the excited triplet state SG can produce singlet oxygen ($^1O_2$) through energy transfer.[82] The $^1O_2$ in solution can further oxidize a chromogenic substrate and results in colour change in solution. The photooxidation reaction can be triggered when SG is intercalated into dsDNA. The chromogenic substrate used in this work is 3,3',5,5'-tetramethylbenzidine (TMB), a widely

used reagent in immunoassays and is the substrate for photooxidation when subjected to an oxidizing agent. The oxidization of TMB (oxTMB) generates an intense colour change from being colorless to blue in the presence of $^1O_2$ (Figure 3.1 right).

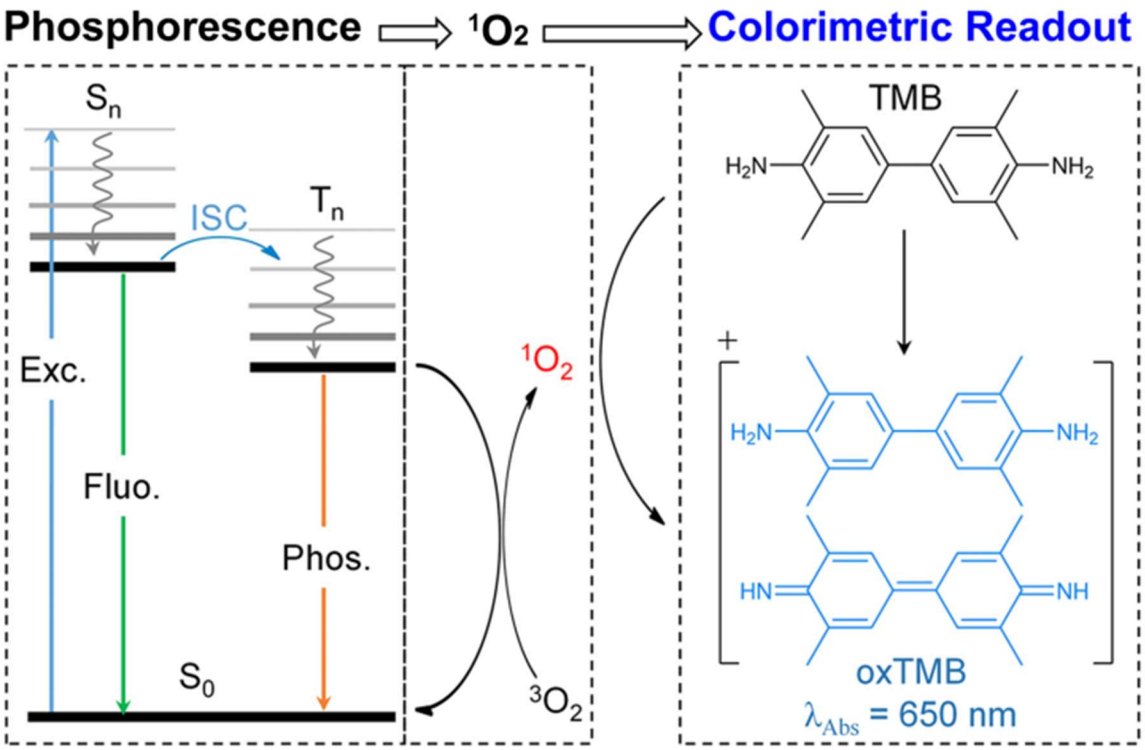

Figure 3.1 The Jablonski diagram shows a plausible mechanism for the FLASH reaction.

3.2.2 FLASH Reader Fabrication and Performance Test.

FLASH Reader Fabrication and Working Principle. The FLASH reader is designed to measure the light-driven color development in *situ* and in real-time by integrating a light irradiation module (a high-intensity cyan LED with wavelength 495nm) with a color sensor

module (Figure 3.2 A & B). The color sensor module contained a silicon photodiodes-based color sensor with red, green, and blue (RGB) filter and an RGB LED for signal generation. Both modules were packaged in a 3D printed housing and operated using Arduino controllers and open-source code (detail design in Experimental section 5.2.2). The reader is switchable between the two modules with programmable irradiation and sensing intervals (Figure 3.2 B). In irradiation mode, the cyan color LED irradiated the sample solution to triggered the TMB photooxidation and in sensing mode the color sensor would measure the TMB absorbance. This repeating irradiation and sensing steps allowed the monitoring of color development in real-time. Of all RGB color channels, the red channel was found to be most sensitive to the colorless-to-blue color transition of TMB (Absorbance max at 650 nm after been oxidized).

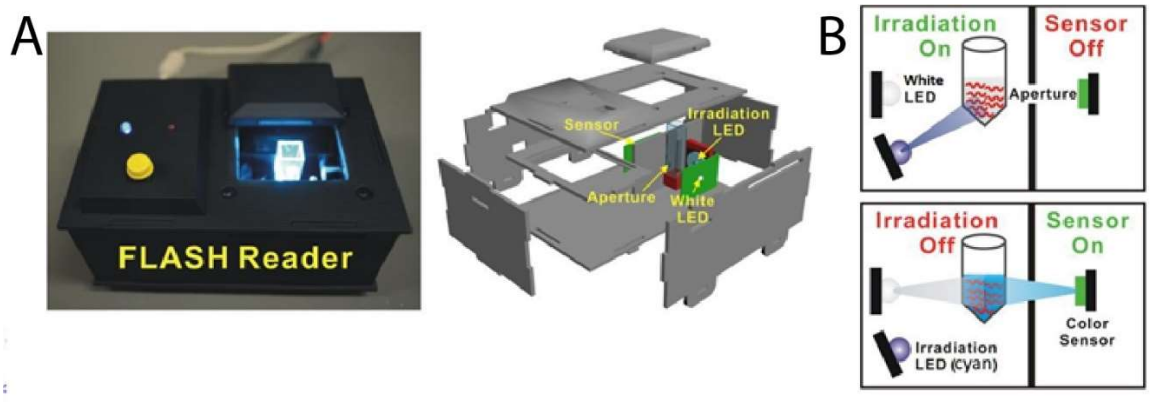

Figure 3.2 Design and operation of FLASH reader. **(A)** Images showing the fully-assembled FLASH reader (left) and critical units (right). **(B)** Schematic illustration of the working principle of the FLASH reader.

Validation of FLASH Reader for NAT. The analytical performance of the FLASH reader was evaluated by using synthetic DNA. A 44-bp HBV DNA was selected as standard DNA

and the FLASH reader was set to measuring the absorbance after every 5 sec irradiations. Figure 3.3 reveals a concentration dependency between the TMB absorbance and the concentration of dsDNA. The dsDNA up to 4 nM concentration can be differentiated after total 1 min irradiation time (Figure 3.3 A), and 0.8nM dsDNA can be differentiated from SG blank upon 5 min irradiation (Figure 3.3 A and B). In this proof-of-principle assay, the dynamic range of FLASH reader was 17−100 nM dsDNA and the detection limit was 5 nM (Calculated from linear regression equation obtained from Figure 3.3 D). The consistency between different trials was tested by repeating 8 trials of FLASH assay with 100nM dsDNA and 2 μM of SG (figure 3.3 C). Figure 3.3 C shows good consistency between each trial with only 3% relative standard deviation. This low detection limit and low error demonstrated the reader is compatible with FLASH assay.

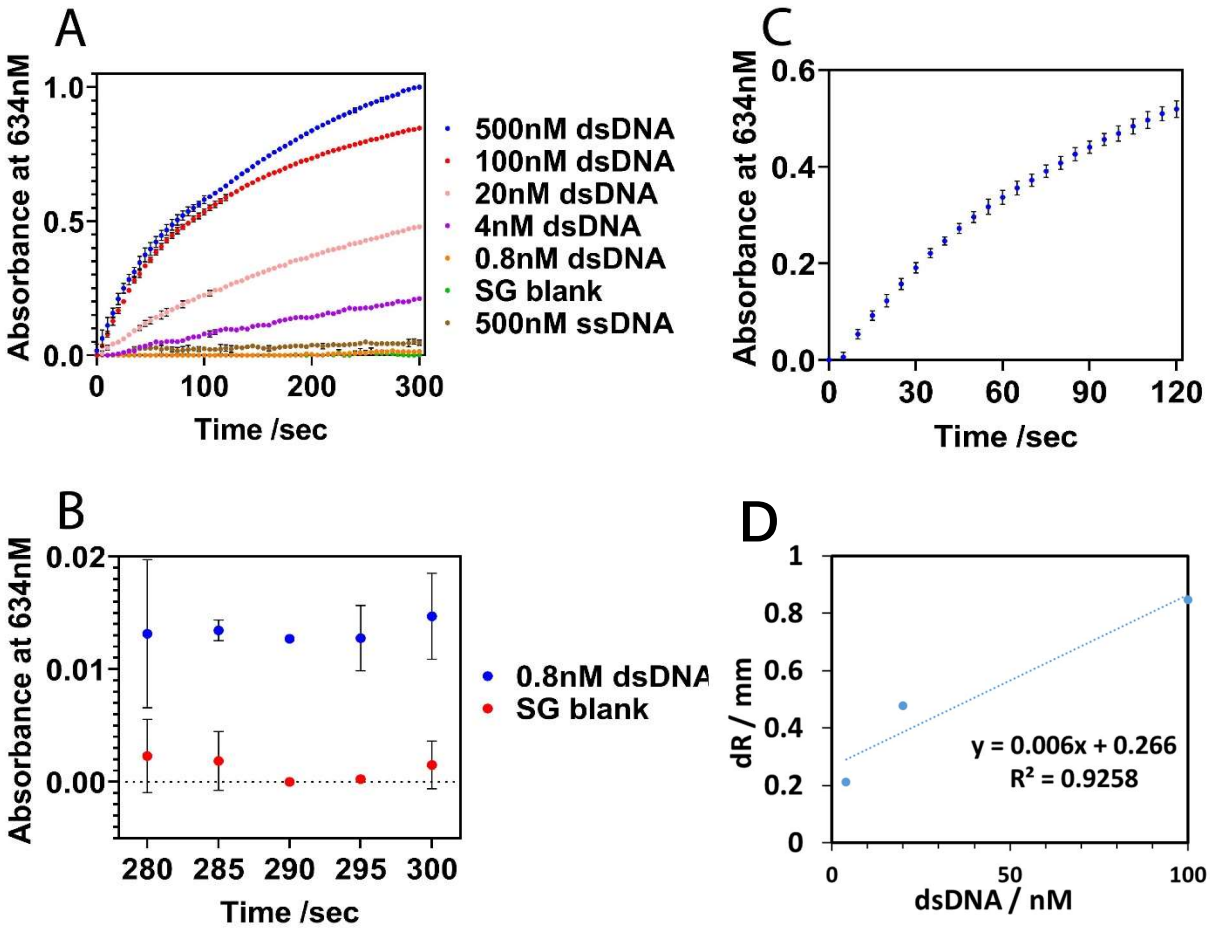

Figure 3.3 FLASH reader performance tests. **(A)** Kinetic data of concentration dependency on the absorbance of FLASH assay by varying concentration of DNA. FLASH reader loaded with 4 μM SG, 0.5 mg/mL TMB and varying concentrations of dsDNA from 0.8 nM to 500 nM or 500 nM ssDNA. Time interval between each points were 5 sec. Each error bar represents one standard deviation from duplicate analyses **(B)** Absorbance data of 0.8nM dsDNA and SG between 280 sec to 300 sec taken from (A). **(C)** Error test by average of 8 trials of FLASH assay by using 100nM dsDNA. **(D)** Linear regression obtained from 4-100 nM dsDNA after 300 sec illumination.

3.2.3 Integration of FLASH Reader with PCR.

To implement FLASH as a simple colorimetric readout for nucleic acid detection and quantification method, it is critical to evaluate its adaptability to standard nucleic acid amplification techniques such as PCR. Instead of bulky bench-top thermal cycler and microplate reader, the FLASH reader and portable thermal cycler (miniPCRTM mini8) was

used in experiment to mimic the on-field test. The analytical performance of the reader was evaluated using a 164-bp synthetic DNA standard corresponding to a gene fragment containing codon 200 on β-tubulin gene, a well-validated genetic marker for *Trichuirs trichiura* (TT) worm identification and drug resistance testing.[83]

Synthetic DNA standards with varying concentrations from 10 aM to 100 fM were amplified by using a portable thermal cycler and detected using the FLASH reader (Figure 3.4 A, top). The standard curve established using the FLASH reader (1 min irradiation) was very similar to that obtained using standard qPCR assays (Figure 3.4 A, bottom), confirming the FLASH reader can perform quantitative NAT with results equivalent to those of commercial qPCR systems. For the final validation of our system, clinical STH worm samples from school-age children who had received anthelminthic therapy were acquired and tested (Figure 3.4 B). Five TT worms and two AL worms were isolated and cleaned from stool samples. Genomic DNAs were extracted on-site in Honduras using a standard magnetic isolation protocol and then transferred to Canada for analyses. The 164-bp gene fragment of β-tubulin gene was amplified using a pair of TT-specific primers and analyzed using both FLASH reader and PAGE. All five TT worm samples showed high absorbance, and two AL worm samples had a low signal as the negative control. Test results using the FLASH reader agreed very well with the PAGE analyses (Figure 3.4 B & Figure 3.5), demonstrating the potential of FLASH assay and reader for on-site disease diagnosis and monitoring.

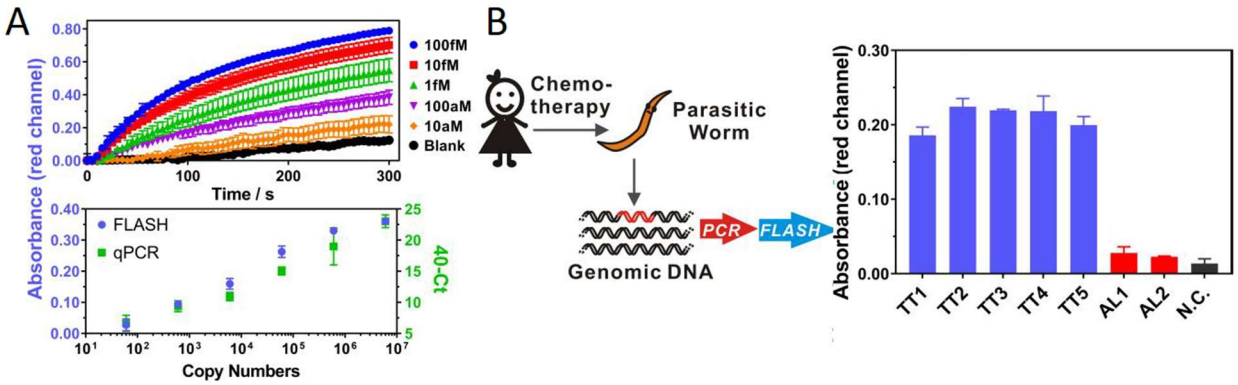

Figure 3.4 Quantification of STH infections by using FLASH PCR. **(A)** Evaluation of the FLASH reader using PCR amplicons produced by DNA standards with original concentrations varying from 10 aM to 100 fM. The quantification capacity of the FLASH reader was compared to a commercial qPCR machine (bottom). Each error bar represents one standard deviation from triplicate analyses. **(B)** Evaluation of FLASH reader for field-based diagnosis by analyzing parasitic worm samples, including TT and AL, expelled from school-age children after chemotherapy at rural areas of Honduras. Each error bar represents one standard deviation from triplicate analyses.

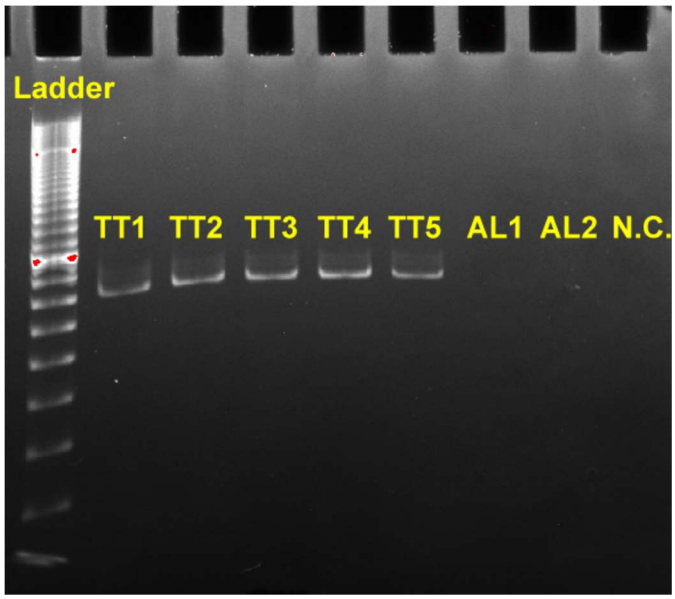

Figure 3.5 Analyzing clinical parasitic worm samples using PAGE gel. From left to right: Lane 1: 20-bp DNA ladder, Lane 2 to 6: five TT worm samples, Lane 7 and 8: two AL worm samples, Lane 9: negative control.

3.2.4 Integration of FLASH Reader with LAMP.

Because of the low instrumental need, isothermal nucleic acid amplification techniques are ideal PCR alternatives for NATs. Here demonstrates the adaptability of FLASH to LAMP, which is one of the most widely used isothermal nucleic acid amplification techniques for diverse applications.

As a proof-of-principle test, a set of six primers were designed to selectively amplify a 192 bp HBV-S gene fragment at location 1081-1272 on the HBV vector (Figure 3.6 A). As each LAMP reaction produces massive dsDNA amplicons in terms of both base pair size and concentration, strong color transitions were observed immediately after light-driven color development for 5s using the FLASH (Figure 3.6 C, D). In addition to the high sensitivity, LAMP is also very well known as a rugged amplification system and much less sensitive to interferences than PCR. The FLASH LAMP could be performed directly in undiluted human serum samples without the need for any extraction or purification steps. To demonstrate the utility of FLASH reader for quantifying LAMP amplicons, we monitored the detection of HBV amplicons that had been amplified by LAMP in undiluted human serum samples for 30 min. With a 5-min color development inside the FLASH reader, HBV positive serum samples with concentrations ranging from 10 aM to 100 fM could be visually discriminated from the negative serum control (Figure 3.6 B). The real-time monitoring of this color development also enabled a quantifiable range from 10 aM to 1 fM (Figure 3.6 B). In addition, FLASH LAMP induced extensive precipitations in HBV positive serum samples, which significantly enhanced the colorimetric readout; whereas the HBV negative serum remained clear (Figure 3.6 C).

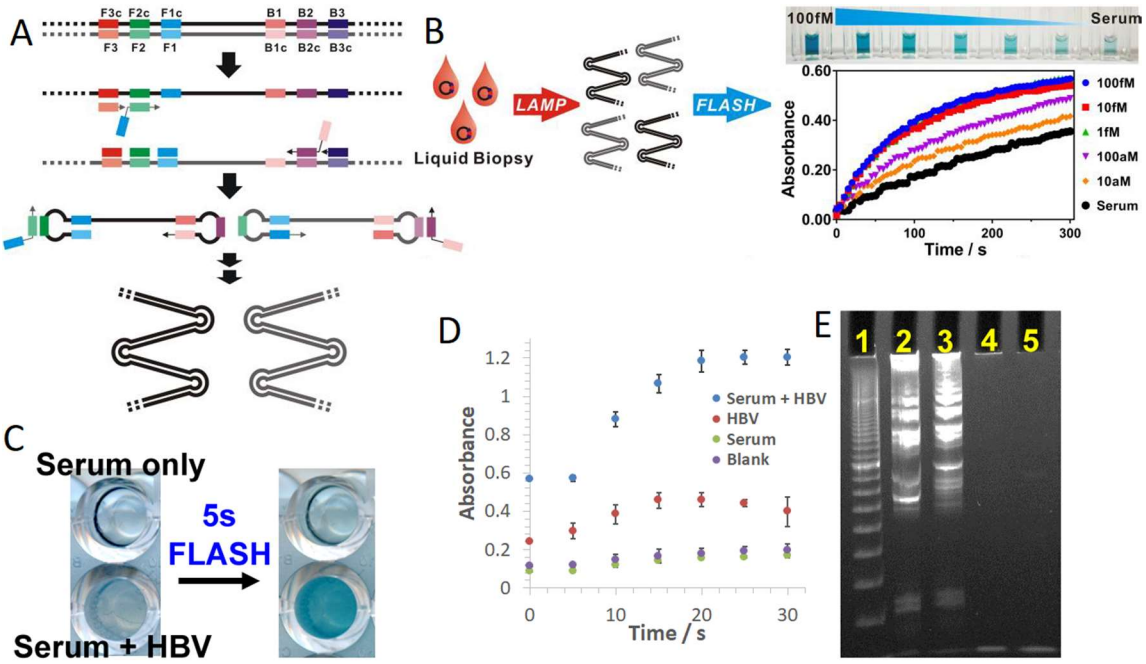

Figure 3.6 Quantification of LAMP amplicons by FLASH reader**. (A)** Schematic illustration of LAMP principle. **(B)** FLASH LAMP for direct analysis of HBV genomic DNA in undiluted human serum samples without the need for any sample preparation steps. **(C)** Characterization of FLASH LAMP for analyzing HBV genomic DNA in undiluted human serum samples through visual examination of spectroscopic analysis **(D)** and comparison with PAGE analysis **(E)** Lane 1 contains 20 bp DNA ladder. Lane 2 and 3 contain LAMP amplicons from 1 fM HBV vector spiked in human serum sample. Lane 4 and 5 contain LAMP reaction mixture in serum sample without spiking. Each error bar represents one standard deviation from duplicate analyses.

3.2.5 FLASH strip.

Although the distance-based nucleic acid quantification assay of qPDR eliminates the need for an external reader, the fluorescence readout still requires a dark room and blue light box to irradiate SG. Colorimetric nucleic acid quantification assay such as the FLASH technique is suitable for qPDR to further simplify data deposition. The paper-based FLASH strip was introduced to further eliminate the need for instrumentation required for FLASH technology. The FLASH strip was fabricated by using the same procedure as qPDR

described in chapter 2 and a thin layer of TMB was pre-deposited homogeneously to the testing zone for color development (Figure 3.7 A). After TMB coating the mixture containing SG and amplified nucleic acids were loaded onto the loading zone on the qPDR strip. After the solution was fully wicked through the TMB coated test zone, the TMB photooxidation reaction was triggered by irradiation using an LED light source (495 nm) for 1 min. Since the TMB photooxidation is only triggered in the presence of SG where SG would be tightly retained at the sample loading zone and can only be eluted into the testing zone in the presence of dsDNA. Therefore, the fluorescence-based readout can be converted into the development of a permanent blue color on FLASH strip (Figure 3.7 B, C, D).

Having established the FLASH assay on FLASH strips the assay compatibility with nucleic acid amplification products was tested. Figure 3.7 B shows the measurement of amplicons produced by direct PCR. The nucleic acid in serum can be amplificated by direct PCR without performing DNA extraction and purification steps. The 1 fM HBV plasmid DNA was spiked into healthy human serum to mimic the clinical samples. The HBV + serum sample then underwent direct PCR and mixed with SG before loaded onto a FLASH strip. Through a distance-development for 10 min followed by a light-driven color development for 1 min, the blue color was observed in the testing zone (Figure 3.7 D). The colorimetric readout clearly differentiated HBV DNA from the blank and was highly consist with the fluorescent readout (Figure 3.7 C).

Here the adaptability of the FLASH strip with LAMP was tested. For LAMP amplification a set of six primers were designed to selectively amplify a 192 bp HBV-S gene fragment (100 aM) at location 1081-1272 on the HBV vector. After amplification the

LAMP products were then mixed with SG and incubated at room temperature for 5 min before loaded onto a FLASH strip. Through a distance-development for 10 min followed by a light-driven color development for 1 min, the FLASH assay clearly differentiates HBV DNA (d_R = 29 mm) from the blank (d_R = 12 mm) without the need for any external reader (Figure 3.7 E).

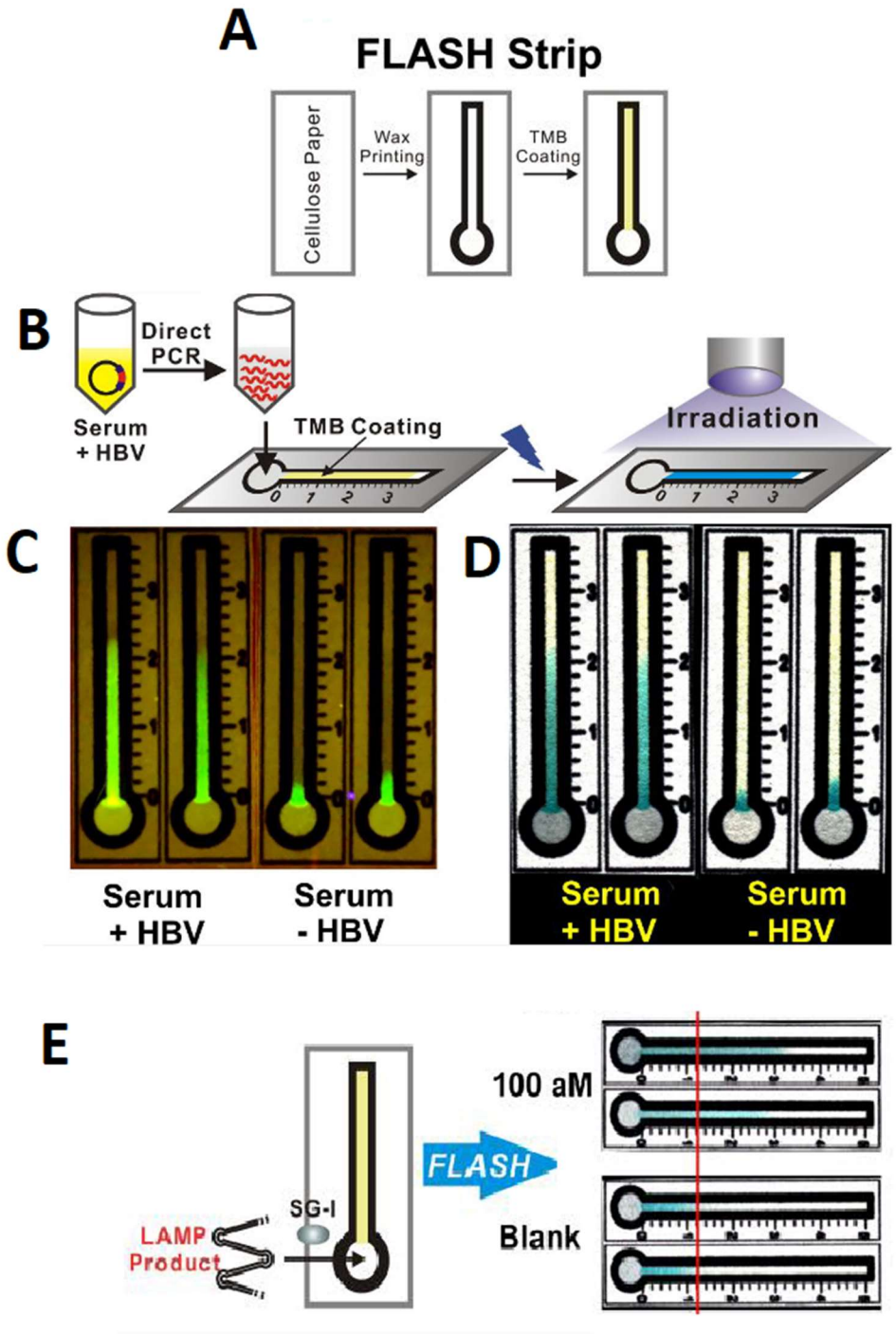

Figure 3.7 Colorimetric detection on qPDR by pre-deposited TMB. **(A)** Schematic illustration of the fabrication process for a TMB coated qPDR **(B)** Schematic illustration of the workflow for distance-based detection of HBV in undiluted human serum samples using direct PCR and TMB coated qPDR. (**C**) Distance development and observation under a blue light lamp. (**D**) Color development using the TMB photooxidation. (**E**) Distance-based detection of HBV genomic DNA using LAMP and TMB coated qPDR.

3.3 Conclusion.

In conclusion, we have developed FLASH technology that harnesses a widely used DNA intercalating probe SG and photooxidation substrate TMB for NAT. The color development requires a direct mixing of nucleic acid amplicons with two chemicals, being SG and TMB, followed by the irradiation using visible light. Regarding field-deployable NATs we have designed and fabricated a FLASH reader by using Arduino controlled irradiation and sensing system. By combing PCR and LAMP with FLASH and a FLASH reader we have proven that FLASH is highly compatible with nucleic acid amplification methods. Although we used FLASH exclusively as an endpoint readout for PCR and LAMP in this work, it is also possible to fabricate real-time FLASH PCR or LAMP systems in the future by adding a heating element. It was also determined that the FLASH assay was compatible with qPDR by pre-depositing TMB onto the test zone of qPDR. Here we developed FLASH strip capable of detecting direct PCR and LAMP amplicons and eliminating the requirement of a lightbox for fluorescent based qPDR.

Chapter 4
Conclusion and Future Work.

In conclusion two portable and inexpensive field-deployable nucleic acid quantification platforms have been developed. The qPDR was fabricated by using unmodified cellulose paper and wax printing technique. Here we exploited the unique chromatographic behavior of DNA and SG on cellulose paper. qPDR quantification of nucleic acids via the retention distance of SG in test zone as a readout eliminates the need for external electronic readers. Additionally qPDR is fully compatible with nucleic acid amplification techniques such as PCR and LAMP and can therefore be readily integrated into the current STH infection diagnostic. It is also possible to expand the applications of aPDR to other diseases by exchanging PCR primers. Through the integration with functional nucleic acids, it is possible to expand the target set of qPDR to non-nucleic-acid targets such as Hg2+ ions. Our next step is to integrate the DNA extraction and isothermal amplification steps with qPDR in order to achieve a real-time on-site disease diagnosis.

The FLASH technique that has been introduced here and with portable platforms results in a simple plug-and-play readout system that can be readily implemented into existing NATs. The simplicity and broad adaptability of FLASH was exemplified using serum and stool samples with varying PCR and LAMP protocols. The compatibility of FLASH with varying engineering platforms such as portable devices and paper-based microfluidics has also been demonstrated by the development and adoption of a FLASH reader and FLASH strip. Unlike signal readouts that make use of additional enzymatic amplifications and/or DNA hybridization, the high sensitivity of FLASH was granted by the chemical nature of DNA intercalating dyes and thus achieved in a mix-and-read manner

without compromising the simplicity and speed of the assay. Both reagents of the FLASH reader and FLASH strip can be pre-mixed and stored. The next step of FLASH is to develop real-time FLASH PCR or LAMP systems. Ongoing efforts in both molecular and device levels, including the screening FLASH reactants and conditions that are fully compatible with real-time PCR or LAMP reactions as well as equipping FLASH readers with heating modules.

Finally, with the desirable features highlighted in this work, we envision both qPDR and FLASH technology will be readily adopted for rapid, robust, and sensitive nucleic acid detection at decentralized settings and open new avenues for disease diagnosis and field-based applications.

Chapter 5
Experimental Section

5.1. Experimental Section for Chapter 2.

5.1.1 Materials and Reagents.

Sodium chloride (NaCl), magnesium chloride ($MgCl_2$), mercury chloride ($HgCl_2$), dimethyl sulfoxide (DMSO), Whatman filter paper (Grade 1), microscope glass slides, paraffin film, sodium citrate ($Na_3C_6H_5O_7$), citrate acid ($H_3C_6H_5O_7$), hydrochloric acid (HCl), sodium hydroxide (NaOH), 10× phosphate buffer saline (10 × PBS), TWEEN 20, polyethylene glycol (PEG) average Mv 100,000, sodium dodecyl sulfate (SDS), and SYBR Green I (SG) dye were purchased from Sigma (Oakville, ON, Canada). Tris-HCl buffer (1M), Urea and citrate acid (2-Hydroxypropane-1,2,3-tricarboxylic acid) monohydrate were purchased from Fisher Scientific (Ottawa, ON, Canada). Sodium Citrate dihydrate was purchased from BioShop (Burlington, ON, Canada). Cetrimonium bromide (CTAB) was purchased from MP Biomedicals (St. Petersburg, Florida, USA). Taq 2 × PCR Master Mix, N,N,N′,N′-tetramethylethylenediamine (TEMED), ammonium persulfate (APS), 40% acrylamide/bisacrylamide solution, and DNA loading buffer were purchased from Bio-Rad Laboratories, Inc. (Mississauga, ON, Canada). NANOpure H_2O (>18.0 MΩ), purified using an Ultrapure Milli-Q water system, was used for all experiments. All synthetic DNA samples (Table 5.1) were purchased from Integrated DNA Technologies (Coralville, IA) and purified using standard desalting.

Table 5.1 Synthetic DNA sequences.

Name		Sequence
44-bp model DNA	Sense	5'-AA ATT CGC AGT CCC CAA CCT CC A ATC ACT CAC CAA CCT CCT GTC-3'
	Antisense	5'-GAC AGG AGG TTG GTG AGT GAT TGG AGG TTG GGG ACT GCG AAT TT-3'
TT-DNA	*TT* Forward-Primer	5'-AGG TTT CAG ATA CAG TTG TAG-3'
	TT Reverse-Primer	5'-CAA ATG ATT TAA GTC TCC G-3'
	164-bp *TT*-DNA Standard	5'-AGG TTT CAG ATA CAG TTG TAG AAC CAT ATA ATG CAA CTC TGT CAG TCC ACC AGT TGG TAG AGA ACA CGG ACG AAA CAT TCT GCA TAG ATA ATG AAG CGC TTT ACG ATA TTT GTT TCC GAA CTT TGA AGT TAA CAA CAC CAA CTT ACG GAG ACT TAA ATC ATT TG-3'
Mercury binding DNA	P1	5'-TTC TTT CTT CCC CTT GTT TGT T-3'
	P2	5'-TTC TTT CTT TCT TTC TTC CCC TTG TTT GTT TGT TTG TT-3'
	P3	5'- TTC TTT CTT CCC CTT GTT TGT TCC CTT CTT TCT TCC CCT TGT TTG TT-3'

5.1.2 qPDR Fabrication.

The qPDR used in this project was printed by XEROX ColorQube 8580 solid ink printer on Whatman No.1 filter paper. The qPDR pattern with a 2.0 mm wide test channel and a 6mm inner diameter loading well was designed on computer by using software Coreldraw x8. The patterned paper was heated at 150 °C for 45 seconds on a hot plate in order to let the ink pattern melted and fully penetrated the filter paper. The device was then fabricated by stacking the patterned paper and a layer of paraffin film on a microscope

glass slide. This sandwiched device was then bonded together by heating on the hot plate at 110°C for 30 s. The final width of the testing zone after fabrication was determined to be 1.5 mm.

5.1.3 Nucleic Acid Quantification Using qPDR.

A typical reaction mixture containing varying concentrations of target nucleic acid and 20 μM SG in reaction buffer was first incubated at room temperature for 5 min and then loaded 10 μL of the mixture into the sample loading zone on qPDR. After sample loading, qPDR was placed on a pocket-size bluelight box (Mini LED Transilluminator, IO Rodeo Inc.) until the reaction mixture completely wicked through the test zone (typically within 10 min). The migration distance was measured in real-time by naked eye examination. To obtain the kinetic data, videos of qPDR in action were taking by a Nikon D600 digital camera. The kinetic curve was then established by converting the video into images at a frequency of 1 snapshot per 20 s. All chromatograms were obtained by first taking photo at 10 min after sample loading using a Nexus 6P smartphone camera and then analyzed using free software ImageJ on computer. When the chromatogram was used to facilitate the measurement of retention distance, a threshold of 15% normalized fluorescence was used. The 15% threshold was determined to be close to the sensitive of human naked eye from survey. Total of 59 people participated in this survey. The picture of qPDR which used in the survey was shown in Figure 5.1. Detail result from each person was shown in table 5.2.

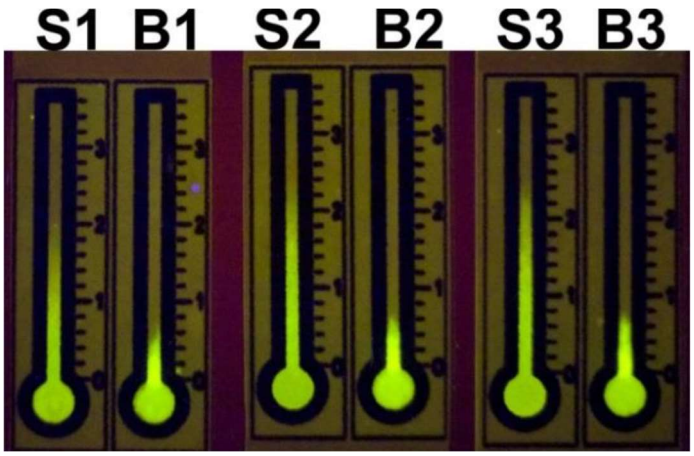

Figure 5.1 Retention distances of 3 dsDNA samples (S1-3) and 3 ssDNA samples (B1-3) on qPDR. Reprinted with permission from Wang, A. G.; Dong, T.; Mansour, H.; Matamoros, G.; Sanchez, A. L.; Li, F., based DNA reader for visualized quantification of soil-transmitted helminth infections. ACS Sens. **2018,** 3, 205-210. Copyright 2018 American chemical Society.

Table 5.2 Retention distance measured by 59 people.

Observer	dsDNA-1 d_R (mm)	dsDNA-2 d_R (mm)	dsDNA-3 d_R (mm)	ssDNA-1 d_R (mm)	ssDNA-2 d_R (mm)	ssDNA-3 d_R (mm)
1	16.20	22.00	22.80	7.50	6.40	7.40
2	19.50	22.00	22.50	5.50	5.70	6.40
3	20.00	22.00	24.00	6.00	6.00	8.00
4	20.00	24.00	24.00	6.00	6.00	6.00
5	18.00	22.10	23.60	5.50	6.20	7.80
6	20.00	22.00	23.00	6.00	6.00	8.00
7	20.00	22.00	24.00	7.00	6.00	8.00
8	20.00	22.00	23.50	6.00	6.50	7.00
9	20.00	24.00	26.00	6.00	6.00	8.00
10	20.00	22.00	24.00	6.00	6.00	8.00
11	16.00	20.00	22.00	5.00	6.00	7.00
12	20.00	23.00	24.00	7.00	6.00	7.00
13	1.20	1.90	22.50	5.30	5.90	6.40
14	20.00	21.00	23.00	5.00	5.00	7.00
15	18.00	20.00	22.00	16.00	16.00	16.00
16	12.00	17.60	22.30	4.00	4.20	6.40
17	20.00	22.10	24.50	7.00	6.00	8.00
18	20.00	22.00	23.00	5.00	6.00	7.00
19	18.90	21.70	22.50	6.50	5.90	7.40
20	20.10	20.40	22.10	5.70	6.10	6.30
21	20.00	22.00	22.00	6.00	6.00	8.00
22	20.00	22.00	23.00	6.00	6.00	8.00
23	19.00	22.00	24.50	7.00	6.00	8.00
24	19.00	22.00	22.00	5.00	5.00	6.50
25	20.00	22.00	21.00	7.00	6.00	7.00
26	19.00	21.00	23.00	6.00	6.00	7.00
27	20.00	22.00	23.00	6.00	6.00	8.00
28	20.00	22.00	22.00	5.00	6.00	7.00
29	20.00	22.00	22.00	6.00	6.00	8.00
30	18.00	22.00	22.00	6.00	6.00	6.00
31	18.00	20.00	22.00	6.00	6.00	8.00
32	20.00	22.00	23.00	6.00	6.00	7.00
33	18.90	21.90	22.50	4.10	4.90	6.20
34	13.00	16.10	18.30	4.50	5.20	6.40
35	20.00	20.10	21.00	5.80	6.00	7.60

36	20.00	22.00	24.00	6.00	6.00	8.00
37	20.00	22.00	24.00	6.00	6.00	8.00
38	18.00	20.00	22.00	4.00	6.00	8.00
39	20.00	24.00	26.00	6.00	6.00	8.00
40	18.50	22.50	23.50	5.90	6.10	7.00
41	20.00	24.00	26.00	7.00	8.00	8.00
42	20.00	23.00	23.00	5.00	6.00	7.00
43	20.00	22.00	24.00	6.00	6.00	7.00
44	20.00	23.00	23.50	6.00	6.00	7.50
45	16.20	22.00	22.80	7.50	6.40	7.40
46	20.10	24.50	23.90	6.20	5.70	8.30
47	18.50	22.00	22.50	5.90	6.30	6.90
48	19.00	22.00	22.00	5.00	5.00	6.50
49	18.90	22.00	22.50	5.00	5.80	6.50
50	18.80	23.00	22.00	6.00	5.90	7.00
51	16.00	20.00	22.00	6.00	6.00	7.00
52	18.30	22.00	23.90	6.10	6.30	8.10
53	16.00	21.50	22.00	4.50	5.00	6.00
54	19.80	21.20	21.50	6.70	7.80	7.50
55	20.00	22.00	22.00	5.00	6.00	8.00
56	18.10	22.30	23.50	5.60	6.10	7.90
57	20.00	22.00	22.00	6.00	6.00	8.00
58	20.00	23.00	24.00	6.00	6.00	7.00
59	20.00	22.00	23.00	6.00	6.00	8.00
Average d_R	19.0	21.8	22.9	6.0	6.1	7.5
Standard deviation	1.70	1.40	1.30	0.80	0.50	0.70
Relative standard deviation	9.10%	6.20%	5.50%	13.50%	9.10%	9.50%
Normalized Fluorescence at d_R	13.9	17.3	14.3	12.8	17.3	9.7
Average Normalized Fluorescence	15.2			13.3		

5.1.4 Effects of SG and Other Auxiliary Reagents on Distance-based DNA Quantification Using qPDR.

Effects of SG Concentration on DNA Quantification. A series of reaction mixtures each containing 40 μM, 20 μM, 10 μM, 5μM, 2.5μM, 1.25 μM SG and 500nM DNA in 0.1M

pH4 citrate buffer were incubated at room temperature for 5 min. The mixture was then loaded and quantified using qPDR using the protocol outline in section 5.1.3.

Effects of Ionic Strength on DNA Quantification. For Na^+ test, a series of reaction mixtures each containing 800 mM, 400 mM, 200 mM, 100 mM, 80 mM, 60 mM, 40 mM NaCl, 20 μM SG, and 500nM DNA in pH4 citrate buffer was incubated at room temperature for 5 min. For Mg^{2+} test, a series of reaction mixtures each containing 400 mM, 200 mM, 100 mM, 50 mM, 25 mM, 12.5 mM $MgCl_2$, 20 μM SG, and 500nM DNA in 0.1M pH4 citrate buffer were incubated at room temperature for 5 min. The mixture was loaded and quantified using qPDR using the protocol outline in section 5.1.3.

Effects of Urea on DNA Quantification. A series of reaction mixtures each containing 4 M, 3 M, 2 M, 1 M, 0 M Urea, 20 μM SG, and 500nM DNA in 0.1M pH4 citrate buffer were incubated at room temperature for 5 min. The mixture was loaded and quantified using qPDR using the protocol outline in section 5.1.3.

Effects of Polyethylene Glycol Concentration on DNA Quantification. A series of reaction mixtures each containing 10 mg/mL, 1 mg/mL, 0.1 mg/mL, 0.01 mg/mL PEG 100,000, 20 μM SG, and 500nM DNA in 0.1M pH4 citrate buffer were incubated at room temperature for 5 min. The mixture was loaded and quantified using qPDR using the protocol outline in section 5.1.3.

Effects of Surfactants on DNA Quantification. For Tween-20 test, a series of reaction mixtures each containing 1.0%, 0.75%, 0.50%, 0.25%, 0.10%, 0.05% Tween-20, 20 μM SG, and 500nM DNA in 0.1M pH4 citrate buffer were incubated at room temperature for 5 min. For SDS test, a series of reaction mixtures each containing 10 mM, 1 mM, 100 μM,

10 μM, 1 μM, 100 nM SDS, 20 μM SG, and 500nM DNA in 0.1M pH4 citrate buffer were incubated at room temperature for 5 min. For CTAB test, a series of reaction mixtures each containing 10 mM, 1 mM, 100 μM, 10 μM, 1 μM, 100 nM, 10 nM CTAB, 20 μM SG, and 500nM DNA in 0.1M pH4 citrate buffer were incubated at room temperature for 5 min. The mixture was loaded and quantified using qPDR using the protocol outline in section 5.1.3.

5.1.5 Quantification of PCR Amplicons Using qPDR.

For a typical test, a series of PCR reaction mixtures each containing 1 pM to 1 aM concentration of 164-bp *TT*-DNA standard and a pair of primers (*TT* forward and reverse primers, 250 nM each) in 1 × Taq master mix were placed in a BioRad T100 thermal cycler. The thermal cycles set up included an initial incubation at 94 °C for 3 min, followed by 35 cycles (30 s denaturation at 94 °C, 30 s annealing at 52 °C, 30 s extension at 72 °C, and repeat) and a final extension at 72 °C for 5 min. After PCR reaction, each amplicon was mixed with SG at a final concentration of 20 μM in 0.1 M pH4 citrate buffer and incubated at room temperature for 5 min. The mixture was loaded and quantified using qPDR using the protocol outline in section 5.1.3.

5.1.6 Clinical STH Samples.

STH worm samples were recovered from eight school-age children infected with *Trichuris trichiura* infection in the rural region of La Hicaca located in the northwestern area of Honduras. Ethical approval was obtained by the National Autonomous University

of Honduras and Brock University. The eight participants received a treatment scheme based on pyrantel pamoate and oxantel pamoate (Conmetel) during the first three days, and Albendazole during a fourth day. The TT worms collected from participants faeces were washed with saline solution and stored in 70% ethanol. Following the recovery of specimens, DNA was extracted using the Automate Express DNA Extraction System (Thermo Fisher Scientific Inc.) with the commercial kit PrepFiler Express BTA, according to the manufacturer's protocol.

5.1.7 Quantification of STH Samples Using qPDR.

A pair of primers (*TT* forward and reverse primers) was designed to amplify a fragment of 164-bp β-tubulin genomic sequence from whipworm *Trichuris trichiura* (TT). For a typical test, the PCR mixture containing 2 ng of *TT* genomic DNA, a pair of primers (250 nM each) in 1 × Taq mater mix was placed in a BioRad T100 thermal cycler. To meet the needs of future uses at rural areas of Honduras, this mixture was amplified using a low cost portable thermal cycler (MiniPCR). The PCR protocol and subsequent detection using qPDR were identical as outlined in section 5.1.5. Two round worm *Ascaris lumbricoides* (AL) genomic samples were also included as negative controls to determine the specificity of the assay. After PCR, each reaction was separated into two equal aliquots, with one aliquot loaded and quantified using qPDR and the other analyzed using PAGE. The samples were then run by 12% native PAGE. Before loading samples to gel, amplicons were mixed with DNA loading buffer at a volume ratio of 5:1. A voltage of 135 V was applied for gel electrophoresis. PAGE gels were imaged by using Gel Doc XR + Gel Documentation System (Biorad, Mississauga, ON, Canada) after ethidium bromide (0.5 μg/mL) staining.

5.1.8 Quantification of Mercury ion (Hg^{2+}) using qPDR.

For a typical test, a solution of varying concentrations of Hg^{2+} in 10 mM Tris-HCl buffer was first mixed with 1 μM mercury detection probe (P1, P2 or P3) and incubated at room temperature for 15 min. The reaction mixture was mixed with 20 μM SG in PBS buffer with 0.1% (v/v) Tween-20 and incubated for 10min at room temperature. The mixture was then loaded and quantified using qPDR with the same protocol as described in section 5.1.3. For mercury detection probe comparison test, 100 nM Hg^{2+} was mixed with varying concentrations of mercury detection probe (P1, P2 or P3) from 0 nM to 1000 nM. Rest steps were the same as above.

5.2 Experimental Section for Chapter 3.

5.2.1 Materials and Reagents.

SYBR Green I (SG) dye, 3,3'5,5'-tetramethylbenzidine (TMB), 10× phosphate buffer saline (10 × PBS), TWEEN 20, 352 polyethylene glycol (PEG) 100,000, sodium citrate ($Na_3C_6H_5O_7$), citrate acid ($H_3C_6H_5O_7$), Whatman No.1 filter paper, microscope glass slides, and paraffin film were purchased from Sigma (Oakville, ON, 355 Canada). Taq 2× PCR Master Mix, iTaqTM Universal SYBR Green Supermix, N,N,N′,N′-tetramethylethylenediamine (TEMED), ammonium persulfate (APS), 40% acrylamide/bis-acrylamide solution, DNA loading buffer, and 20 bp DNA ladder were purchased from Bio-Rad Laboratories, Inc. (Mississauga, ON, Canada). Luna Universal qPCR Master Mix and Monarch PCR & DNA Cleanup Kit were purchased from New England BioLabs

(Whitby, ON, Canada). Phusion Blood Direct PCR kit were purchased from Thermo Fisher Scientific (Whitby, ON, Canada). QIAamp Circulating Nucleic Acid Kit and QIAprep Spin Miniprep Kit were purchased from Qiagen Inc. (Toronto, ON, Canada). QuntiFluor dsDNA quantification kit was purchased from Promega (Madison, WI). All synthetic DNA templates and primers were purchased from Integrated DNA Technologies (Coralville, IA) and purified using standard desalting. All DNA sequences were listed in Table 5.3 and Table 5.4.

Table 5.3 PCR templates and primers.

Original species	Target sequence	Size (bp)	Forward primer	Reverse primer
HBV oligo	5'- AGA CTC GTG GTG GAC TTC TCT CAA TTT TCT AGG GGG AAC ACC CGT GTG TCT TGG CCA AAA TTC GCA GTC CCA AAT CTC CAG TCA CTC ACC AAC CTG TTG TCC TCC AAT TTG TCC TGG TTA TCG CTG GAT GTG TCT GCG GCG TTT TAT CAT CTT CCT CTG CAT CCT GCT GCT ATG CCT CAT CT -3'	182	5'-AGA CTC GTG GTG GAC TTC -3'	5'- AGA TGA GGC ATA GCA GCA-3'
plasmid HBV 1.3-mer WT replicon	5'-TAT CGC TGG ATG TGT CTG CGG CGT TTT ATC ATC TTC CTC TTC ATC CTG CTG CTA TGC CTC ATC TTC TTG TTG GTT CTT CTG GAC TAT CAA GGT ATG TTG CCC GTT TGT CCT CTA ATT CCA GGA TCC TCA ACA ACC AGC ACG GGA CCA TGC CGG ACC TGC ATG ACT ACT GCT CAA GGA ACC TCT ATG TAT CCC TCC TGT TGC TGT ACC AAA CCT TCG GAC GGA AA-3'	224	5'- TAT CGC TGG ATG TGT CTG CG-3'	5'-TTT CCG TCC GAA GGT TTG GT-3'
	5'- CCT CAA CAA CCA GCA CGG GAC CAT GCC GGA CCT GCA TGA CTA CTG CTC AAG GAA CCT CTA TGT ATC CCT CCT GTT GCT GTA CCA AAC CTT CGG ACG GAA ATT GCA CCT GTA TTC CCA TCC CAT CAT CCT GGG CTT TCG GAA AAT TCC TAT GGG AGT GGG CCT CAG CCC GTT TCT CCT GGC TCA GTT TAC TAG TGC CAT TTG TTC AGT GGT TCG TAG GGC T -3'	220	5- CCT CAA CAA CCA GCA CGG GA-3'	5- AGC CCT ACG AAC CAC TGA AC-3'
Trichuris trichiura oligo/ genomic DNA	5'- AGG TTT CAG ATA CAG TTG TAG AAC CAT ATA ATG CAA CTC TGT CAG TCC ACC AGT TGG TAG AGA ACA CGG ACG AAA CAT TCT GCA TAG ATA ATG AAG CGC TTT ACG ATA TTT GTT TCC GAA CTT TGA AGT TAA CAA CAC CAA CTT ACG GAG ACT TAA ATC ATT TG -3'	164	5'- AGG TTT CAG ATA CAG TTG TAG -3'	5'- CAA ATG ATT TAA GTC TCC G -3'

Table 5.4 LAMP templates and primers.

Original species	Target sequence	Size (bp)	Primer sets	
plasmid HBV 1.3-mer WT replicon	5'- TCC TCA CAA TAC CGC AGA GTC TAG ACT CGT GGT GGA CTT CTC TCA ATT TTC TAG GGG AAA CTA CCG TGT GTC TTG GCC AAA ATT CGC AGT CCC CAA CCT CCA ATC ACT CAC CAA CCT CTT GTC CTC CAA TTT GTC CTG GTT ATC GCT GGA TGT GTC TGC GGC GTT TTA TCA TCT TCC TCT TCA TCC TGC TGC -3'	192	5'- GTTGGGGACT GCGAATTTTG GCTTTTTAGA CTCGTGGTGG ACTTCT-3'	5'- TCACTCACCAA CCTCTTGTCC TTTTTAAAAC GCCGCAGACA CAT-3'
			5'-GGTAGTTCCC CCTAGAAA ATTGAG-3'	5'-AATTTGTCC TGGTTAT CGCTGG-3'
			5'-TCCTCACAATA CCGCAGAGT-3'	5'-GCAGCAGGATG AAGAGGAAT-3'

5.2.2 Fabrication of FLASH Reader.

The FLASH reader is designed to consist of a high-power blue (495 nm) LED for FLASH irradiation and an in-*situ* color sensing system modified from an IO Rodeo colorimeter. The housing of the reader was designed using 3D MAX and 3D printed using a Stratasys Object30 Pro printer with UV curable acrylic materials (figure 5.2 a). The blue LED was temporally programmable using Arduino control board to achieved the precise activation and termination of the FLASH reaction (figure 5.2 b). Specifically, the control system consisted of two correlating circuit loops. The circuit 1 contained a LED driver (output: 4V-5V, 600mA, direct current) which was connected with 110V alternating current, and a LED with 495nm wavelength was linked with a relay (model: SRD-05VDC-SL-C) serving as a switch for the irradiation LED. The voltage common collector (VCC) of the relay wired to the Arduino 5V pin (purple wire) and the relay input was wired to Arduino ground (GND) pin (yellow wire). The circuit 2 consisted of a red LED as an

indicator connected to Arduino GND (black wire) and powered by 5V Arduino digital pin 4 (blue wire) through a resistor (165Ω) and further wired to relay GND (green wire). A tact switch was also wired with red LED through the black wire and connected to 5V Arduino digital pin 8 (red wire) through another resistor (165Ω). Before pressing the tact switch the loop through the red LED was set to open and since the loop also wired to relay GND the relay in circuit 1 was in closure due to both VCC and GND has 5V power. Once pressed the tact switch, the loop through Arduino digital pin 8 to GND was set to open and the voltage of digital pin 8 would drop from 5V to almost 0V. The Arduino board was pre-programmed to shut down the power of digital pin 4 for 5 seconds once it detected the voltage drop in digital pin 8. Because of no power supply through digital pin 4, the red LED would turn off and the power relay would turn on since relay GND dropped to 0V and VCC remained on 5V. Besides the electronic and optical systems, all other components including the sample holder, the LED holder, mechanical components, and housing were fabricated using the 3D printing.

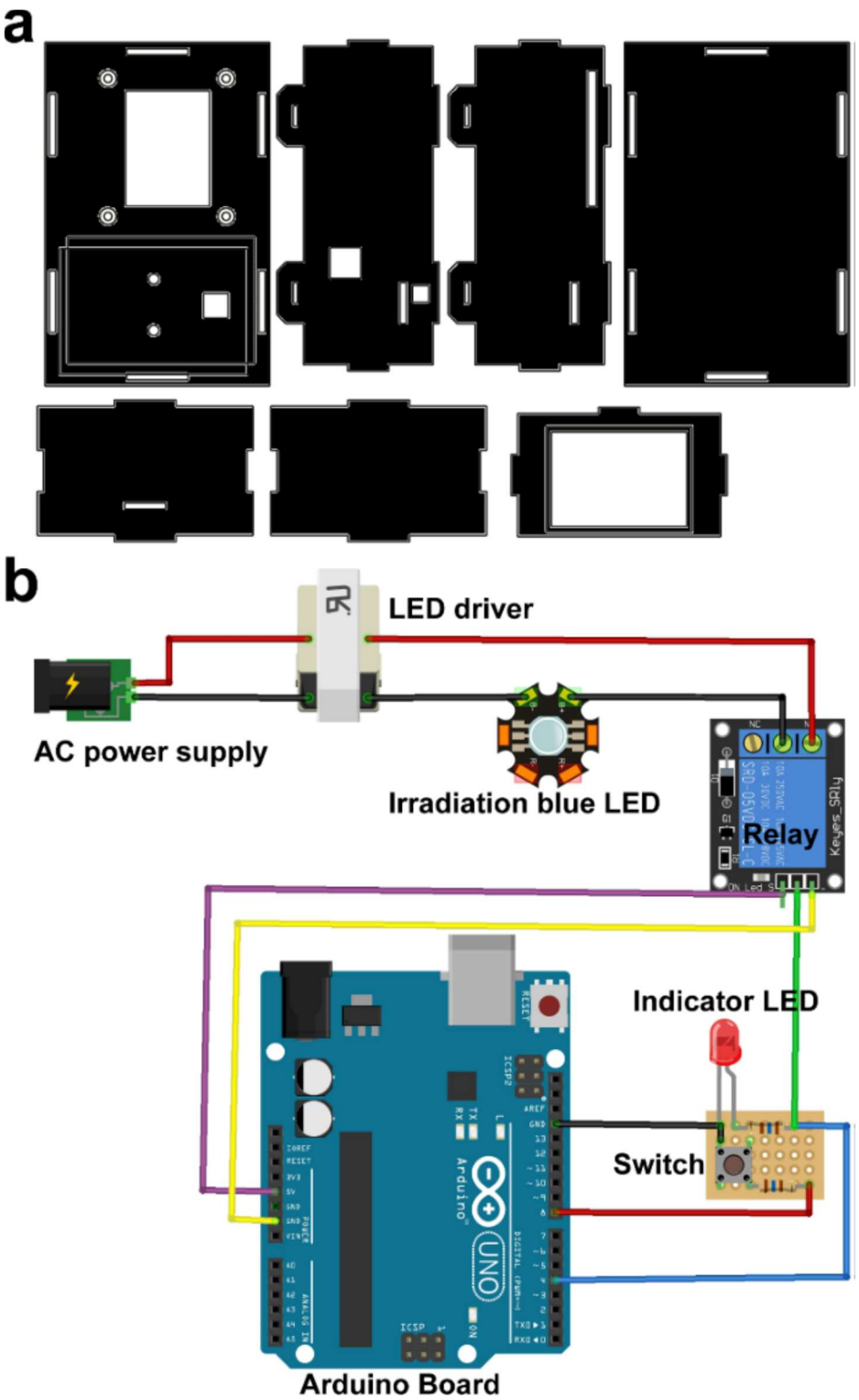

Figure 5.2 Schematic illustration of the housing (**a**) and electrical (**b**) designs of the FLASH reader.

5.2.3 NAT using the FLASH Reader.

In a typical FLASH reader assay, reaction mixtures (200 µL) containing 20 µl of synthetic DNA standards, PCR or LAMP amplicons, 4 µM of SG and 0.5 mg/mL of TMB in 0.1M pH 4 citrate buffer were loaded into a micro cuvette and irradiated using the irradiation LED (495nm wavelength) to triggered the TMB photooxidation. The FLASH reader was powered and controlled by laptop. The absorbance of 200 µL of 0.1 M citrate buffer was measured as background. For samples analyzed using FLASH reader, absorbance of solution at 634 nm (red channel) was measured and recorded after each 5 sec irradiation (including absorbance at 0 sec). Data was transmitted and saved on laptop through cable.

5.2.4 Validation of the FLASH reader Performance.

A series of reaction mixtures each containing 500 nM, 100 nM, 20 nM, 4nM, 0.8nM, 44-bp HBV dsDNA or 500 nM 44-bp ssDNA, 4 µM SG and 0.5 mg/mL TMB in 0.1M pH4 citrate buffer were incubated at room temperature for 5 min. The mixture was then loaded into microcuvette and quantified using FLASH reader using the protocol outline in section 5.2.3. The total irradiation time was 5 min.

For error test, 8 trials of reaction mixtures each containing 100 nM 44-bp HBV dsDNA, 4 µM SG and 0.5 mg/mL TMB in 0.1M pH4 citrate buffer were incubated at room temperature for 5 min. The mixture was then loaded into microcuvette and quantified using FLASH reader using the protocol outline in section 5.2.3. The total irradiation time was 1 min.

5.2.5 Preparation of HBV Containing Human Serum Samples and DNA Isolation.

HBV containing human serum samples were prepared to mimic the real clinical serum samples. To do so, varying concentrations of HBV vector or synthetic genomic fragment were spiked into human serum samples that were obtained from health donors (Sigma). For a typical standard PCR test, total DNA was extracted from the HBV containing human serum samples using QIAamp DNA Blood Mini Kit according to the manufacturer's protocol. Briefly, 200 μL of serum samples were mixed with 20 μL protease and 200 μL of lysis buffer and incubated at 56°C for 10 minutes. Then 200 μL of ethanol were added to the mixture and loaded onto the columns. After washing the columns, total serum DNA was finally eluted into TE buffer at desired volumes (6 μL – 50 μL).

5.2.6 Clinical STH Samples.

STH worm samples were obtained for the same procedure as section 5.1.6.

5.2.7 Deploying FLASH PCR for STH Infections.

Each PCR reaction mixture (25 mL) contains 1 × Taq Master Mix, a pair of primers at a final concentration of 125 nM each, and the target nucleic acid template. The reactions were carried out using a miniPCRTM mini8 Thermal Cycler. A typical PCR reaction included an initial incubation at 94 °C for 3 min, followed by 35 PCR cycles (denaturation at 94 °C for 3 min, annealing for 15 s, extension at 72°C for 15s, and repeat), and a final extension at 72°C for 5 min.

For PCR using 164-bp synthetic DNA standard (Trichuris trichiura oligo/genomic DNA), a series of reaction mixtures each containing 10 aM, 100 aM, 1 fM, 10 fM, 100 fM DNA and a pair of corresponding primers (125nM each, table 5.3). For PCR using DNA obtained from five TT worms and two AL worms, the primers were the same as using for 164-bp synthetic DNA standard. The rest of reagents and PCR protocol were the same as above.

After PCR, a series of reaction mixtures (200 μL) each containing 20 μL PCR amplicons, 4 μM SG and 0.5 mg/mL TMB in 0.1M pH4 citrate buffer were incubated at room temperature for 5 min. The mixture was then loaded into microcuvette and quantified using FLASH reader using the protocol outline in section 5.2.3. For 164-bp synthetic DNA standard, the total irradiation time was 5 min. For DNA obtained from worms, the total irradiation time was 1 min.

The performance of the FLASH reader was validated against a commercial qPCR machine (BioRad CFX96™ IVD Real-Time PCR Detection System) with two commercial kits (SYBR Green Master Mix Bio-Rad and Luna Universal qPCR Master Mix, NEB).

5.2.8 Direct PCR.

Serum samples can be amplificated using the direct PCR protocol without the need for DNA extraction. A typical reaction mixture (25 μL) contained 1× Phusion Blood Direct PCR Master Mix, a pair of primers at a final concentration of 125 nM each, and 2 μL of HBV DNA containing human serum samples. A typical direct PCR reaction included a cell lysis step at 98°C for 5 min, followed by 35 PCR cycles (denaturation at 98 °C for 15 s,

annealing for 5 s, and extension at 72°C for 15s, and repeat), and a final extension at 72°C for 1 min. The resulting PCR product was purified using a Monarch PCR & DNA Cleanup Kit to remove the interferences before the subsequent analyses.

5.2.9 LAMP.

The LAMP reactions (25 μL) containing 1x WarmStart® LAMP Kit, 1.6 μM of FIP (5'- GTTGGGGACT GCGAATTTTG GCTTTTTAGA CTCGTGGTGG ACTTCT-3') and BIP (5'-TCACTCACCAA CCTCTTGTCC TTTTTAAAAC GCCGCAGACA CAT-3') primer, 0.4 μM of LF (5'-GGTAGTTCCC CCTAGAAA ATTGAG-3') and LB (5'-AATTTGTCC TGGTTAT CGCTGG-3') primer, 0.4 μM of F3 (5'-TCCTCACAATA CCGCAGAGT-3') and B3 (5'- GCAGCAGGATG AAGAGGAAT-3') primer, and varying concentration of 192-bp HBV vector (Table 5.4) or human serum samples were incubated at 65°C for 30 min.

After LAMP, a series of reaction mixtures (200 μL) each containing 20 μL LAMP amplicons, 4 μM SG and 0.5 mg/mL TMB in 0.1M pH4 citrate buffer were incubated at room temperature for 5 min. The mixture was then loaded into microcuvette and quantified using FLASH reader using the protocol outline in section 5.2.3.

5.2.10 Gel Electrophoresis.

The PCR or LAMP products were analyzed by 6% PAGE with a typical voltage of 110 v. Gels were then stained with ethidium bromide (0.5 μg/mL) and visualized using a Gel Doc™ XR+ Gel Documentation System (Biorad, Mississauga, ON, Canada).

5.2.10 Distance-based NAT Using FLASH Strip.

The FLASH strip was fabricated by depositing a layer of TMB onto the test zone of qPDR. TMB was first dissolved in acetone with the concentration of 20 mg/mL. The TMB was then deposited onto the test zone on qPDR by using pipette. Total 5 μL of TMB were deposited onto 45 mm^2 (1.5mm×30mm) of test zone on qPDR.

For a typical test, a reaction mixture containing PCR or LAMP amplicons were mixed with 0.1M pH4 citrate buffer containing SG and PEG 100,000 at a ratio of 4: 6. The final concentration of SG was 20 μM and the final concentration of PEG 100,000 was 1 mg/mL in reaction mixture. The reaction mixture was then incubated at room temperature for 5 min and loaded onto the sample loading zone of the FLASH strip for the distance development. After the solution was fully wicked through test zone (~10 min), the strip was irradiated under LED (3W, 495nm) for 1 min for the light-driven color development.

References

1. Dong, T.; Wang, G. A.; Li, F. Shaping up field-deployable nucleic acid testing using microfluidic paper-based analytical devices. *Anal. Bioanal. Chem.* **2019**, 411, 4401-4414.
2. Boehme, C. C.; Nicol, M. P.; Nabeta, P.; Michael, J. S.; Gotuzzo, E.; Tahirli, R.; Gler, M. T.; Blakemore, R.; Worodria, W.; Gray, C. Feasibility, diagnostic accuracy, and effectiveness of decentralised use of the Xpert MTB/RIF test for diagnosis of tuberculosis and multidrug resistance: a multicentre implementation study. *The lancet* **2011,** *377*, 1495-1505.
3. Niemz, A.; Ferguson, T. M.; Boyle, D. S. Point-of-care nucleic acid testing for infectious diseases. *Trends Biotechnol.* **2011,** *29*, 240-250.
4. Urdea, M.; Penny, L. A.; Olmsted, S. S.; Giovanni, M. Y.; Kaspar, P.; Shepherd, A.; Wilson, P.; Dahl, C. A.; Buchsbaum, S.; Moeller, G. Requirements for high impact diagnostics in the developing world. *Nature* **2006,** *444*, 73.
5. Yager, P.; Domingo, G. J.; Gerdes, J. Point-of-care diagnostics for global health. *Annu. Rev. Biomed. Eng.* **2008,** *10*.
6. Reboud, J.; Xu, G.; Garrett, A.; Adriko, M.; Yang, Z.; Tukahebwa, E. M.; Rowell, C.; Cooper, J. M. Paper-based microfluidics for DNA diagnostics of malaria in low resource underserved rural communities. *Proc. Natl. Acad. Sci.* **2019,** *116*, 4834-4842.
7. Yeh, E. C.; Fu, C. C.; Hu, L.; Thakur, R.; Feng, J.; Lee, L. P. Self-powered integrated microfluidic point-of-care low-cost enabling (SIMPLE) chip. *Sci. Adv.* **2017,** *3*, e1501645.
8. Valentini, P.; Pompa, P. P. A universal polymerase chain reaction developer. *Angew. Chem. Int. Ed.* **2016,** *55*, 2157-2160.
9. Chung, H. J.; Castro, C. M.; Im, H.; Lee, H.; Weissleder, R. A magneto-DNA nanoparticle system for rapid detection and phenotyping of bacteria. *Nat. Nanotechnol.* **2013,** *8*, 369.
10. Soleymani, L.; Fang, Z.; Sargent, E. H.; Kelley, S. O. Programming the detection limits of biosensors through controlled nanostructuring. *Nat. Nanotechnol.* **2009,** *4*, 844.
11. Gootenberg, J. S.; Abudayyeh, O. O.; Lee, J. W.; Essletzbichler, P.; Dy, A. J.; Joung, J.; Verdine, V.; Donghia, N.; Daringer, N. M.; Freije, C. A. Nucleic acid detection with CRISPR-Cas13a/C2c2. *Science* **2017,** *356*, 438-442.
12. Pardee, K.; Green, A. A.; Takahashi, M. K.; Braff, D.; Lambert, G.; Lee, J. W.; Ferrante, T.; Ma, D.; Donghia, N.; Fan, M. Rapid, low-cost detection of Zika virus using programmable biomolecular components. *Cell* **2016,** *165*, 1255-1266.
13. Chen, J. S.; Ma, E.; Harrington, L. B.; Da Costa, M.; Tian, X.; Palefsky, J. M.; Doudna, J. A. CRISPR-Cas12a target binding unleashes indiscriminate single-stranded DNase activity. *Science* **2018,** *360*, 436-439.
14. Hajian, R.; Balderston, S.; Tran, T.; deBoer, T.; Etienne, J.; Sandhu, M.; Wauford, N. A.; Chung, J.-Y.; Nokes, J.; Athaiya, M. Detection of unamplified target genes via CRISPR–Cas9 immobilized on a graphene field-effect transistor. *Nat. Biomed. Eng.* **2019,** *3*, 427.
15. Du, Y.; Pothukuchy, A.; Gollihar, J. D.; Nourani, A.; Li, B.; Ellington, A. D. Coupling sensitive nucleic acid amplification with commercial pregnancy test strips. *Angew. Chem. Int. Ed.* **2017,** *56*, 992-996.

16. Myhrvold, C.; Freije, C. A.; Gootenberg, J. S.; Abudayyeh, O. O.; Metsky, H. C.; Durbin, A. F.; Kellner, M. J.; Tan, A. L.; Paul, L. M.; Parham, L. A. Field-deployable viral diagnostics using CRISPR-Cas13. *Science* **2018,** *360*, 444-448.
17. Mabey, D.; Peeling, R. W.; Ustianowski, A.; Perkins, M. D. Tropical infectious diseases: diagnostics for the developing world. Nature Reviews Microbiology 2004, 2, 231.
18. Petryayeva, E.; Algar, W. R. Toward point-of-care diagnostics with consumer electronic devices: the expanding role of nanoparticles. *RSC Adv.* **2015,** *5*, 22256-22282.
19. Cate, D. M.; Adkins, J. A.; Mettakoonpitak, J.; Henry, C. S. Recent developments in paper-based microfluidic devices. *Anal. Chem.* **2014,** *87*, 19-41.
20. Gong, M. M.; Sinton, D. Turning the page: advancing paper-based microfluidics for broad diagnostic application. *Chem. Rev.* **2017,** *117*, 8447-8480.
21. Magro, L.; Escadafal, C.; Garneret, P.; Jacquelin, B.; Kwasiborski, A.; Manuguerra, J. C.; Monti, F.; Sakuntabhai, A.; Vanhomwegen, J.; Lafaye, P. Paper microfluidics for nucleic acid amplification testing (NAAT) of infectious diseases. *Lab Chip* **2017,** *17*, 2347-2371.
22. Updegraff, D. M. Semimicro determination of cellulose inbiological materials. *Anal. Biochem.* **1969,** *32*, 420-424.
23. Kontturi, E.; Meriluoto, A.; Penttilä, P. A.; Baccile, N.; Malho, J. M.; Potthast, A.; Rosenau, T.; Ruokolainen, J.; Serimaa, R.; Laine, J. Degradation and crystallization of cellulose in hydrogen chloride vapor for high-yield isolation of cellulose nanocrystals. *Angew. Chem. Int. Ed.* **2016,** *55*, 14455-14458.
24. Martinez, A. W.; Phillips, S. T.; Butte, M. J.; Whitesides, G. M. Patterned paper as a platform for inexpensive, low-volume, portable bioassays. *Angew. Chem. Int. Ed.* **2007,** *46*, 1318-1320.
25. Fronczek, C. F.; San Park, T.; Harshman, D. K.; Nicolini, A. M.; Yoon, J.-Y. Paper microfluidic extraction and direct smartphone-based identification of pathogenic nucleic acids from field and clinical samples. *RSC Adv.* **2014,** *4*, 11103-11110.
26. Govindarajan, A.; Ramachandran, S.; Vigil, G.; Yager, P.; Böhringer, K. A low cost point-of-care viscous sample preparation device for molecular diagnosis in the developing world; an example of microfluidic origami. *Lab Chip* **2012,** *12*, 174-181.
27. Li, X.; Luo, L.; Crooks, R. M. Low-voltage paper isotachophoresis device for DNA focusing. *Lab Chip* **2015,** *15*, 4090-4098.
28. Gong, M. M.; Nosrati, R.; San Gabriel, M. C.; Zini, A.; Sinton, D. Direct DNA analysis with paper-based ion concentration polarization. *J. Am. Chem. Soc.* **2015,** *137*, 13913-13919.
29. Rosenfeld, T.; Bercovici, M., Amplification-free detection of DNA in a paper-based microfluidic device using electroosmotically balanced isotachophoresis. *Lab Chip* **2018,** *18*, 861-868.
30. Rohrman, B. A.; Richards-Kortum, R. R. A paper and plastic device for performing recombinase polymerase amplification of HIV DNA. *Lab Chip* **2012,** *12*, 3082-3088.
31. Liu, M.; Hui, C. Y.; Zhang, Q.; Gu, J.; Kannan, B.; Jahanshahi-Anbuhi, S.; Filipe, C. D.; Brennan, J. D.; Li, Y. Target-induced and equipment-free DNA amplification with a simple paper device. *Angew. Chem. Int. Ed.* **2016,** *55*, 2709-2713.
32. Seok, Y.; Joung, H.-A.; Byun, J.-Y.; Jeon, H.-S.; Shin, S. J.; Kim, S.; Shin, Y.-B.; Han, H. S.; Kim, M.-G. A paper-based device for performing loop-mediated isothermal

amplification with real-time simultaneous detection of multiple DNA targets. *Theranostics* **2017,** *7*, 2220.
33. Yang, Z.; Xu, G.; Reboud, J.; Ali, S. A.; Kaur, G.; McGiven, J.; Boby, N.; Gupta, P. K.; Chaudhuri, P.; Cooper, J. M. Rapid veterinary diagnosis of bovine reproductive infectious diseases from semen using paper-origami DNA microfluidics. *ACS Sens.* **2018,** *3*, 403-409.
34. Chow, W. H. A.; McCloskey, C.; Tong, Y.; Hu, L.; You, Q.; Kelly, C. P.; Kong, H.; Tang, Y.-W.; Tang, W. Application of isothermal helicase-dependent amplification with a disposable detection device in a simple sensitive stool test for toxigenic Clostridium difficile. *J. Mol. Diagn.* **2008,** *10*, 452-458.
35. Shetty, P.; Ghosh, D.; Singh, M.; Tripathi, A.; Paul, D. Rapid amplification of Mycobacterium tuberculosis DNA on a paper substrate. *RSC Adv.* **2016,** *6*, 56205-56212.
36. Lafleur, L. K.; Bishop, J. D.; Heiniger, E. K.; Gallagher, R. P.; Wheeler, M. D.; Kauffman, P.; Zhang, X.; Kline, E. C.; Buser, J. R.; Kumar, S. A rapid, instrument-free, sample-to-result nucleic acid amplification test. *Lab Chip* **2016,** *16*, 3777-3787.
37. Toley, B. J.; Covelli, I.; Belousov, Y.; Ramachandran, S.; Kline, E.; Scarr, N.; Vermeulen, N.; Mahoney, W.; Lutz, B. R.; Yager, P. Isothermal strand displacement amplification (iSDA): a rapid and sensitive method of nucleic acid amplification for point-of-care diagnosis. *Analyst* **2015,** *140*, 7540-7549.
38. Choi, J. R.; Hu, J.; Tang, R.; Gong, Y.; Feng, S.; Ren, H.; Wen, T.; Li, X.; Abas, W. A. B. W.; Pingguan-Murphy, B. An integrated paper-based sample-to-answer biosensor for nucleic acid testing at the point of care. *Lab Chip* **2016,** *16*, 611-621.
39. Connelly, J. T.; Rolland, J. P.; Whitesides, G. M. "Paper machine" for molecular diagnostics. *Anal. Chem.* **2015,** *87*, 7595-7601.
40. Xu, G.; Nolder, D.; Reboud, J.; Oguike, M. C.; van Schalkwyk, D. A.; Sutherland, C. J.; Cooper, J. M. Paper-Origami-Based Multiplexed Malaria Diagnostics from Whole Blood. *Angew. Chem. Int. Ed.* **2016,** *55*, 15250-15253.
41. Bender, A. T.; Borysiak, M. D.; Levenson, A. M.; Lillis, L.; Boyle, D. S.; Posner, J. D. Semiquantitative nucleic acid test with simultaneous isotachophoretic extraction and amplification. *Anal. Chem.* **2018,** *90*, 7221-7229.
42. Tang, R.; Yang, H.; Gong, Y.; You, M.; Liu, Z.; Choi, J. R.; Wen, T.; Qu, Z.; Mei, Q.; Xu, F. A fully disposable and integrated paper-based device for nucleic acid extraction, amplification and detection. *Lab Chip* **2017,** *17*, 1270-1279.
43. Phillips, E. A.; Moehling, T. J.; Bhadra, S.; Ellington, A. D.; Linnes, J. C. Strand displacement probes combined with isothermal nucleic acid amplification for instrument-free detection from complex samples. *Anal. Chem.* **2018,** *90*, 6580-6586.
44. Choi, J. R.; Liu, Z.; Hu, J.; Tang, R.; Gong, Y.; Feng, S.; Ren, H.; Wen, T.; Yang, H.; Qu, Z. Polydimethylsiloxane-paper hybrid lateral flow assay for highly sensitive point-of-care nucleic acid testing. *Anal. Chem.* **2016,** *88*, 6254-6264.
45. He, Y.; Zeng, K.; Zhang, S.; Gurung, A. S.; Baloda, M.; Zhang, X.; Liu, G. Visual detection of gene mutations based on isothermal strand-displacement polymerase reaction and lateral flow strip. *Biosens. Bioelectron.* **2012,** *31*, 310-315.
46. Xu, Y.; Liu, Y.; Wu, Y.; Xia, X.; Liao, Y.; Li, Q. Fluorescent probe-based lateral flow assay for multiplex nucleic acid detection. *Anal. Chem.* **2014,** *86*, 5611-5614.

47. Dragan, A.; Pavlovic, R.; McGivney, J.; Casas-Finet, J.; Bishop, E.; Strouse, R.; Schenerman, M.; Geddes, C. SYBR Green I: fluorescence properties and interaction with DNA. *J. Fluoresc.* **2012,** *22*, 1189-1199.
48. Cosa, G.; Focsaneanu, K. S.; McLean, J.; McNamee, J.; Scaiano, J. Photophysical Properties of Fluorescent DNA-dyes Bound to Single-and Double-stranded DNA in Aqueous Buffered Solution. *Photochem. Photobiol.* **2001,** *73*, 585-599.
49. Roy, S.; Mohd-Naim, N. F.; Safavieh, M.; Ahmed, M. U. Colorimetric nucleic acid detection on paper microchip using loop mediated isothermal amplification and crystal violet dye. *ACS Sens.* **2017,** *2*, 1713-1720.
50. Gootenberg, J. S.; Abudayyeh, O. O.; Kellner, M. J.; Joung, J.; Collins, J. J.; Zhang, F. Multiplexed and portable nucleic acid detection platform with Cas13, Cas12a, and Csm6. *Science* **2018,** *360*, 439-444.
51. Mao, X.; Ma, Y.; Zhang, A.; Zhang, L.; Zeng, L.; Liu, G. Disposable nucleic acid biosensors based on gold nanoparticle probes and lateral flow strip. *Anal. Chem.* **2009,** *81*, 1660-1668.
52. Ali, M. M.; Aguirre, S. D.; Xu, Y.; Filipe, C. D.; Pelton, R.; Li, Y. Detection of DNA using bioactive paper strips. *Chem. Commun.* **2009,** 6640-6642.
53. Hu, J.; Wang, L.; Li, F.; Han, Y. L.; Lin, M.; Lu, T. J.; Xu, F. Oligonucleotide-linked gold nanoparticle aggregates for enhanced sensitivity in lateral flow assays. *Lab Chip* **2013,** *13*, 4352-4357.
54. Takalkar, S.; Baryeh, K.; Liu, G. Fluorescent carbon nanoparticle-based lateral flow biosensor for ultrasensitive detection of DNA. *Biosens. Bioelectron.* **2017,** *98*, 147-154.
55. Noor, M. O.; Hrovat, D.; Moazami-Goudarzi, M.; Espie, G. S.; Krull, U. J. Ratiometric fluorescence transduction by hybridization after isothermal amplification for determination of zeptomole quantities of oligonucleotide biomarkers with a paper-based platform and camera-based detection. *Anal. Chim. Acta* **2015,** *885*, 156-165.
56. Noor, M. O.; Krull, U. J. Camera-based ratiometric fluorescence transduction of nucleic acid hybridization with reagentless signal amplification on a paper-based platform using immobilized quantum dots as donors. *Anal. Chem.* **2014,** *86*, 10331-10339.
57. Doughan, S.; Uddayasankar, U.; Krull, U. J. A paper-based resonance energy transfer nucleic acid hybridization assay using upconversion nanoparticles as donors and quantum dots as acceptors. *Anal. Chim. Acta* **2015,** *878*, 1-8.
58. Doughan, S.; Uddayasankar, U.; Peri, A.; Krull, U. J. A paper-based multiplexed resonance energy transfer nucleic acid hybridization assay using a single form of upconversion nanoparticle as donor and three quantum dots as acceptors. *Anal. Chim. Acta* **2017,** *962*, 88-96.
59. Lu, J.; Ge, S.; Ge, L.; Yan, M.; Yu, J. Electrochemical DNA sensor based on three-dimensional folding paper device for specific and sensitive point-of-care testing. *Electrochim. Acta* **2012,** *80*, 334-341.
60. Teengam, P.; Siangproh, W.; Tuantranont, A.; Vilaivan, T.; Chailapakul, O.; Henry, C. S. Electrochemical impedance-based DNA sensor using pyrrolidinyl peptide nucleic acids for tuberculosis detection. *Anal. Chim. Acta* **2018,** *1044*, 102-109.
61. Li, X.; Scida, K.; Crooks, R. M. Detection of hepatitis B virus DNA with a paper electrochemical sensor. *Anal. Chem.* **2015,** *87*, 9009-9015.

62. Scida, K.; Li, B.; Ellington, A. D.; Crooks, R. M. DNA detection using origami paper analytical devices. *Anal. Chem.* **2013,** *85*, 9713-9720.
63. Allen, P. B.; Arshad, S. A.; Li, B.; Chen, X.; Ellington, A. D. DNA circuits as amplifiers for the detection of nucleic acids on a paperfluidic platform. *Lab Chip* **2012,** *12*, 2951-2958.
64. Ying, N.; Ju, C.; Sun, X.; Li, L.; Chang, H.; Song, G.; Li, Z.; Wan, J.; Dai, E. Lateral flow nucleic acid biosensor for sensitive detection of microRNAs based on the dual amplification strategy of duplex-specific nuclease and hybridization chain reaction. *PloS one* **2017,** *12*, e0185091.
65. Green, A. A.; Silver, P. A.; Collins, J. J.; Yin, P. Toehold switches: de-novo-designed regulators of gene expression. *Cell* **2014,** *159*, 925-939.
66. Pardee, K.; Green, A. A.; Ferrante, T.; Cameron, D. E.; DaleyKeyser, A.; Yin, P.; Collins, J. J., Paper-based synthetic gene networks. *Cell* **2014,** *159*, 940-954.
67. Noh, H.; Phillips, S. T. Fluidic timers for time-dependent, point-of-care assays on paper. *Anal. Chem.* **2010,** *82*, 8071-8078.
68. Yamada, K.; Suzuki, K.; Citterio, D., Text-displaying colorimetric paper-based analytical device. *ACS Sens.* **2017,** *2*, 1247-1254.
69. Wang, A. G.; Dong, T.; Mansour, H.; Matamoros, G.; Sanchez, A. L.; Li, F., based DNA reader for visualized quantification of soil-transmitted helminth infections. *ACS Sens.* **2018,** *3*, 205-210.
70. Sechi, D.; Greer, B.; Johnson, J.; Hashemi, N. Three-dimensional paper-based microfluidic device for assays of protein and glucose in urine. *Anal. Chem.* **2013,** *85*, 10733-10737.
71. Cate, D. M.; Dungchai, W.; Cunningham, J. C.; Volckens, J.; Henry, C. S. Simple, distance-based measurement for paper analytical devices. *Lab Chip* **2013,** *13*, 2397-2404.
72. Noor, M. O.; Krull, U. J. Paper-based solid-phase multiplexed nucleic acid hybridization assay with tunable dynamic range using immobilized quantum dots as donors in fluorescence resonance energy transfer. *Anal. Chem.* **2013,** *85*, 7502-7511.
73. Lewis, G. G.; DiTucci, M. J.; Phillips, S. T. Quantifying Analytes in Paper-Based Microfluidic Devices Without Using External Electronic Readers. *Angew. Chem. Int. Ed.* **2012,** *51*, 12707-12710.
74. Lewis, G. G.; Robbins, J. S.; Phillips, S. T. Point-of-care assay platform for quantifying active enzymes to femtomolar levels using measurements of time as the readout. *Anal. Chem.* **2013,** *85*, 10432-10439.
75. Tian, T.; Li, J.; Song, Y.; Zhou, L.; Zhu, Z.; Yang, C. J. Distance-based microfluidic quantitative detection methods for point-of-care testing. *Lab Chip* **2016,** *16*, 1139-1151.
76. Wei, X.; Tian, T.; Jia, S.; Zhu, Z.; Ma, Y.; Sun, J.; Lin, Z.; Yang, C. J. Target-responsive DNA hydrogel mediated "stop-flow" microfluidic paper-based analytic device for rapid, portable and visual detection of multiple targets. *Anal. Chem.* **2015,** *87*, 4275-4282.
77. Zhang, Y.; Zhou, C.; Nie, J.; Le, S.; Qin, Q.; Liu, F.; Li, Y.; Li, J. Equipment-free quantitative measurement for microfluidic paper-based analytical devices fabricated using the principles of movable-type printing. *Anal. Chem.* **2014,** *86*, 2005-2012.
78. Meisburger, S. P.; Sutton, J. L.; Chen, H.; Pabit, S. A.; Kirmizialtin, S.; Elber, R.; Pollack, L. Polyelectrolyte properties of single stranded DNA measured using SAXS and

single-molecule FRET: Beyond the wormlike chain model. *Biopolymers* **2013,** *99*, 1032-1045.
79. Zhou, Y.; Huang, Q.; Gao, J.; Lu, J.; Shen, X.; Fan, C. A dumbbell probe-mediated rolling circle amplification strategy for highly sensitive microRNA detection. *Nucleic Acids Res.* **2010,** *38*, e156-e156.
80. Diawara, A.; Drake, L. J.; Suswillo, R. R.; Kihara, J.; Bundy, D. A.; Scott, M. E.; Halpenny, C.; Stothard, J. R.; Prichard, R. K. Assays to detect β-tubulin codon 200 polymorphism in Trichuris trichiura and Ascaris lumbricoides. *PLoS Neglected Trop. Dis.* **2009,** *3*, e397.
81. Ono, A.; Togashi, H. Highly selective oligonucleotide-based sensor for mercury (II) in aqueous solutions. *Angew. Chem. Int. Ed.* **2004,** *43*, 4300-4302.
82. Zhang, X.; Huang, C.; Xu, S.; Chen, J.; Zeng, Y.; Wu, P.; Hou, X. Photocatalytic Oxidation of TMB with the Double Stranded DNA–SYBR Green I Complex for Label-Free and Universal Colorimetric Bioassay. *Chem. Commun.* **2015**, 51, 14465–14468.
83. Rashwan, N.; Scott, M.; Prichard, R., Rapid Genotyping of β-tubulin Polymorphisms in Trichuris trichiura and Ascaris lumbricoides. *PLoS Neglected Trop. Dis.* **2017,** *11*, e0005205.